Journal of Physics G: Nuclear and
Particle Physics

Rare and exclusive few-body decays of the Higgs, Z, W bosons, and the top quark

Rare and exclusive few-body decays of the Higgs, Z, W bosons, and the top quark

David d'Enterria [1,*] and Văn Dũng Lê [2,†]

[1] CERN, EP Department, CH-1211 Geneva, Switzerland
[2] University of Science - Ho Chi Minh National University, Vietnam

We perform an extensive survey of rare and exclusive few-body decays —defined as those with branching fractions $\mathcal{B} \lesssim 10^{-5}$ and two or three final particles— of the Higgs, Z, W bosons, and the top quark. Such rare decays can probe physics beyond the Standard Model (BSM), constitute a background for exotic decays into new BSM particles, and provide precise information on quantum chromodynamics factorization with small nonperturbative corrections. We tabulate the theoretical $\mathcal{B}$ values for almost 200 rare decay channels of the four heaviest elementary particles, indicating the current experimental limits in their observation. Among those, we have computed for the first time ultrarare Higgs boson decays into photons and/or neutrinos, H and Z radiative decays into leptonium states, radiative H and Z quark-flavour-changing decays, and semiexclusive top-quark decays into a quark plus a meson, while updating predictions for a few other rare H, Z, and top quark partial widths. The feasibility of measuring each of these unobserved decays is estimated for p-p collisions at the high-luminosity Large Hadron Collider (HL-LHC), and for e^+e^- and p-p collisions at the future circular collider (FCC).

CONTENTS

* david.d'enterria@cern.ch
† dunglvht@gmail.com

I. INTRODUCTION

With the discovery of the Higgs boson at the CERN Large Hadron Collider (LHC) about ten years ago [1, 2], the full particle content of the Standard Model (SM) of particle physics has become fully fixed. Among the 17 existing elementary particles (6 quarks, 6 leptons, 4 gauge bosons, and the scalar boson), the top quark, the Higgs and the electroweak (W, Z) bosons are the most massive ones. Studying in detail the properties of the four heaviest elementary particles, with masses around the electroweak scale $\Lambda_{\rm EW} \approx \mathcal{O}(100$ GeV), is an important priority in precision SM studies and in searches for new physics beyond it (BSM). At the LHC, the large center-of-mass energies and integrated luminosities (up to $\mathcal{L}_{\rm int} = 3$ ab^{-1} at the end of the high-luminosity, HL-LHC, phase) [3] available in proton-proton (p-p) collisions, as well as the many ab^{-1} to be integrated in the very clean "background-free" e^+e^- collision environment of the next planned lepton collider facilities, such as the Future Circular collider (FCC-ee) [4] or the CEPC [5], will allow the collection of very large H, W, Z, and top-quark data samples. In addition, and despite much more complicated background conditions than at e^+e^- colliders, p-p collisions at $\sqrt{s} = 100$ TeV planned at FCC-hh [6] will produce unprecedented numbers of W, Z, Higgs, and top particles. The very large data samples expected at these machines will make it possible to measure many of their rare few-body decays —understood here as decays into two or three final-state particles, with branching fractions below $\mathcal{B} \approx 10^{-5}$—, which remain unobserved to date. Broadly speaking, in this work we consider three types of rare few-body decays shown in Fig. 1: (i) decays into three lighter gauge bosons (or one gauge boson plus two neutrinos), (ii) decays into a lighter gauge boson plus a single hadronic (or leptonic) bound system in the form of a quarkonium (or leptonium) state, and (iii) exclusive decays into two quarkonium bound states. The reason for the rarity of the first type of decays is the fact that they proceed through suppressed (heavy particle) loops, whereas the second and third decay modes occur very scarcely because the probability to form a single (let alone double) -onium bound state, out of the outgoing quarks or leptons of the primary decay, is very small.

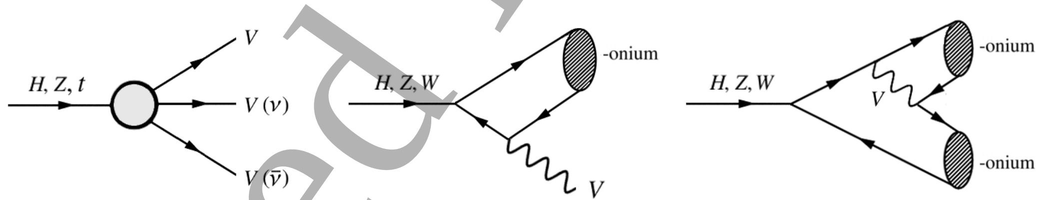

FIG. 1. Examples of schematic diagrams of rare and exclusive two- and three-body decays of the Higgs, Z, and W bosons, and of the top quark. The leftmost diagram shows a rare decay into two or three gauge bosons V = Z, W, γ (or into a gauge boson plus two neutrinos ν) through virtual loops (grey circle). The center and rightmost diagrams show, respectively, typical exclusive decays into a gauge boson (mostly a photon) plus an onium bound state, and into two onium states (dashed blobs).

The incentives for the study of such decays are multiple, with some specificities depending on the decaying "mother" particle. A first general motivation for their study is the possibility that new physics phenomena alter some very rare partial decay widths. Precision tests of suppressed (or forbidden) processes in the SM —such as flavour changing neutral currents (FCNC), or processes violating lepton flavour (LFV) or lepton flavour universality (LFUV)— are powerful probes of BSM physics that have been mostly studied so far in b-quark decays [7, 8]. Unlike in the latter case where, due to the relatively low masses of the B hadrons involved, large power corrections to the decay rates lead to sizable theoretical uncertainties, power corrections in decays of the electroweak and Higgs bosons and top quark are under better theoretical control thanks to the large boost of the final-state hadrons. More concrete motivations are succinctly mentioned next for each particle. In the case of the Higgs boson, very rare decays with photons and/or neutrinos (Fig. 1, left) lead to experimental signatures that are identical to potential exotic BSM Higgs decays [9, 10], and therefore need to be well estimated as background(s) for the latter. Exclusive Higgs decays such as those shown in Fig. 1 (center) are sensitive to the Yukawa couplings of the charm and lighter quarks [11–15], as well as to FCNC

H → qq′ decays, which are otherwise very difficult to access experimentally due to the smallness of the quark masses involved, and/or their heavily suppressed loop-induced rates [10]. In the Z boson case, specific decay modes allow probing FCNC couplings (which are loop- and Glashow–Iliopoulos–Maiani (GIM) [16] suppressed processes in the SM) in a model-independent way [17, 18]. In addition, rare decays of the H and Z bosons shown in Fig. 1 where the onium state decays into diphotons or dileptons, constitute a background for different searches for exotic BSM decays [19], such as e.g., $Z \to \gamma\, a(\gamma\gamma)$ with a being an axion-like particle [20] or a graviton [21] decaying into photons; or $H \to A'(\ell^+\ell^-) + X$ where a dark photon A′ further decays into a $\ell^+\ell^-$ lepton pair [22]. The measurements of exclusive decays of the W boson [23–25] and of the top quark [26] have also been suggested e.g., as an alternative means to determine the W boson and top quark masses via two- or three-body invariant mass analysis, free of invisible neutrinos or (messy) jets involved in the inclusive decay modes. In the top quark case, the study of its suppressed radiative decay rates, induced by the offdiagonal parts of the quark dipole moments, has been of interest for many decades because they also provide an experimentally clean probe for new physics [27]. Of particular importance are precision studies of rare FCNC decays such as $t \to Zc$, $t \to \gamma c$, and $t \to cg$, for which many BSM extensions can enhance their branching ratios by orders of magnitude, thereby yielding compelling phenomenology [27, 28].

Theoretically, the calculation of the partial widths of the few-body decays schematically shown in Fig. 1 (left) are carried out through an expansion of the underlying virtual loops in the electroweak (EW) and/or quantum chromodynamics (QCD) couplings (α and α_s, respectively), at a given order of perturbative accuracy. First calculations were computed at leading order (LO), but more recent results exist at next-to-leading-order (NLO) accuracy. With regards to the center and right diagrams of Fig. 1, the formalism of QCD factorization [29–33] is a well-established approach to study and compute rates for hard exclusive processes with individual hadrons in the final state. Within this framework, the production of the final state occurs in two stages: first, a pair of quarks is produced in a short-distance partonic process; second, the quarks form a given hadronic bound state. The short-distance physics at the energy scale of the initial heavy particle is appropriately separated from the long-distance dynamics governing the formation of the final hadron(s), and the decay amplitudes can be therefore obtained from the convolution of hard-scattering functions calculable in perturbative QCD (pQCD) and nonlocal hadronic matrix elements. These latter objects, called light-cone distribution amplitudes (LCDAs), are nonperturbative and scale-dependent functions that encode the infrared physics of the final hadron formation. The decay amplitudes are formally given as expansions in the ratio of the two (hard and soft) scales in the problem, given by the large energy released $E = m_X/2$ in the process and the final hadron mass, respectively. In the cases of interest in this work, the hard scale is set by the heavy mass of the decaying bosons or top quark, $\mu_{hard} \approx \Lambda_{EW}$ rendering the impact of nonperturbative power corrections at typical hadronization energy scales $\Lambda_{QCD} \approx 0.2$ GeV, $\mathcal{O}(\Lambda_{QCD}/\Lambda_{EW}) \lesssim 10^{-3}$, under control. The studies of exclusive decays of the H, Z, W bosons, and top quark, therefore not only provide a sensitive test of the SM but, in particular, also stringent tests of the QCD factorization formalism, including constraints on poorly known aspects of the nonperturbative formation of hadronic bound states. In the case of final states with charm and bottom quarks, they can bring forward valuable insights into partially conflicting mechanisms of heavy quarkonium production [34, 35].

The main purpose of this work is to present a comprehensive summary of the current theoretical and experimental status of rare and exclusive few-body decays of the four heaviest SM particles. We have first collected all calculations and experimental upper limits for rates of rare and exclusive decays existing in the literature, revised them, and complemented them with ~50 additional channels estimated here for the first time. In total, we provide a list of about 200 predicted rare decays branching ratios, and identify those that are potentially observable at the HL-LHC, or at FCC, and those with negligible rates unless some BSM physics enhances them. This document should therefore help guide and prioritize future experimental and theoretical studies of the different channels. The paper is organized as follows. Section II provides an overall description of the theoretical and experimental details of the branching ratios compiled for each decay channel, as well as an explanation of how estimates of future experimental upper limits are derived. Sections III, IV, V, and VI present, respectively, a detailed list of all rare decays of the Higgs, Z, and W bosons, and top quark, including revised branching fractions for a few channels, as well as ultrarare H decays, H and Z decays into leptonium states, radiative H and Z quark-flavour-changing decays, and semiexclusive top-quark decays into a quark plus a meson, computed here for the first time. The paper is closed with a summary of the main findings.

II. RESULTS

The rare decays results covered in this work are organized in tables per decaying particle listing their theoretical branching fractions, their current experimental upper limits, and future bounds expected at HL-LHC, FCC-ee, and FCC-hh colliders. Here, we discuss first the theoretical models collected, followed by an explanation of the method used to estimate future experimental limits. The numerical values of the relevant SM parameters used in the (re)calculations of a few branching fractions are also provided.

A. Theoretical predictions

For all rare decays collected here, we indicate the theoretical framework used to calculate their corresponding branching fractions. All channels with hadronic final states (Fig. 1, center and right) have been obtained through various implementations of the QCD factorization formalism, using different prescriptions to describe the meson form-factors and to evolve them using the renormalization group equations. We provide here a succinct description of each model so that their acronyms listed below are understandable. The concrete models employed mostly depend on the identity (mass) of the underlying quarks and associated final hadron(s), which defines their kinematics and relevant energy scales. Thus, for example, the form-factors of heavy (charm and/or bottom) mesons also include short-distance physics at energy scales of the heavy-quark mass ($m_{\mathrm{Q}} \gg \Lambda_{\mathrm{QCD}}$, for Q = c, b), which are often described in terms of long-distance matrix elements (LDMEs) rather than LCDAs

1. Light-cone (LC) factorization

A common method for computing exclusive light-hadron production in high-energy decays is given by the so-called amplitude expansion in the light cone (LC), where the perturbatively small expansion parameter is the chirality factor m_{q}/E (with m_{q} and E being the mass of the produced quark and its typical energy, respectively), and the meson form-factors are nonperturbative objects described by LCDAs [33] that encode the internal motion of the quark-antiquark pair inside their bound state, constrained by QCD sum rules [36, 37]. The LC approach implements directly QCD factorization by describing the production of a given final state as a convolution of a hard scattering kernel times the LCDA object. As an example, for the case of the exclusive decay of a heavy particle X into a meson M plus a photon (X → M + γ), the decay amplitude can be written schematically as

$$A(\mathrm{X} \to \mathrm{M} + \gamma) \sim f_{\mathrm{M}} \int_0^1 \mathrm{d}x\, H_{\mathrm{M}}(x,\mu)\phi_{\mathrm{M}}(x,\mu), \tag{1}$$

where f_{M} is the meson decay constant, x is the momentum fraction carried out by the outgoing meson, $H_{\mathrm{M}}(x,\mu)$ is the hard scattering kernel, calculable in pQCD from the relevant matrix-element diagrams, and evaluated at the energy scale μ of the decay, and $\phi_{\mathrm{M}}(x)$ is the LCDA object, which at LO can be interpreted as the amplitude for finding a quark with longitudinal momentum fraction x inside the meson. The f_{M} constant is a parameter that describes the strength of the interaction between a meson and its decay products. It is connected with the form factor of the SM transition current sandwiched between the vacuum and the meson states, which for pseudoscalar (P) and vector meson (VM) mesons (with masses $m_{\mathrm{P,VM}}$ and wavefunctions $P(k)$ and $VM(k)$ at four-momentum k) read, respectively,

$$\begin{aligned} \langle P(k)|\overline{q}_1(0)\gamma^{\mu}\gamma^5 q_2(0)|0\rangle &= -i f_{\mathrm{P}} k^{\mu}, \\ \langle VM(k)|\overline{q}_1(0)\gamma^{\mu} q_2(0)|0\rangle &= -i f_{\mathrm{VM}} m_{\mathrm{VM}} \varepsilon^{*\mu}_{\mathrm{VM}}. \end{aligned} \tag{2}$$

Here above, $\gamma^{\mu,5}$ are Dirac gamma matrices, and $\varepsilon^{*\mu}_{\mathrm{VM}}$ is the polarization vector of the meson. The f_{M} numerical values are obtained from experimental measurements of electromagnetic meson decays widths into leptons (of mass m_ℓ) or photons

$$\begin{aligned} &\Gamma(\mathrm{VM} \to \ell^+\ell^-) = \frac{4\pi\alpha^2(m_{\mathrm{VM}})}{3} Q_{\mathrm{q}}^2 \frac{f_{\mathrm{VM}}^2}{m_{\mathrm{VM}}}, \\ &\Gamma(\mathrm{P} \to \gamma\gamma) = 4\pi\alpha^2(m_{\mathrm{P}}) Q_{\mathrm{q}}^4 \frac{f_{\mathrm{P}}^2}{m_{\mathrm{P}}}, \qquad \Gamma(\mathrm{P}^\pm \to \ell^\pm \nu_\ell) = \frac{\pi\, \alpha^2(m_{\mathrm{P}}) f_{\mathrm{P}}^2\, m_{\mathrm{P}}\, m_\ell^2}{16 m_{\mathrm{Z}}^4 \cos^4\theta_{\mathrm{w}} \sin^4\theta_{\mathrm{w}}} \left[1 - \left(\frac{m_\ell}{m_{\mathrm{P}}}\right)^2\right]^2 |V_{\mathrm{q_1 q_2}}|^2, \end{aligned} \tag{3}$$

where α is the QED coupling, Q_{q} the meson quark electric charge, θ_{w} is the weak mixing angle, m_{Z} the Z boson mass, and $|V_{\mathrm{q_1 q_2}}|$ the Cabibbo–Kobayashi–Maskawa (CKM) matrix element between the two constituent quarks.

Higher-order pQCD corrections can be included in Eq. (1) through the evolution of $H_{\mathrm{M}}(x,\mu)$ from the m_{X} down to the meson mass scale. In the simplest approximation where one ignores the internal motion of quarks inside the mesons, the LCDA takes the form $\phi(x,\mu) = \delta(x)$ or $\phi(x,\mu) = x\delta(x)$ for even and odd states, respectively, where $\delta(x)$ is the Dirac delta function, and the whole meson information in Eq. (1) is encoded in the f_{M} parameter. In such a delta-approximation scheme, one can then write e.g., the partial decay width of a Z boson into an exclusive $\mathrm{M}^0 + \gamma$ final state (for a parity-even meson state M^0) as [38]

$$\Gamma_\delta(\mathrm{Z} \to \mathrm{M}^0 + \gamma) = \frac{\pi\alpha f_{\mathrm{M}}^2 Q_{\mathrm{q}}}{6\cos^2\theta_{\mathrm{w}} \sin^2\theta_{\mathrm{w}} m_{\mathrm{Z}}}. \tag{4}$$

2. *Soft-Collinear Effective Theory (SCET)*

As an alternative to the LC approach, many decay modes involving light mesons have been calculated using Soft-Collinear Effective Theory (SCET) [39], where QCD factorization is rephrased in the language of effective field theory (EFT) [40] to properly address the problem of the multiple scales appearing in the calculations. The SCET framework provides a systematic expansion of $\mathrm{X} \to \mathrm{M}+\mathrm{Y}$ decay amplitudes in powers of a small expansion parameter $\lambda = \Lambda_{\mathrm{QCD}}/E$ (with $E = m_{\mathrm{X}}/2$ the meson energy), and allows proper resummation of the large logarithms in the ratios of scales $\log(m_{\mathrm{M}}/m_{\mathrm{X}})^n$ given by the mass of the mother particle and that of the mesonic final state, which spoil the convergence of the perturbative expansion. Most often SCET is combined with LCDA. At the scale of the large energies released in EW and Higgs boson decays, even charm and bottom quarks can be treated as light quarks, and hence heavy-quark mesons can be described by LCDAs. In a few other calculations, the EFT approach is combined with form-factors based on the nonrelativistic quark model (NRQM) [41]. Final-state mesons containing one light and one heavy quark can be instead described in Heavy-Quark Effective Theory (HQET) where the LCDA describes the hadronic physics at two distinct scales, m_{Q} and Λ_{QCD}, of which the former should be tractable by perturbative methods [42]. In HQET, the hadronic matrix elements are expressed as a combination of perturbatively computable coefficients and new, suitably defined, hadronic matrix elements that exploit the constraints provided by heavy quark symmetries [43] on the nonperturbative matrix elements at low scales.

At leading order in the SCET expansion, the $\mathrm{X} \to \mathrm{M}+\gamma$ decay amplitude can be written in a factorized form as [44]:

$$A = \sum_i \int \mathrm{d}t\, C_i(t,\mu)\, \langle M(k)|\bar{q}(t\bar{n})\frac{\bar{\not{n}}}{2}\Gamma_i[t\bar{n},0]q(0)|0\rangle + \text{power corrections}, \tag{5}$$

where i runs over different combinations of gamma matrices Γ_i that have the appropriate spin structure to form the meson M with wavefunction $M(k)$ from a suitable quark-antiquark pair ($\mathrm{q\bar{q}}$) combination; $n, \bar{n}$ are four-momenta in the lightcone basis[1]; the Wilson coefficients $C_i(t,\mu)$ are calculable hard-scattering EFT coefficients that depend on the process and are evaluated at a factorization scale (μ) that can be determined in a matching computation from perturbation theory. The meson matrix element in Eq. (5) has a direct connection with the meson form factor given by Eqs. (2), through [45]:

$$\begin{aligned}\langle M(k)|\bar{q}(t\bar{n})\frac{\bar{\not{n}}}{2}\Gamma_i[t\bar{n},0]q(0)|0\rangle &= -if_{\mathrm{M}}E\int_0^1 \mathrm{d}x e^{ixt\bar{n}\cdot k}\phi_{\mathrm{M}}(x,\mu); \quad \mathrm{M} = \mathrm{P}, \mathrm{VM}_{\parallel} \\ \langle VM(k)_{\perp}|\bar{q}(t\bar{n})\frac{\bar{\not{n}}}{2}\Gamma_i[t\bar{n},0]q(0)|0\rangle &= -if^{\perp}_{\mathrm{VM}}(\mu)E\varepsilon^{\perp*\mu}_{\mathrm{VM}}\int_0^1 \mathrm{d}x e^{ixt\bar{n}\cdot k}\phi^{\perp}_{\mathrm{VM}}(x,\mu),\end{aligned} \tag{6}$$

where $E = \bar{n}\cdot k/2$; and $\perp, \parallel$ stand for transverse and longitudinal polarizations of the meson. These last expressions can be thought of as the generalization of the relation of matrix elements to decay constants in the nonlocal case: in the local time limit $t \to 0$, the matrix elements of Eq. (6) translate into Eq. (2). To make the connection to the LC approach clearer, we can further take the Fourier transform of $C_i(t,\mu)$ and call it hard scattering kernel $H_{\mathrm{M}}(x,\mu) \equiv \int \mathrm{d}t\, C_{\mathrm{M}}(t,\mu)\, e^{ixt\bar{n}\cdot k}$. We then have a form of the factorized scattering amplitude

$$A = -if_{\mathrm{M}}E\int_0^1 \mathrm{d}x H_{\mathrm{M}}(x,\mu)\phi_{\mathrm{M}}(x,\mu) + \text{ power corrections}, \tag{7}$$

which looks like the LC decay amplitude given by the convolution of hard-scattering kernels with meson LCDA of Eq. (1). One can also expand the LCDAs in terms of Gegenbauer polynomials as [45]

$$\phi_{\mathrm{M}}(x,\mu) = 6x(1-x)\left[1 + \sum_{n=1}^{\infty} a_n^{\mathrm{M}}(\mu)\, C_n^{3/2}(2x-1)\right], \tag{8}$$

with coefficients $a_n^{\mathrm{M}}(\mu)$, moments of the LCDA, that can be obtained from nonperturbative approaches such as lattice QCD, or QCD sum rules. At the electroweak scale, the LCDAs are close to the asymptotic $6x(1-x)$ form. Thus for the asymptotic case, one has e.g., that the $\mathrm{Z} \to \mathrm{M}^0 + \gamma$ partial decay width amounts to [44]:

$$\Gamma(\mathrm{Z} \to \mathrm{M}^0 + \gamma) = \frac{\pi\alpha(0)f_{\mathrm{M}}^2}{6\cos^2\theta_{\mathrm{w}}\sin^2\theta_{\mathrm{w}}m_{\mathrm{Z}}}\left[1 - \frac{10}{3}\frac{\alpha_{\mathrm{s}}(m_z)}{\pi}\right]. \tag{9}$$

[1] In the rest frame of a decaying particle X (with mass $m_{\mathrm{X}} \gg m_{\mathrm{M}}$), the 4-momenta of the two final-state particles are $k_1^{\mu} = n^{\mu}E$ and $k_2^{\mu} = \bar{n}^{\mu}E$, where $E = m_{\mathrm{X}}/2$ is the energy of the final particles in the X rest frame, and the light-cone vectors satisfy $n\cdot\bar{n} = 2$.

This asymptotic expression is similar to that of the delta approximation in Eq. (4) with an extra term that includes higher QCD coupling, $\alpha_s(m_Z)$, corrections coming from a better approximation of the LCDA.

3. Non-Relativistic QCD (NRQCD)

The formation of heavy quarkonium in the decay of a massive particle X is a multi-scale problem involving the hard scale given by m_X, the heavy-flavour quark mass m_Q, the relative momentum of the heavy quark pair $m_Q v$, and the binding energy of the heavy quark pair $m_Q v^2$, where v is the typical relative velocity of the heavy quarks inside the meson. Since $m_X \gg mv \gg mv^2 \gg \Lambda_{QCD}$, the simple static limit applied for light quarks is not sufficient for these systems. Therefore, for heavy quark-antiquark bound states such as charmonium, bottomonium, and bottom-charm (B_c) mesons, a third class of models is often used where in addition to the usual expansion in powers of α_s, the interactions are organized as an expansion in v. Since $v^2 \approx 0.3, 0.1$ for charmonium and bottomonium, respectively, the heavy quarks are nonrelativistic and described in a Non-Relativistic QCD (NRQCD) approach [46]. In the NRQCD framework, the decay width of a heavy particle X into a given quarkonium meson M(n) with quantum numbers $n = {}^{2s+1}L_J^{[1,8]}$ (corresponding to a state with spin s, orbital angular momentum L, total angular momentum J, in the [1] or [8] colour singlet or octet representations, respectively), $X \to M(n) + Y$, factorizes as

$$d\Gamma[X \to M(n) + Y] = \sum_n d\hat{\Gamma}[X \to (Q\overline{Q})_n + Y]\,\langle O^M(n)\rangle, \tag{10}$$

where the amplitude $\sum_n d\hat{\Gamma}[X \to (Q\overline{Q})_n + Y] \propto \frac{1}{2m_X}|\mathcal{A}|^2 d\Phi_3$ can be computed perturbatively, and $\langle O^M(n)\rangle$ are LDMEs which, for the colour singlet (CS) states, are related to the radial quarkonium wavefunction at the origin $|R^M(0)|$. For S-wave quarkonia at LO in v, the $({}^1S_0^{[1]})$ and $({}^3S_1^{[1]})$ states are the sole to contribute, and their LDMEs read

$$\langle O^{\eta_c}({}^1S_0^{[1]})\rangle = \frac{N_c}{2\pi}|R^{\eta_c}(0)|^2, \quad \langle O^{J/\psi}({}^3S_1^{[1]})\rangle = \frac{3N_c}{2\pi}|R^{J/\psi}(0)|^2, \tag{11}$$

for the singlet charmonium ground states, where $N_c = 3$ is the number of colours. The LDMEs for the CS contributions can be obtained from the electromagnetic decays of quarkonia into dileptons or diphotons [47, 48], or from potential models. The NRQCD encapsulates two different mechanisms to describe the evolution of the heavy-flavour quark pair into a quarkonium meson, such as the colour-singlet model (CSM), and the colour-octet model (COM). In the CSM, the $Q\overline{Q}$ pairs are produced in CS states at the hard-scattering scale m_X, and their quantum numbers are conserved during hadronization. The COM requires the extra radiation of gluons, and its contributions are more suppressed than in inclusive reactions, but has also been considered in a few cases. Beyond the non relativistic description of NRQCD, the relativistic quark model (RQM) [49] has been also employed in a few exclusive decay processes involving heavy quarkonia. The NRQCD calculations of heavy particle decays into quarkonia have been performed at LO, NLO, or next-to-NLO (NNLO) accuracy, resumming in some cases also leading (LL) or next-to-leading (NLL) logarithms.

The production of a bottom meson $B \equiv (b\overline{q})_n = B_{u,d}, B_s, B_c$ in the heavy particle decay process $X \to \overline{B} + Y$, can be described in a NRQCD-inspired heavy-quark recombination model [50] where the width takes the form

$$d\Gamma[X \to \overline{B} + Y] = \sum_n d\hat{\Gamma}[X \to (b\overline{q})_n + Y]\,\rho[(b\overline{q})_n \to \overline{B}], \tag{12}$$

with $(b\overline{q})_n$ representing the Fock state of the bottom b and accompanying $\overline{q}$ quark, and the factor $\rho[(b\overline{q})_n \to \overline{B}]$ is a nonperturbative probability for $(b\overline{q})_n$ to evolve into the $\overline{B}$ meson. In the case of $B_c^\pm$ production, the nonperturbative transition $(b\overline{q})_n \to \overline{B}_c$ follows a definite velocity power-counting because the relative velocity of the charm and bottom quarks in the rest frame of the bottom meson (like that of the two bottom quarks in the Υ case) are small. This latter assumption is not fulfilled in the $B_{u,d,s}$ cases, where the Fock state $(b\overline{q})_n$ contributions to the $\overline{B}$ meson with different quantum numbers (e.g., in colour or angular momentum) are not necessarily suppressed, as aforementioned (although for practical purposes, the only relevant states are $n = {}^1S_0^{[1]}, {}^3S_1^{[1]}, {}^1S_0^{[8]}, {}^3S_1^{[8]}$ [50]). By using the heavy-quark spin symmetry [46], one can further reduce the nonperturbative transition probabilities ρ from four to two as [51]

$$\rho_1^{\overline{B}} \equiv \rho[(b\overline{q})_{{}^1S_0^{[1]}} \to \overline{B}], \quad \rho_8^{\overline{B}} \equiv \rho[(b\overline{q})_{{}^1S_0^{[8]}} \to \overline{B}], \quad 3\rho_{1,8}^{\overline{B}} = \rho[(b\overline{q})_{{}^3S_1^{[1,8]}} \to \overline{B}], \tag{13}$$

where the ρ_1 and ρ_8 probabilities can then be related to the standard LDMEs, $\langle O^{\overline{B}}({}^{2s+1}L_J^{[c]})\rangle$, via

$$\langle O^{\overline{B}}({}^1S_0^{[1]})\rangle = 2N_c\frac{4m_b m_q^2}{3}\rho_{1,8}^{\overline{B}}, \quad \langle O^{\overline{B}}({}^1S_0^{[8]})\rangle = \left(N_c^2 - 1\right)\frac{4m_b m_q^2}{3}\rho_{1,8}^{\overline{B}}, \quad \langle O^{\overline{B}}({}^3S_1^{[1,8]})\rangle = 3\langle O^{\overline{B}}({}^1S_0^{[1,8]})\rangle, \tag{14}$$

where m_b is the bottom quark mass, $m_{\bar{q}} = m_{\bar{d}}, m_{\bar{s}} \approx 0.3$ GeV are the constituent light quark masses. The concrete application of the formulas above for the semiexclusive decay of a top quark into a B-meson plus an up-type quark, $t \to \overline{B}^0_{(s)} + q$ (discussed in Section VI C), results in the following widths at LO in the QCD coupling α_s [51]:

$$\begin{aligned}\Gamma(t \to \overline{B}^0 + q) &= \left(\rho_1^{\overline{B}} + 8\rho_8^{\overline{B}}\right)|V_{qd}|^2 \frac{\alpha^2\pi}{9} \frac{m_{\bar{d}}^2(m_t^2 - m_b^2)^2(m_t^2 + m_b^2)}{m_t^3 m_W^4 \sin^4\theta_w}\left[1 + O\left(\frac{m_q}{m_b}\right)\right],\\ \Gamma(t \to \overline{B}^0_s + q) &= \frac{|V_{qs}|^2}{|V_{qd}|^2}\frac{m_{\bar{s}}^2}{m_{\bar{d}}^2}\Gamma(t \to \overline{B}^0 + q)\,, \end{aligned} \quad (15)$$

with similar (yet longer) expressions available in Ref. [51] for the $t \to \Upsilon + q$ decays.

B. Experimental limits

As we will see below, predictions for rare decays of the electroweak and Higgs bosons, and the top quark, have branching fractions in the 10^{-5} to 10^{-15} range (or even down to 10^{-22} for positronium + photon final states). Such tiny branching fractions are very challenging experimentally, and no such decays have yet been observed for any of the particles. To provide an idea of the size of the data samples of $W^\pm$, Z, H, and t particles discussed in this work, Table I collects their total number produced in past, current, and future colliders. The LEP numbers of W and Z bosons are obtained from the LEP-I and LEP-II electroweak summaries [52, 53], and indicate that no rare decay mode with rates below 10^{-7} and 10^{-5} for the Z and W bosons, respectively, has ever been probed in the clean experimental conditions of an e^+e^- collider. We note, somehow curiously, that the last LEP-II operation, which integrated 2.46 fb^{-1} over $\sqrt{s}$ = 189–209 GeV [54], featured a Higgs cross section of $\sigma_H \approx 3$ fb (adding Higgsstrahlung and weak-boson-fusion production processes) [55], and therefore LEP-II *did* produce a few Higgs(125 GeV) boson counts (however, the Higgs searches at the time were optimized for the associated production of a m_H = 115 GeV scalar boson plus an onshell Z boson, for which the H(125 GeV) signal would not have been visible). For the next e^+e^- machine, we focus on FCC-ee because it is the planned facility with the largest data samples expected to be collected [56]. The FCC-ee numbers in Table I cover the time span of the baseline 15-year program with four interaction points and four dedicated runs under consideration: Z-pole, WW threshold, HZ Higgstrahlung, and $t\bar{t}$ threshold. The largest data sample of all will be for Z bosons, for which $6 \cdot 10^{12}$ particles will be produced. The number of H bosons at FCC-ee includes those produced in the HZ (1.45×10^6) and $t\bar{t}$ (+330k events) runs, plus via WW → H at all runs (+125k). Although, in much more complicated background conditions than in e^+e^- collisions, the HL-LHC (with 3 ab^{-1}of p-p collisions at $\sqrt{s}$ = 14 TeV collected per ATLAS/CMS experiment) and the FCC-hh (p-p at $\sqrt{s}$ = 100 TeV with 30 ab^{-1}) will truly serve as W, Z, Higgs, and top factories. We also list the number of the four massive particles produced at the Tevatron in p-$\bar{p}$ collisions at $\sqrt{s}$ = 1.96 TeV, as there exist still a couple of competitive rare decay limits from the CDF experiment. The hadron collider numbers in Table I are obtained from the corresponding production cross sections for each particle multiplied by the integrated luminosity quoted (plus the contribution from $t\bar{t} \to W^+W^- + X$ decays for the $W^\pm$ counting). The cross sections at hadron colliders have been either obtained from the existing literature [57] or, when not readily available or not fully up-to-date, have been recomputed at next-to-next-to-leading-order (NNLO) accuracy with MCFM v.8.0 [58] with the NNPDF3.1_NNLO parton distribution functions (PDFs) [59]. Theoretical (scale, PDF) uncertainties are at most 10% and not quoted.

The largest yield increases across colliders are factors of $6 \cdot 10^3$, $3 \cdot 10^5$, and $4 \cdot 10^5$ for W, Z, and H bosons, respectively, going from LEP to FCC-ee, and a factor of $9 \cdot 10^4$ for top quarks from Tevatron to HL-LHC. As of today (end of 2023), measurements at LEP, Tevatron, and LHC have been able to set upper limits at 95% confidence level (CL) in about one-fourth of the ~200 rare channels considered here. The most stringent experimental rare decays limits are listed in the tables below, including in some cases new results which are not yet available in the 2023 PDG decays listings [60]. One key goal of our work is to provide reasonable expectations of the achievable upper bounds at the HL-LHC, FCC-ee, and FCC-hh. The corresponding extrapolations are obtained through three different means:

1. For a few decay channels, there exist dedicated ATLAS and/or CMS studies that have determined the expected limits at the end of the HL-LHC phase [61–66]. For such cases, we provide directly the expected limits (multiplied by $\sqrt{2}$ to account for the statistical combination of two experiments, ATLAS + CMS) with their bibliographical reference.

2. For those channels where LHC limits exist today in measurements with a given integrated luminosity (labelled e.g., "$\mathcal{L}_{int}$(13 TeV)" next), but for which no dedicated studies exist for HL-LHC, we estimate the latter by assuming that they will be statistically improved by the size of the final data sample, namely by the ratio of squared-root

TABLE I. Total number of Higgs, Z, and W bosons, and top quarks produced (or expected to be produced) in e^+e^- collisions at LEP and FCC-ee, as well as in p-$\bar{p}$ at Tevatron, and in p-p collisions at HL-LHC, and FCC-hh. For e^+e^- colliders, the Z-pole, Higgstrahlung and Higgs weak-fusion, and pair production (WW, $t\bar{t}$) cross sections (without ISR) are indicated. At LEP and FCC-ee, the numbers of W bosons and top-quarks consider two bosons and two quarks produced per collision at the $e^+e^- \to W^+W^-$, $t\bar{t}$ thresholds. For hadron machines, the integrated luminosities and the NNLO production cross section for each particle are indicated. All top quark numbers are for pair production (i.e., the number of events are multiplied by two), and the number of W bosons is the $(W^+ + W^-)$ sum including also the contributions from $t\bar{t}$ decays.

Collider	$W^\pm$ bosons		Z bosons		H bosons		top quarks	
	σ(W)	N(W)	σ(Z)	N(Z)	σ(H)	N(H)	$\sigma(t\bar{t})$	N(top)
LEP	4.0 pb	0.8×10^5	59 nb	2×10^7	~2, 1 fb	~5	–	–
FCC-ee	4.0 pb	5×10^8	59 nb	6×10^{12}	200, 30 fb	1.9×10^6	0.5 pb	3.8×10^6
Increase factor LEP $\mapsto$ FCC-ee	1	6250	1	300, 000	70, 30	400, 000	–	–
Tevatron (1.96 TeV, 10 fb^{-1})	25.3 nb	2.5×10^8	7.6 nb	7.6×10^7	1.1 pb	1.1×10^4	7.1 pb	1.4×10^5
HL-LHC (14 TeV, 2×3 ab^{-1})	200 nb	1.2×10^{12}	62.5 nb	3.8×10^{11}	58 pb	3.5×10^8	1 nb	1.2×10^{10}
FCC-hh (100 TeV, 30 ab^{-1})	1300 nb	4.1×10^{13}	415 nb	1.2×10^{13}	0.93 nb	2.8×10^{10}	35 nb	2.1×10^{12}
Increase factor Tevatron $\mapsto$ HL-LHC	8	4800	8.2	5000	52.7	31 800	141	86 000
Increase factor HL-LHC $\mapsto$ FCC-hh	6.5	34	6.7	32	16	80	35	175

integrated luminosities $\sqrt{2 \times 3\ \mathrm{ab}^{-1}/\mathcal{L}_{\mathrm{int}}(13\ \mathrm{TeV})}$, where the factor of two assumes an ATLAS + CMS combination. For individual LHC measurements carried out with the full Run-2 integrated luminosity of around 140 fb^{-1}, this translates into an expected HL-LHC improvement of more than a factor of six. Bounds estimated that way are conservative, as they ignore improvements in the data analyses (e.g., optimization of the event selection, enlarged categorization depending on the production mode, adoption of more advanced statistical profiling methods, etc.), increased particle production cross sections (from collision energies rising from 13 to 14 TeV), and possible multi-experiment combinations (e.g., adding results from LHCb) for some channels. We have checked that our simple statistical approximation here gives limits comparable to those obtained with the method 1) above whenever dedicated studies are available.

3. For those channels where the best limits today are from Tevatron, the corresponding HL-LHC extrapolation is obtained also statistically, by multiplying the current bound by the square-root of the ratio of the number of decaying particles X between Tevatron and HL-LHC, $\sqrt{N_X(\mathrm{HL\text{-}LHC})/N_X(\mathrm{Tevatron})}$. According to the increase factors quoted in Table I, this implies an improvement of about a factor of 70 in the expected W and Z bosons upper bounds. Such an estimate is conservative as, in general, the overall acceptance/efficiency of the ATLAS/CMS detectors is larger than that of CDF.

Finally, for the FCC-ee and FCC-hh cases, whenever a given decay channel has a branching fraction commensurate with the expected number of particles produced (i.e., whenever $\mathcal{B} \times N_X \gtrsim 1$, where N_X are the FCC numbers given in Table I for any given particle), it will appear listed as "producible at FCC-ee/FCC-hh". Assuming that potential backgrounds are small and/or well under control, as is often the case at e^+e^- colliders, and even more so at FCC-ee where very precise detector performances are being required [56], observation can be achieved with a handful of events. Such an assumption is unwarranted at hadron colliders, such as FCC-hh, where at least 100 signal events are typically required to suppress backgrounds in searches for rare prompt decays of Higgs and Z bosons [67, 68]. Future detector and experimental analysis progresses at the FCC-hh could make it less critical than for the LHC. It is conceivable that much more advanced data analysis techniques will be available by the time this new energy-frontier collider starts to operate, which can render observable some producible decays.

C. Input parameters of the calculations

For the numerical evaluation of various theoretical expressions for branching fractions computed in this work, the input parameters listed in Table II are used. This include leptonium and quark and boson masses and widths (left column), couplings and CKM matrix elements (center column), and hadron masses and form-factor parameters: decay constants f_{M} and HQET first inverse moments λ_{M} (right column).

TABLE II. Numerical values of SM parameters used here in theoretical calculations of various branching fractions. Most of the values are from the PDG [60] (the leptonium masses, $m_{\ell\ell}$, are given as twice the single lepton masses, ignoring tiny binding energies), except for those where a specific reference is provided.

masses and widths		couplings and CKM elements		meson masses and form-factor parameters (in GeV)			
m_{ee}	1.02991 MeV	$\alpha(0)$	1/137.036	$m_{\pi^\pm}$	0.13957	f_π	0.1304 [45]
$m_{\mu\mu}$	0.21126 GeV	$\alpha(m_{\mathrm{Z}})$	1/128.943	$m_{\mathrm{K}^\pm}$	0.493677	f_{K}	0.1562 [45]
$m_{\tau\tau}$	3.5537 GeV	$\alpha_s(m_{\mathrm{Z}})$	0.1180	$m_{\rho^\pm}$	0.77526	f_ρ	0.212 [45]
m_{c}	1.50 GeV	$\sin^2\theta_{\mathrm{w}}$	0.2351	$m_{\mathrm{K}^{*\pm}}$	0.89166	f_{K^*}	0.203 [45]
m_{b}	4.18 GeV	$\mathrm{G_F}$	$1.1664\cdot10^{-5}$ GeV^{-2}	m_ϕ	1.0194	f_ϕ	0.223 [14]
m_{t}	172.69 GeV	$\lvert V_{\mathrm{ud,cs}}\rvert$	0.974	$m_{\mathrm{D}^\pm}$	1.86966	f_{D}	0.212 [69]
m_{W}	80.377 GeV	$\lvert V_{\mathrm{us,cd}}\rvert$	0.225			λ_{D}	0.354 [70]
m_{Z}	91.188 GeV	$\lvert V_{\mathrm{cb,ts}}\rvert$	0.041	$m_{\mathrm{D}_s^\pm}$	1.96835	$f_{\mathrm{D_s}}$	0.2499 [69]
m_{H}	125.25 GeV	$\lvert V_{\mathrm{ub}}\rvert$	0.00382	$m_{\mathrm{D}^{*0}}$	2.007	$f_{\mathrm{D}^{*0}}$	1.28 f_{D} [71]
Γ_{W}	2.085 GeV	$\lvert V_{\mathrm{tb}}\rvert$	0.999	$m_{\mathrm{D}^{*\pm}}$	2.01027	f_{D^*}	1.28 f_{D} [71]
$\Gamma_{\mathrm{W}\to\mu\nu}$	0.1063 Γ_{W}	$\lvert V_{\mathrm{td}}\rvert$	0.0086	$m_{\mathrm{D}_s^{*\pm}}$	2.1123	$f_{\mathrm{D}_s^*}$	1.26 $f_{\mathrm{D_s}}$ [71]
Γ_{Z}	2.4955 GeV			$m_{\mathrm{B}^\pm}$	5.27934	f_{B}	0.190 [69]
$\Gamma_{\mathrm{Z}\to\ell\ell}$	0.0337 Γ_{Z}					λ_{B}	0.338 [72]
Γ_{H}	4.1 MeV [73]			$m_{\mathrm{B}^{*\pm,0}}$	5.32471	f_{B^*}	0.941 f_{B} [74]
$\Gamma_{\mathrm{H}\to\gamma\gamma}$	$2.5\cdot10^{-3}$ Γ_{H}					$f_{\mathrm{B_s}}$	0.2303 [69]
Γ_{t}	1.331 GeV [75]					$\lambda_{\mathrm{B_s}}$	0.438 [76]
				$m_{\mathrm{B}_s^{*0}}$	5.415	$f_{\mathrm{B}_s^*}$	0.953 $f_{\mathrm{B_s}}$ [74]
				$m_{\mathrm{B}_c^\pm}$	6.27447	$f_{\mathrm{B_c}}$	0.427 [74]
				$m_{\mathrm{B}_c^{*\pm}}$	6.32877 [74]	$f_{\mathrm{B}_c^*}$	0.988 $f_{\mathrm{B_c}}$ [74]

III. RARE HIGGS BOSON DECAYS

A. Rare two-, three-, and four-body Higgs boson decays

Figure 2 shows rare decays of the H boson into two neutrinos, three photons, a photon plus two neutrinos, and four photons, respectively. Calculations of rates for these processes, which proceed via virtual loops in the SM, do not exist in most cases to our knowledge. Since they are very suppressed and have no obvious phenomenological impact, they are not included in the standard Higgs decay codes [73], although they are intriguing for diverse reasons exposed below. We have therefore computed them with the MadGraph5_aMC@NLO program [77] with QCD and EW loop corrections up to NLO accuracy [78, 79] using the input parameters of Table II. The corresponding results are listed in Table III.

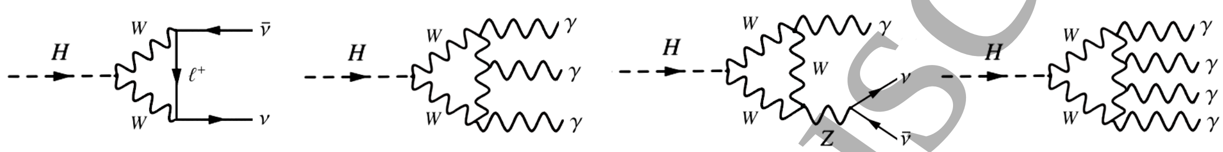

FIG. 2. Representative diagrams of rare 2-, 3-, and 4-body decays of the H boson into photons and/or neutrinos.

The first calculation is that of the invisible two-body Higgs boson decay into a neutrino-antineutrino pair, which is infinitesimal in the SM ($\mathcal{B} \approx 10^{-36}$) compared to the standard invisible (four-neutrino) $H \to ZZ^\star \to 4\nu$ decay ($\mathcal{B} \approx 0.1\%$) [73]. However, since the SM assumption of massless ν's is incorrect, the $H \to \nu\bar{\nu}$ decay can receive extra contributions depending on the mechanism of neutrino mass generation actually realized in nature. Therefore, it is a process worth keeping an eye on, when considering invisible Higgs decays and accounting for massive neutrinos. The second ultrarare Higgs decay of interest here is $H \to 3\gamma$. At variance with the naive assumption that it is forbidden for a scalar particle to decay into three photons, because such a process violates charge-conjugation (C) symmetry, $C(H) = 0 \neq C(3\gamma) = (-1)^3 = -1$, such a decay is possible, albeit extremely suppressed, for EW-induced decays. In a situation akin to the case of the triphoton decay of the scalar positronium state (para-positronium), which is forbidden in QED but not in the EW theory [80, 81], such a Higgs decay can proceed through W loops. Since $H \to 3\gamma$ violates C-symmetry, it must also violate parity in order to conserve CP and, therefore, the final state must be composed of three spatially symmetric photons with vanishing total angular momentum. As a consequence, this partial width features an utterly small $\mathcal{O}(10^{-40})$ probability. Thus, any potential experimental observation of $H \to 3\gamma$ would require an enhancement of the SM rate by up to 40 orders-of-magnitude, and it would be a strong signal of BSM physics. The third diagram of Fig. 2 shows the photon-plus-neutrinos decay, which proceeds through Z and W loops and, since

TABLE III. Compilation of rare Higgs decays to two neutrinos, three or four photons, and a photon plus two neutrinos. For each decay, we provide the theoretical branching fraction computed here with the MadGraph5_aMC@NLO MC (called MG5_aMC, hereafter). The last two columns indicate whether the decay can be produced at FCC-ee/FCC-hh.

				Exp. limits		Producible at	
		Branching fraction	Framework	2023	HL-LHC	FCC-ee	FCC-hh
H →	$\nu + \bar{\nu}$	7.2×10^{-36}	NLO SM, MG5_aMC (this work)	–	–	✘	✘
	$\gamma + \nu + \bar{\nu}$	$(3.74 \pm 0.01) \times 10^{-4}$	NLO SM, MG5_aMC (this work)	–	–	✓	✓
		3.4×10^{-4}	NLO SM [82]				
	$\gamma + \gamma + \gamma$	1.0×10^{-40}	NLO SM, MG5_aMC (this work)	–	–	✘	✘
	$\gamma + \gamma + \gamma + \gamma$	$(4.56 \pm 0.01) \times 10^{-12}$	NLO SM, MG5_aMC (this work)	–	–	✘	✘

the neutrino pair goes undetected, it appears experimentally as an unbalanced monophoton decay of the Higgs boson. Such a final state is shared by many exotic BSM Higgs decays [9], and it is worth computing its SM rate. This decay is actually the least rare considered in this whole survey, and has a branching fraction of $\mathcal{B} = 3.74 \cdot 10^{-4}$ that is about 20% larger than the naive estimate given by $\mathcal{B}(H \to Z\gamma) = 1.54 \cdot 10^{-3}$ [73] combined with $\mathcal{B}(Z \to \nu\bar{\nu}) = 0.200$ [60]. This is so because extra W-induced channels (not shown in Fig. 2) contribute to the amplitude. Last but not least, it is interesting to compute the 4-photon decay of the Higgs boson as it may constitute a background for exotic decays into a pair of light axion-like or scalar particles, each of which further decays into two photons, $H \to a(\gamma\gamma)\, a(\gamma\gamma)$. The Higgs 4γ decay has a branching fraction of $\mathcal{B} = 4.56 \cdot 10^{-12}$, which is 28 orders-of-magnitude larger than the 3-γ one, as C and P conservation is not an issue here, and the rate is only suppressed due to the presence of heavy charged-particle loops. Among all rare channels discussed in this section, LHC searches have been performed to date for the 4γ final state alone [68, 83–86] (searches for 3γ decays have focused on Z' resonances off the Higgs peak [68]), but unfortunately, the limits have been set only on the process $H \to a(\gamma\gamma)a(\gamma\gamma)$ with two intermediate ALPs decaying into photons. It would not be difficult for ATLAS/CMS to recast these searches into upper bounds on the $H \to 4\gamma$ "continuum" decay.

B. Exclusive Higgs decays into a gauge boson plus a meson

Since it is extremely difficult to experimentally access the Yukawa couplings to first- ($q = u, d, s$) and second- (c) generation quarks, due to the smallness of the $H \to q\overline{q}, c\overline{c}$ decay widths, and the very large QCD jet backgrounds at the LHC, it has been proposed to constrain those couplings via rare exclusive decays into a photon (or a gauge boson) plus a vector meson [11–15]. The relevant Feynman diagrams for the $H \to V + M$ (where $V = Z, W^{\pm}, \gamma$, and M = meson) decays in the SM are shown in Fig. 3. The first diagram represents LO amplitudes where the Higgs boson directly couples to a quark-antiquark pair that radiates a gauge boson and forms the mesonic bound state. The second diagram depicts indirect contributions to the decay amplitude, where the scalar boson decays first into two gauge bosons, one of which transforms (offshell) into a hadron state via $V^* \to q\overline{q}$. The third diagram shows the radiative FCNC decay into a photon plus a flavoured meson, through a double W loop. The indirect diagram provides the dominant contribution to the decay rates due to the smallness of the Yukawa couplings to the first- and second-generation quarks, and the largest sensitivity to the Higgs–quark coupling comes from the (destructive) interference of the two amplitudes. Thus, for example, the $H \to \gamma + J/\psi, \gamma + \phi$ modes allow direct access to the flavour-diagonal coupling of the Higgs to the charm and strange quarks, respectively, while the $H \to \gamma + \rho, \gamma + \omega$ decays can probe the Higgs couplings to up and down quarks. The radiative decays $H \to \gamma + M$, where $M = K^{*0}, D^{*0}, B_s^{*0}, B_d^{*0}$ – which in the SM can only proceed through a virtual W boson because the photon (and Z) splitting preserves flavour, or through the direct process in BSM scenarios with flavour-violating Higgs decays – provide possibilities to probe BSM flavour-violating q-q' Higgs couplings [13, 87].

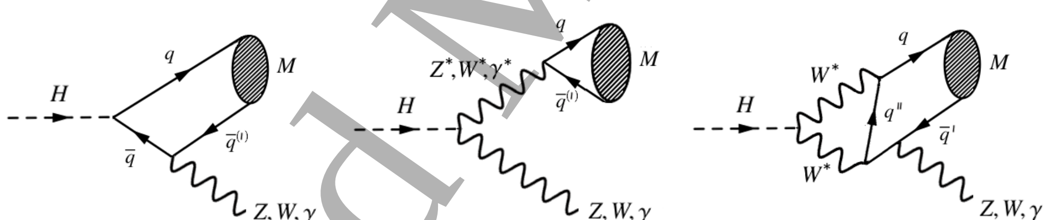

FIG. 3. Schematic diagrams of exclusive decays of the H boson into a meson plus a gauge boson: direct (left), indirect (center), and W-loop (right) processes. The solid fermion lines represent quarks, and the gray blob represents the mesonic bound state.

The indirect amplitude, in which the virtual photon or Z boson couples to the vector meson through the matrix element of a local current, can be parameterized in terms of a single hadronic parameter: the vector-meson decay constant f_M (see Table II). This quantity can be directly obtained from the experimental measurements of the vector-meson leptonic partial decay width (which proceeds through the EW annihilation $q\overline{q} \to \gamma^*, Z^* \to \ell^+\ell^-$), given by

$$\Gamma(M \to \ell^+\ell^-) = \frac{4\pi Q_M^2 f_M^2}{3m_M}\alpha^2(m_M), \tag{16}$$

where Q_M is the relevant combination of quark electric charges, and m_M the mass of the meson. Corrections due to the offshellness of the photon and to the contribution of the $H \to \gamma Z^*$ process are suppressed by m_M^2/m_H^2 and $m_M^2/(m_Z^2 - m_M^2)$, respectively, and hence very small [14]. The direct amplitudes, which are much smaller than the indirect ones except for the heaviest $H \to \gamma + \Upsilon$ decay, have been calculated theoretically by different groups. The hierarchy $m_M \ll m_H$ implies that the vector meson is emitted at very high energy $E_M \gg m_M$ in the Higgs boson rest frame. The constituent partons of the vector meson can thus be described by energetic particles moving collinear to the direction of M, and QCD factorization, either in the SCET or NRQCD incarnation, can be employed to compute them.

1. *Higgs decays into a photon plus a vector meson*

Table IV lists the corresponding theoretical predictions and experimental limits for Higgs decays into a photon plus a vector meson, and Fig. 4 displays them in graphical form. Theoretical $\mathcal{B}$ values are in the range of $\mathcal{O}(10^{-5}$–$10^{-9})$, with larger rates for decays into the lightest vector mesons due to the inverse dependence on the meson mass of the $\mathrm{V}^{(*)} \to \mathrm{q\overline{q}}$ transitions of the dominant indirect process, as per Eq. (16). Experimental upper bounds have been set for all decays at the LHC [88–92] except for the $\mathrm{H} \to \gamma + \mathrm{D}, \gamma + \mathrm{B}$ ones, but it seems that evidence for a few of those SM decays will only possible at FCC-ee. The heaviest bottomonium radiative decays will require the number of Higgs bosons produced in a machine like FCC-hh.

TABLE IV. Compilation of exclusive Higgs decays to a photon plus a meson. For each decay, we provide the predicted branching fraction(s) and the theoretical approach used to compute it, as well as the current experimental upper limit and that estimated for HL-LHC. The last two columns indicate whether the decay can be produced at FCC-ee/FCC-hh.

				Exp. limits		Producible at	
$\mathrm{H} \to \gamma\ +$	M	Branching fraction	Framework	2023	HL-LHC	FCC-ee	FCC-hh
$\mathrm{H} \to \gamma\ +$	ρ^0	$(1.68 \pm 0.08) \times 10^{-5}$	SCET+LCDA [14]	$< 8.8 \times 10^{-4}$ [88]	$\lesssim 6.8 \times 10^{-5}$	✓	✓
	ω	$(1.48 \pm 0.08) \times 10^{-6}$	SCET+LCDA [14]	$< 1.5 \times 10^{-4}$ [91]	$\lesssim 2.2 \times 10^{-5}$	✓	✓
	ϕ	$(2.31 \pm 0.11) \times 10^{-6}$	SCET+LCDA [14]	$< 4.8 \times 10^{-4}$ [88]	$\lesssim 3.7 \times 10^{-5}$	✓	✓
	J/ψ	$(2.95 \pm 0.17) \times 10^{-6}$	SCET+LCDA [14]	$< 2.0 \times 10^{-4}$ [93]	$\lesssim 3.9 \times 10^{-5}$ [62]	✓	✓
		$(3.01 \pm 0.15) \times 10^{-6}$	NRQCD (NLL)+LDME [94]				
		$\left(2.99^{+0.16}_{-0.15}\right) \times 10^{-6}$	NRQCD+LCDA [95]				
	$\psi(2S)$	$(1.3 \pm 0.0) \times 10^{-6}$	SCET+LCDA [14]	$< 9.9 \times 10^{-4}$ [92, 93]	$\lesssim 1.4 \times 10^{-4}$	✓	✓
	$\Upsilon(1S)$	$\left(4.61^{+1.76}_{-1.23}\right) \times 10^{-9}$	SCET+LCDA [14]	$< 2.5 \times 10^{-4}$ [93]	$\lesssim 3.8 \times 10^{-5}$	✘	✓
		$\left(9.97^{+4.04}_{-3.03}\right) \times 10^{-9}$	NRQCD (NLL)+LDME [94]				
		3.0×10^{-8}	NRQCD (NLO)+LDME [96]				
		$\left(5.22^{+2.02}_{-1.70}\right) \times 10^{-9}$	NRQCD+LCDA [95]				
	$\Upsilon(2S)$	$\left(2.34^{+0.76}_{-1.00}\right) \times 10^{-9}$	SCET+LCDA [14]	$< 4.2 \times 10^{-4}$ [93]	$\lesssim 6.4 \times 10^{-5}$	✘	✓
		$\left(2.62^{+1.39}_{-0.91}\right) \times 10^{-9}$	NRQCD (NLL)+LDME [94]				
		1.4×10^{-8}	NRQCD (NLO)+LDME [96]				
		$\left(1.42^{+0.72}_{-0.57}\right) \times 10^{-9}$	NRQCD+LCDA [95]				
	$\Upsilon(3S)$	$\left(2.13^{+0.76}_{-1.12}\right) \times 10^{-9}$	SCET+LCDA [14]	$< 3.4 \times 10^{-4}$ [93]	$\lesssim 5.2 \times 10^{-5}$	✘	✓
		$\left(1.87^{+1.05}_{-0.69}\right) \times 10^{-9}$	NRQCD (NLL)+LDME [94]				
		1.1×10^{-8}	NRQCD (NLO)+LDME [96]				
		$\left(9.1^{+4.8}_{-3.8}\right) \times 10^{-10}$	NRQCD+LCDA [95]				

2. *Higgs decays into a photon plus a flavoured meson*

The third diagram of Fig. 3 shows the radiative decay into a photon plus a flavoured meson. In the SM, this FCNC process can only proceed through a double W loop, and we are not aware of any theoretical calculation of these rates to date. We estimate here the branching fractions for $\mathrm{H} \to \gamma + \mathrm{M}$ with $\mathrm{M} = \mathrm{K}^{*0}, \mathrm{D}^{*0}, \mathrm{B}_s^{*0}, \mathrm{B}_d^{*0}$, which are all excited vector states, as explained below. On the one hand, calculations for the inclusive flavour-changing $\mathrm{H} \to \mathrm{qq}'$ rates exist [87, 97, 98], but without the photon emission and the exclusive final-state meson formation. These predicted FCNC Higgs branching fractions, $\mathcal{B}(\mathrm{H} \to \mathrm{qq}') \equiv \mathcal{B}(\mathrm{H} \to \mathrm{q\overline{q}}' + \mathrm{q}'\overline{\mathrm{q}})$, amount to $\mathcal{B}(\mathrm{H} \to \mathrm{uc}) = (2.7 \pm 0.5) \cdot 10^{-20}$, $\mathcal{B}(\mathrm{H} \to \mathrm{ds}) = 1.19 \cdot 10^{-11}$, $\mathcal{B}(\mathrm{H} \to \mathrm{db}) = (3.8 \pm 0.6) \cdot 10^{-9}$, and $\mathcal{B}(\mathrm{H} \to \mathrm{sb}) = (8.9 \pm 1.5) \cdot 10^{-8}$ [98]. On the other hand, the work of [13] determined the branching fractions of radiative Higgs flavoured-meson decays assuming (arbitrary) $\mathcal{O}(1)$ flavour-changing Yukawa couplings. Combining the results of [13, 98], the branching ratios of Higgs radiatively decaying into flavoured neutral mesons can be determined through the following EFT + LCDA-based expression

$$\mathcal{B}\left(\mathrm{H} \to \gamma + \mathrm{M}(\mathrm{qq}')\right) = \frac{1}{8\pi}\left(\frac{f_{\mathrm{M}} m_{\mathrm{M}}}{2\,\lambda_{\mathrm{M}}(\mu)}\frac{m_{\mathrm{b}}}{v} Q_{\mathrm{q}}\right)^2 \frac{\mathcal{B}(\mathrm{H} \to \mathrm{qq}')}{2\, m_{\mathrm{H}}\, \Gamma_{\mathrm{H}}}, \tag{17}$$

where $v \approx 246$ GeV is the Higgs vacuum expectation value, and all other quantities have been already defined. For the numerical evaluation of the meson HQET first inverse moment $\lambda_{\mathrm{M}}(\mu)$, which plays an important role when working

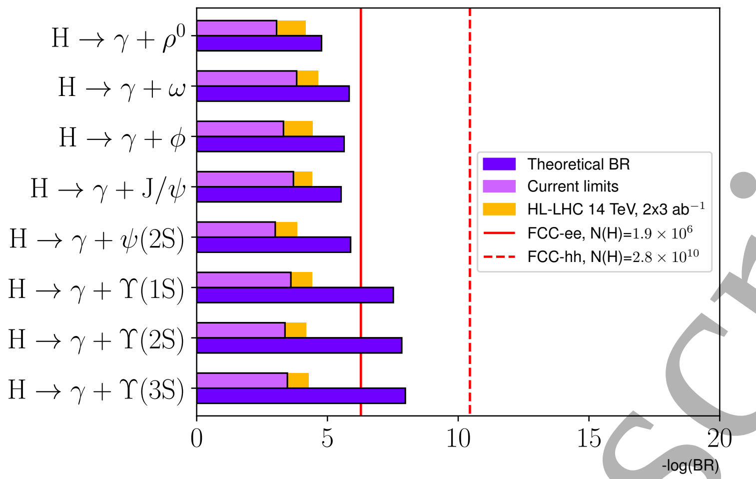

FIG. 4. Branching ratios (in negative log scale) of exclusive $H \to \gamma$ + vector-meson decays. Most recent theoretical predictions (blue bars) compared to current experimental upper limits (violet) and expected HL-LHC bounds (orange). The red vertical lines indicate the FCC-ee (solid) and FCC-hh (dashed) reach based only on the total number of H bosons to be produced at both facilities.

out rates for exclusive decays involving charm and bottom mesons [70, 99], we have used the values quoted in Table II with $\lambda_{B_s^{*0}} = \lambda_{B_d^{*0}} = \lambda_B$, and $\lambda_{D_s^{*0}} = \lambda_D$. For the K^{*0} decay, we simply took $O(10^{-8}) \times \mathcal{B}(H \to ds)$ for the predicted rate. The theoretical branching fractions for such exclusive FCNC radiative decays are extremely suppressed, in the range of $O(10^{-14}$–$10^{-26})$. Therefore, flavoured meson decays of the Higgs boson appear utterly rare to be visible at any current or future collider, and therefore a very clean probe of BSM physics that may enhance Higgs FCNC decays. One experimental limit has been recently set for the $H \to \gamma + K^{*0}$ channel at $O(10^{-5})$ [91], to be compared with our $O(10^{-19})$ SM prediction.

TABLE V. Compilation of exclusive Higgs decays to a photon plus a flavoured meson. For each decay, we provide the branching fraction predicted using Eq. (17), as well as the current experimental upper limit and that estimated for HL-LHC. The last two columns indicate whether the decay can be produced at FCC-ee/FCC-hh.

				Exp. limits		Producible at	
$H \to \gamma$ +	M	Branching fraction	Framework	2023	HL-LHC	FCC-ee	FCC-hh
$H \to \gamma$ +	K^{*0}	1.0×10^{-19}	EFT+LCDA (this work)	$< 8.9 \times 10^{-5}$ [91]	$\lesssim 1.3 \times 10^{-5}$	✘	✘
	D^{*0}	7.0×10^{-27}	EFT+LCDA (this work)	$< 1.0 \times 10^{-3}$ [100]	$\lesssim 1.5 \times 10^{-4}$	✘	✘
	$\overline{B}^{*0}$	8.6×10^{-16}	EFT+LCDA (this work)	–	–	✘	✘
	$\overline{B}_s^{*0}$	1.9×10^{-14}	EFT+LCDA (this work)	–	–	✘	✘

3. *Higgs decays into a Z boson plus a meson*

Higgs decays of the form $H \to Z + M$ involve neutral currents and are very similar to the radiative decays just discussed. However, an important difference with respect to the γ + meson decays, is that the interference terms between the direct and indirect amplitudes are smaller. Although these decays are less useful for measuring the Higgs couplings to light quarks, they probe the important effective H-γ-Z coupling, and provide independent constraints on the meson distribution amplitudes. In addition, they constitute a background for exotic BSM decays of the Higgs boson into, e.g., a Z boson plus an ALP ($H \to Z + a$) [101]. Table VI compiles the theoretical predictions and experimental limits for Higgs decay branching ratios into a Z boson plus a vector meson, and Fig. 6 presents them in graphical form. All decays have rates in the 10^{-5}–10^{-6} range with small differences across models for the same channel, except for the $H \to Z + \rho$ case where the calculations of [12] and [102] differ by a factor of six, seemingly because the former had neglected the indirect contributions. Experimental upper bounds have been set for a few channels listed in Table VI,

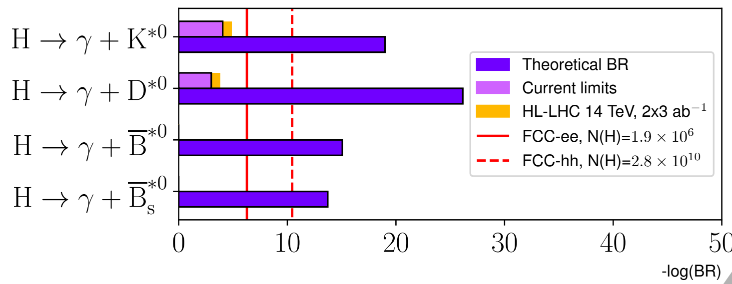

FIG. 5. Branching fractions (in negative log scale) of exclusive $\mathrm{H} \to \gamma+$ flavoured-meson decays. Our predictions via Eq. (17) (blue bars) are compared to current experimental upper limits (violet) and expected HL-LHC bounds (orange). The vertical red lines indicate the FCC-ee (solid) and FCC-hh (dashed) reach based only on the total number of H bosons to be produced at both facilities.

and they are in the $O(10^{-2}$–$10^{-3})$ range[2]. In general, the experimental $\mathrm{H} \to \mathrm{Z}+\mathrm{M}$ limits are about a factor of ten worse than their $\mathrm{H} \to \gamma + \mathrm{M}$ counterparts because of the extra events lost from the requirement of Z boson identification via dilepton decays (with $\mathcal{B} \approx 3\%$ for each lepton pair). The HL-LHC will be able to set upper bounds about 100 times below the expected SM branching fractions, and it appears that experimental evidence will only be possible at FCC-ee for all of them. Bottomonia-plus-Z decays have the largest rates, but no bound has been set to date for them.

[2] We note that one could a priori also derive limits for $\mathcal{B}(\mathrm{H} \to \mathrm{Z} + \eta_\mathrm{c})$ and $\mathcal{B}(\mathrm{H} \to \mathrm{Z} + \eta_\mathrm{b})$ from a recent 95% CL upper limit on the cross section for the $\mathrm{H} \to \mathrm{Z}(\ell\ell)\mathrm{a}(\gamma\gamma)$ process over $m_a \approx$ 1–30 GeV performed by the CMS Collaboration [101]. However, the upper bound cross sections measured at the $m_a = m_{\eta_\mathrm{c},\eta_\mathrm{b}} \approx 2.9,\ 9.4$ GeV mass points ($\sigma \lesssim 7,\ 2.1$ fb, corresponding to $\mathcal{B}(\mathrm{H} \to \mathrm{Z} + \mathrm{a}) \lesssim 0.002,\ 0.62 \cdot 10^{-3}$ after normalizing by the Higgs production cross section and correcting for the dilepton decays of the Z boson) are too weak to place any sensible constrain on these $\mathcal{B}$.

TABLE VI. Compilation of exclusive Higgs decays to Z boson plus a meson. For each decay, we provide the predicted branching fraction(s) and the theoretical approach used to compute it, as well as the current experimental upper limit and that estimated for HL-LHC. The last two columns indicate whether the decay can be produced at FCC-ee/FCC-hh.

$H \to Z$ +	M	Branching fraction	Framework	Exp. limits 2023	Exp. limits HL-LHC	Producible at FCC-ee	Producible at FCC-hh
$H \to Z$ +	π^0	$(2.3 \pm 0.1) \times 10^{-6}$	EFT+NRQM [10]	–	–	✓	✓
		$(2.3 \pm 0.1) \times 10^{-6}$	EFT+LCDA [102]				
	η	$(8.3 \pm 0.9) \times 10^{-7}$	EFT+LCDA [102]	–	–	✓	✓
	ρ^0	$(1.4 \pm 0.1) \times 10^{-5}$	EFT+NRQM [10]	$< 1.2\times 10^{-2}$ [103]	$\lesssim 1.8 \times 10^{-3}$	✓	✓
		$(7.19 \pm 0.29) \times 10^{-6}$	EFT+LCDA [102]				
	ω	$(1.6 \pm 0.1) \times 10^{-6}$	EFT+NRQM [10]	–	–	✓	✓
		$(5.6 \pm 0.2) \times 10^{-7}$	EFT+LCDA [102]				
	η'	$(1.24 \pm 0.13) \times 10^{-6}$	EFT+LCDA [102]	–	–	✓	✓
	ϕ	$(4.2 \pm 0.3) \times 10^{-6}$	EFT+NRQM [10]	$< 3.6\times 10^{-3}$ [103]	$\lesssim 5.4 \times 10^{-4}$	✓	✓
		$(2.42 \pm 0.10) \times 10^{-6}$	EFT+LCDA [102]				
	η_c	$(1.0 \pm 0.1) \times 10^{-5}$	EFT+NRQM [10]	–	–	✓	✓
		$(1.0 \pm 0.0) \times 10^{-5}$	EFT+LCDA [104]				
	J/ψ	3.4×10^{-6}	NRQCD (NLO)+LMDE [105]	$< 1.9\times 10^{-3}$ [106]	$\lesssim 2.1 \times 10^{-4}$ [64]	✓	✓
		3.2×10^{-6}	EFT+NRQM [107]				
		$(2.3 \pm 0.1) \times 10^{-6}$	EFT+LCDA [102]				
	$\psi(2S)$	1.5×10^{-6}	EFT+NRQM [107]	$< 6.6\times 10^{-3}$ [106]	$\lesssim 1.0 \times 10^{-3}$	✓	✓
	η_b	$(2.69 \pm 0.05) \times 10^{-5}$	EFT+LCDA [104]	–	–	✓	✓
		$\left(4.739^{+0.276}_{-0.244}\right) \times 10^{-5}$	EFT (NLO)+LCDA [108]				
	$\Upsilon(1S)$	1.7×10^{-5}	NRQCD (NLO)+LMDE [105]	–	–	✓	✓
		1.7×10^{-5}	EFT+NRQM [107]				
		$(1.54 \pm 0.06) \times 10^{-5}$	EFT+LCDA [102]				
	$\Upsilon(2S)$	8.9×10^{-6}	EFT+NRQM [107]	–	–	✓	✓
		$(7.5 \pm 0.3) \times 10^{-6}$	EFT+LCDA [102]				
	$\Upsilon(3S)$	6.7×10^{-6}	EFT+NRQM [107]	–	–	✓	✓
		$(5.63 \pm 0.24) \times 10^{-6}$	EFT+LCDA [102]				

4. *Higgs decays into a W boson plus a meson*

The charged $H \to W^{\pm}M^{\mp}$ decays (corresponding to the diagrams of Fig. 3 with W bosons in the final state) differ qualitatively from the neutral radiative decays discussed above, because the W attaches itself to a charged current, and one can probe flavour-violating couplings of the Higgs boson. The theoretical complication is that the W has both transverse and longitudinal polarizations, yielding lengthier analytical expressions [12, 102]. Table VII lists the theoretical predictions for Higgs decays into a $W^{\pm}$ boson plus a charged meson, and Fig. 7 presents them in graphical form. The rates for these processes range roughly between 10^{-5} and 10^{-10} with small differences between models for the same final state. The EFT + NRQM theoretical predictions of Ref. [10], which update the $\mathcal{B}$ numerical values computed in [12] (but have likely a typo in the $\mathcal{B}(H \to B^{*\pm}W^{\mp}) = 10^{-5}$ rate, which should be 10^{-10}), agree with the alternative EFT + LCDA rates of Ref. [102]. There has been no experimental search to date at the LHC for any of these 11 decays. The most promising channel, with a $\mathcal{O}(10^{-5})$ branching fraction, is $H \to W^{\pm} + \rho^{\mp}$ with the rho meson decaying into two pions with almost 100% probability, but seemingly experimental evidence for 7 (all) of them will only be possible at FCC-ee (FCC-hh).

C. Radiative Higgs leptonium decays

Figure 8 shows the diagrams of the decay of the Higgs boson into a photon or a Z boson plus a leptonium state $(\ell^+\ell^-)$, where $(\ell^+\ell^-) = (e^+e^-)$, $(\mu^+\mu^-)$, $(\tau^+\tau^-)$ represent positronium, dimuonium, and ditauonium bound states, respectively.

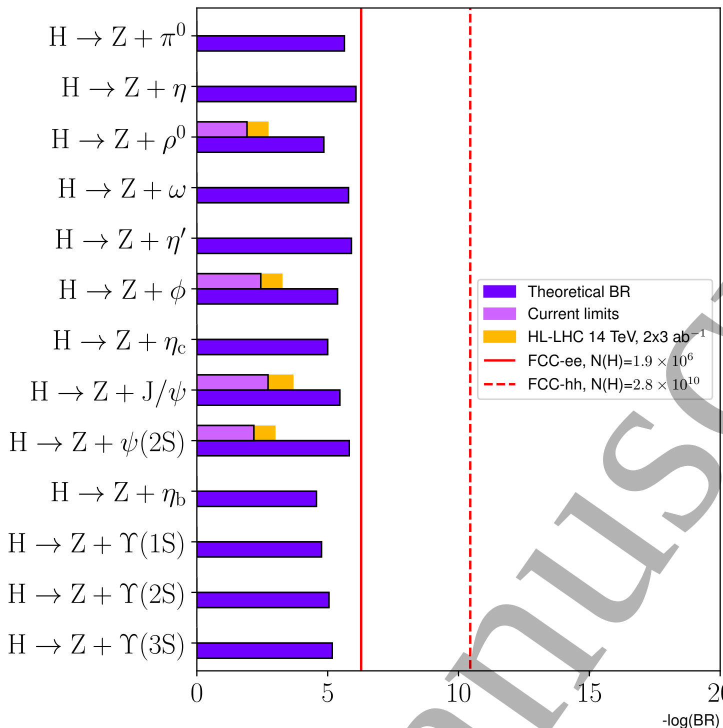

FIG. 6. Branching ratios (in negative log scale) of exclusive H → Z + meson decays. The most recent theoretical predictions (blue bars) are compared to current experimental upper limits (violet) and expected HL-LHC bounds (orange). The red vertical lines indicate the FCC-ee (solid) and FCC-hh (dashed) reach based only on the total number of H bosons to be produced at both machines.

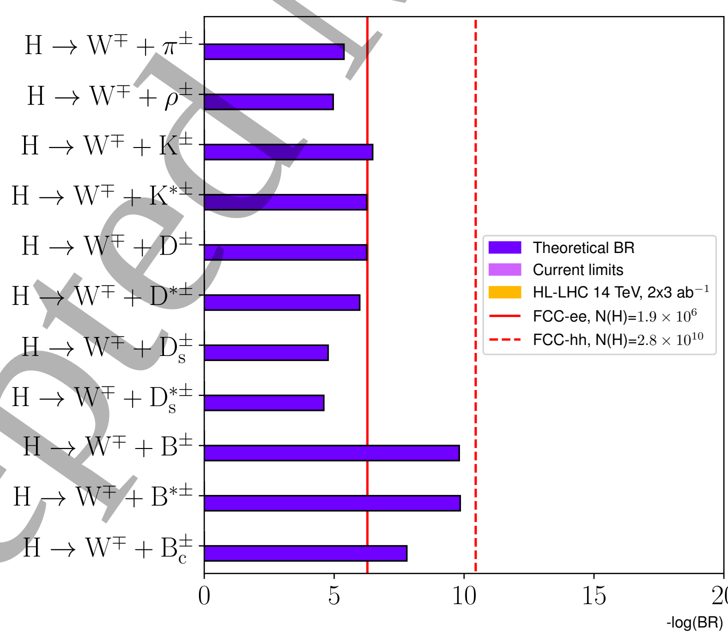

FIG. 7. Branching fractions (in negative log scale) of exclusive H → $W^{\pm}$ + meson decays. The theoretical predictions are shown as blue bars. The red vertical lines indicate the FCC-ee (solid) and FCC-hh (dashed) reach based only on the total number of H bosons to be produced at both facilities.

TABLE VII. Compilation of exclusive Higgs decays to W boson plus a meson. For each decay, we provide the predicted branching fraction(s) and the theoretical approach used to compute it. The last two columns indicate whether the decay can be produced at FCC-ee/FCC-hh.

H → W	+	M	Branching fraction	Framework	Exp. limits 2023	Exp. limits HL-LHC	Producible at FCC-ee	Producible at FCC-hh
$H \to W^{\mp}$	+	$\pi^{\pm}$	$(4.2 \pm 0.2) \times 10^{-6}$	EFT+NRQM [10]	–	–	✓	✓
			$(4.3 \pm 0.2) \times 10^{-6}$	EFT+LCDA [102]				
		$\rho^{\pm}$	$(1.5 \pm 0.1) \times 10^{-5}$	EFT+NRQM [10]	–	–	✓	✓
			$(1.09 \pm 0.05) \times 10^{-5}$	EFT+LCDA [102]				
		$K^{\pm}$	$(3.3 \pm 0.1) \times 10^{-7}$	EFT+NRQM [10]	–	–	✘	✓
			$(3.3 \pm 0.1) \times 10^{-7}$	EFT+LCDA [102]				
		$K^{*\pm}$	$(4.3 \pm 0.2) \times 10^{-7}$	EFT+NRQM [10]	–	–	✘	✓
			$(5.6 \pm 0.4) \times 10^{-7}$	EFT+LCDA [102]				
		$D^{\pm}$	$(5.8 \pm 0.6) \times 10^{-7}$	EFT+NRQM [10]	–	–	✓	✓
			$(5.6 \pm 0.5) \times 10^{-7}$	EFT+LCDA [102]				
		$D^{*\pm}$	$(1.3 \pm 0.1) \times 10^{-6}$	EFT+NRQM [10]	–	–	✓	✓
			$(1.04 \pm 0.14) \times 10^{-6}$	EFT+LCDA [102]				
		$D_s^{\pm}$	$(1.6 \pm 0.1) \times 10^{-5}$	EFT+NRQM [10]	–	–	✓	✓
			$(1.71 \pm 0.11) \times 10^{-5}$	EFT+LCDA [102]				
		$D_s^{*\pm}$	$(3.5 \pm 0.2) \times 10^{-5}$	EFT+NRQM [10]	–	–	✓	✓
			$(2.51 \pm 0.19) \times 10^{-5}$	EFT+LCDA [102]				
		$B^{\pm}$	$(1.6 \pm 0.4) \times 10^{-10}$	EFT+NRQM [10]	–	–	✘	✓
			$(1.54 \pm 0.40) \times 10^{-10}$	EFT+LCDA [102]				
		$B^{*\pm}$	$(1.3 \pm 0.2) \times 10^{-5}$	EFT+NRQM [10]	–	–	✓	✓
			$(1.41 \pm 0.36) \times 10^{-10}$	EFT+LCDA [102]				
		$B_c^{\pm}$	$(1.6 \pm 0.2) \times 10^{-8}$	EFT+NRQM [10]	–	–	✘	✓
			$(8.21 \pm 0.83) \times 10^{-8}$	EFT+LCDA [102]				

Depending on the accompanying gauge boson (Z or γ), leptonium can be produced in spin triplet (ortho) and/or spin singlet (para) states. Such decays are similar to the exclusive radiative decays into mesons shown in Fig. 3, but changing the quark lines for lepton lines. Of course, in the SM there is no unlike-flavour leptonic decay possible, at variance with the $H \to W^{\pm} + M$ case. However, in the presence of BSM physics leading to LFV Higgs decays, $(\ell\ell')$ bound states could be formed directly in exclusive radiative decays. We provide here an estimate of the decay rates for the SM processes by considering the similar $H \to \gamma + M$, $Z + M$ processes, and changing the quarkonium form-factors by leptonium ones. If such decays were to be produced with relatively large rates, they would provide interesting cross checks for any LFUV effects potentially observed with the "open" leptons [109].

The overall probability for forming an onium bound state is determined by one single parameter: its radial wave-function at the origin of the space coordinate, which for leptonium bound states (of principal quantum number n) reads [110],

$$|\phi_{n,(\ell\ell)}(r=0)|^2 = \frac{(m_\ell \alpha(0))^3}{8\pi n^3}. \quad (18)$$

Since the QED coupling is much smaller than the QCD one, $\alpha(m_{\ell\ell}) \ll C_F \alpha_s(m_{q\bar{q}})$, and since the charged lepton masses are smaller than the quark masses of the same generation, $m_{\ell\ell} \ll m_{q\bar{q}}$, the ratio $[\alpha(0) m_{\ell\ell}/(\alpha_s(m_{q\bar{q}}) m_{q\bar{q}})]^3$ is very small, and one can anticipate that those decays will be orders-of-magnitude more suppressed than the $H \to \gamma + M(q\bar{q})$ ones discussed in Section III B.

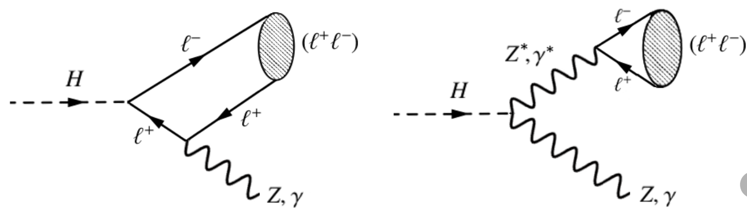

FIG. 8. Schematic diagrams of exclusive decays of the H boson into a photon or a Z boson plus a leptonium state in the direct (left) and indirect (right) processes. The solid fermion lines represent leptons, the gray blob represents the leptonium bound state.

We start by calculating the branching fraction for the $\mathrm{H} \to \gamma + (\ell^+\ell^-)$ process in which, due to charge-conjugation conservation, the leptonium can only be in the ortho $(\ell^+\ell^-)_1$ state. The partial width of this decay can be derived from the similar expressions for quarkonium vector mesons [11], namely

$$\mathcal{B}(\mathrm{H} \to \gamma + (\ell^+\ell^-)_1) = \frac{1}{8\pi}\,\frac{\mathrm{m}_\mathrm{H}^2 - \mathrm{m}_{\ell\ell}^2}{\mathrm{m}_\mathrm{H}^2\,\Gamma_\mathrm{H}}\,|\mathcal{A}_\mathrm{dir} + \mathcal{A}_\mathrm{ind}|^2\,, \tag{19}$$

with the direct and indirect amplitudes corresponding to the diagrams of Fig. 8 left and right, respectively, and where the $\mathrm{H} \to \gamma + \mathrm{Z}^*$ contribution followed by the $\mathrm{Z}^* \to (\ell^+\ell^-)_1$ transition is negligible compared to the corresponding $\mathrm{H} \to \gamma + \gamma^*$ one. These two amplitudes can be written as a function of the wavefunction at the origin $\phi_{\mathrm{n},(\ell\ell)}(0)$, as follows

$$\mathcal{A}_\mathrm{dir} = 2Q_\ell\,\sqrt{4\pi\alpha(0)}\left(\sqrt{2}\mathrm{G}_\mathrm{F}\,m_{\ell\ell}\right)^{1/2}\frac{m_\mathrm{H}^2 - m_{\ell\ell}^2}{\sqrt{m_\mathrm{H}}(m_\mathrm{H}^2 - m_{\ell\ell}^2/2 - 2m_\ell^2)}\,\phi_{\mathrm{n},(\ell\ell)}(0), \tag{20}$$

$$\mathcal{A}_\mathrm{ind} = \frac{Q_\ell\,\sqrt{4\pi\alpha(0)}\,f_{\ell\ell}}{m_{\ell\ell}}\left(16\pi\Gamma_{\mathrm{H}\to\gamma\gamma}\right)^{1/2}\frac{m_\mathrm{H}^2 - m_{\ell\ell}^2}{m_\mathrm{H}^2} = -\frac{2Q_\ell\,\sqrt{4\pi\alpha(0)}}{m_{\ell\ell}^{3/2}}\left(16\pi\Gamma_{\mathrm{H}\to\gamma\gamma}\right)^{1/2}\frac{m_\mathrm{H}^2 - m_{\ell\ell}^2}{m_\mathrm{H}^2}\,\phi_{\mathrm{n},(\ell\ell)}(0)\,, \tag{21}$$

where for the second equality of the indirect component, we have adopted the Van Royen–Weisskopf formula [111, 112] to relate the leptonium decay constant, f_M, to its wavefunction at the origin:

$$f_\mathrm{M}^2 = 4N_\mathrm{c}\frac{|\phi_\mathrm{M}(0)|^2}{m_\mathrm{M}}. \tag{22}$$

Here, the particle M can be either a pseudoscalar/vector meson or an ortho-/para-leptonium state, and the number of colours $N_\mathrm{c} = 1$ is used for the latter. We choose $\phi_\mathrm{M}(0)$ to be real, and then the decay constant f_M comes with a phase that decides the interference between indirect and direct amplitudes. In this work, we choose the (positive) phase that yields a destructive interference similar to the quarkonium case [11]. Since $m_{\ell\ell} \ll m_\mathrm{H}$, plugging Eq. (18) into (21), one can see that the indirect amplitudes are independent of the leptonium masses. Using Eqs. (19)–(21) with the numerical values of Table II, we determine the radiative ortholeptonium ($n = 1$) branching fractions listed in the first three rows of Table VIII. The radiative ortholeptonium decays of the Higgs boson have all numerically similar $O(10^{-12})$ rates for the three leptons, they have not been searched-for to date at the LHC, and only a future machine such as the FCC-hh can try to set upper limits on them at about 10 times their SM values. The experimental search has a very clean signature characterized by a secondary vertex from the boosted $(\ell^+\ell^-)_1$ decay, which lead to significantly displaced triphotons (for positronium and dimuonium), $\mathrm{e}^+\mathrm{e}^-$ pairs (for dimuonium and ditauonium), or $\mu^+\mu^-$ pairs (for ditauonium).

We determine next the rates of the $\mathrm{H} \to \mathrm{Z} + (\ell^+\ell^-)$ decays. At variance with the photon case, these decays have a massive final-state gauge boson that can be in a longitudinal polarization state. As a consequence, both scalar (para-) and vector (ortho-) leptonium states can be produced, whereas in the $\mathrm{H} \to \gamma + (\ell^+\ell^-)_1$ case, the leptonium could only be a (transversely polarized) ortho state. We consider first the Higgs decays into Z-boson-plus-ortholeptonium by properly adapting the theoretical expressions for the similar $\mathrm{H} \to \mathrm{Z} + \mathrm{VM}$ decays, where VM are quarkonia vector mesons such as $\mathrm{J}/\psi, \Upsilon$ [107]. The corresponding $\mathrm{Z} + (\ell^+\ell^-)_1$ decay width can then be written as

$$\Gamma(\mathrm{H} \to \mathrm{Z} + (\ell^+\ell^-)_1) = \Gamma_1 + \Gamma_2 + \Gamma_3, \tag{23}$$

where Γ_1, Γ_2, and Γ_{12} are the contributions from $\mathrm{H} \to \mathrm{Z} + \mathrm{Z}^* \to \mathrm{Z} + (\ell^+\ell^-)_1$, $\mathrm{H} \to \mathrm{Z} + \gamma^* \to \mathrm{Z} + (\ell^+\ell^-)_1$, and their interference, respectively. Defining $r_\mathrm{Z} = m_\mathrm{Z}^2/m_\mathrm{H}^2$, $r_{\ell\ell} = m_{\ell\ell}^2/m_\mathrm{H}^2$, $\lambda(a,b,c)$ is the Källén function, and the HγZ effective coupling $C_{Z\gamma} \approx 5.54$ [113], these individual partial widths can be expressed as follows

$$\Gamma_1 = \frac{m_\mathrm{H}^3 (g_{\ell\ell} f_{\ell\ell})^2}{16\pi v^4} \frac{\lambda^{1/2}(1, r_\mathrm{Z}, r_{\ell\ell})}{(1 - r_{\ell\ell}/r_\mathrm{Z})^2} [(1 - r_\mathrm{Z} - r_{\ell\ell})^2 + 8 r_\mathrm{Z} r_{\ell\ell}],$$
$$\Gamma_2 = \frac{\alpha(0)^3 f_{\ell\ell}^2 Q_\ell^2 m_\mathrm{H}^3}{32\pi^2 v^2 \sin^2\theta_\mathrm{W}} \frac{C_{Z\gamma}^2}{m_{\ell\ell}^2} \lambda^{1/2}(1, r_\mathrm{Z}, r_{\ell\ell})[(1 - r_\mathrm{Z} - r_{\ell\ell})^2 + 2 r_\mathrm{Z} r_{\ell\ell}],$$
$$\Gamma_{12} = \frac{3\alpha(0)^2 f_{\ell\ell}^2 g_{\ell\ell} Q_\ell m_\mathrm{H} C_{Z\gamma}}{8\pi \cos\theta_\mathrm{W} \sin^2\theta_\mathrm{W} v^2} \frac{\lambda^{1/2}(1, r_\mathrm{Z}, r_{\ell\ell})}{1 - r_{\ell\ell}/r_\mathrm{Z}} (1 - r_\mathrm{Z} - r_{\ell\ell}), \quad (24)$$

with $v \approx 246$ GeV, and $g_{\ell\ell} = T_3^\ell - 2Q_\ell \sin^2\theta_\mathrm{W} = 1/2 + 2\sin^2\theta_\mathrm{W}$ (where Q_ℓ is the lepton charge, and T_3^ℓ its third component of the weak isospin). Using the expressions above with the numerical values of Table II, we determine the branching fractions listed in the second three rows of Table VIII. The $\mathrm{H} \to \mathrm{Z} + (\ell^+\ell^-)_1$ decays have $O(10^{-10}$–$10^{-13})$ rates, and they have not been searched-for to date at the LHC. Given the negligible rates, only a high-luminosity machine such as FCC-hh would be able to provide limits approaching the SM values for the most probable $\mathrm{H} \to \mathrm{Z} + (\mathrm{e}^+\mathrm{e}^-)_1$ final state, with a particularly unique search for a Z boson accompanied by triphotons, or an $\mathrm{e}^+\mathrm{e}^-$ pair[3], issuing from a significantly displaced vertex from the secondary positronium decay.

Lastly, we compute the rates of the $\mathrm{H} \to \mathrm{Z} + (\ell^+\ell^-)_0$ decays, whose width can be written using similar expressions for the $\mathrm{H} \to \mathrm{Z} + \mathrm{M}$ decays (where M is a pseudoscalar meson) [102], as follows

$$\Gamma(\mathrm{H} \to \mathrm{Z} + (\ell^+\ell^-)_0) = \frac{m_\mathrm{H}^3}{4\pi v^4} \lambda^{3/2}(1, r_\mathrm{Z}, r_{\ell\ell}) \left| F^{\mathrm{Z}+\ell\ell_0} \right|^2 \text{ with } F^{\mathrm{Z}+\ell\ell_0} = F_\mathrm{dir}^{\mathrm{Z}+\ell\ell_0} + F_\mathrm{ind}^{\mathrm{Z}+\ell\ell_0}. \quad (25)$$

The contribution from the direct amplitude to the partial width (25) amounts to

$$F_\mathrm{dir}^{\mathrm{Z}+\ell\ell_0} = -f_{\ell\ell}\, a_\ell \frac{m_\ell^2}{m_\mathrm{H}^2} \frac{1 - r_\mathrm{Z}^2 + 2 r_\mathrm{Z} \ln r_\mathrm{Z}}{(1 - r_\mathrm{Z})^3}, \quad (26)$$

with $a_\ell = T_3^\ell/2 = 1/4$, which is suppressed by a factor $m_{\ell\ell}^2/m_\mathrm{H}^2$ or m_ℓ^2/m_H^2, that makes it completely negligible (the contribution to the final $(\tau\tau)_0$ amplitude is of about 0.09%). The contribution from the indirect amplitude to the width (25) reads

$$F_\mathrm{ind}^{\mathrm{Z}+\ell\ell_0} = f_{\ell\ell}\, a_\ell. \quad (27)$$

Using the expressions above with the numerical values of Table II, we determine Z-plus-paraleptonium decay rates, $\mathrm{H} \to \mathrm{Z} + (\ell^+\ell^-)_0$, that amount to 10^{-12}–10^{-16} (three last rows of Table VIII).

All branching fractions computed here for Higgs decays into Z or γ plus leptonium are listed in Table VIII and shown in graphical form in Fig. 9. As aforementioned, the decay rates are minuscule, in the $O(10^{-10}$–$10^{-16})$ range, and in the absence of BSM effects enhancing them, only a machine producing as many Higgs bosons as the FCC-hh can attempt to observe the $\mathrm{H} \to \mathrm{Z} + (3\gamma)$ with a displaced triphoton vertex from the late orthopositronium $(ee)_1 \to 3\gamma$ decay, or $\mathrm{H} \to \mathrm{Z} + (\ell^+\ell^-)$ with a displaced dielectron from the magnetic-field-induced breaking of orthopositronium into its constituents. Limits on final states containing the dimuonium and ditauonium states can be set by searching for very displaced secondary vertices from their $\mathrm{e}^+\mathrm{e}^-, \mu^+\mu^-$ decays.

D. Exclusive Higgs decays into two mesons

Figure 10 shows representative diagrams of the exclusive decay of the Higgs boson into two mesons, which can proceed through a multitude of intermediate states coupling to the scalar particle: quarks, gluons, virtual EW gauge

[3] The boosted positronium would have an extremely long path-length (its natural triphoton decay, with lifetime $c\tau = 142$ ns, would take place many km(!) away from the interaction point: $L = (c\tau)(\beta * \gamma) \approx 1450$ km, for $\beta\gamma \approx (m_\mathrm{H} - m_\mathrm{Z})/m_{(\mathrm{ee})} \approx 3.4\,10^4$), but the bound state would be first broken into its constituent $\mathrm{e}^+\mathrm{e}^-$ pair by the detector magnetic field [114].

TABLE VIII. Compilation of exclusive Higgs decays to a photon or a Z boson plus an ortho- $(\ell^+\ell^-)_1$ or para- $(\ell^+\ell^-)_0$ leptonium state (only the ground states, $n = 1$, are considered). For each decay, we provide the prediction of its branching fraction computed here. The last two columns indicate whether the decay can be produced at FCC-ee/FCC-hh.

H → V	+	$(\ell\ell)$	Branching fraction	Framework	Exp. limits 2023	Exp. limits HL-LHC	Producible at FCC-ee	Producible at FCC-hh
		$(ee)_1$	3.5×10^{-12}	(this work)	–	–	✘	✘
$H\to\gamma$	+	$(\mu\mu)_1$	3.5×10^{-12}	(this work)	–	–	✘	✘
		$(\tau\tau)_1$	2.2×10^{-12}	(this work)	–	–	✘	✘
		$(ee)_1$	5.2×10^{-13}	(this work)	–	–	✘	✘
		$(\mu\mu)_1$	5.7×10^{-13}	(this work)	–	–	✘	✘
		$(\tau\tau)_1$	1.4×10^{-11}	(this work)	–	–	✘	✘
$H\to Z$	+	$(ee)_0$	2.7×10^{-16}	(this work)	–	–	✘	✘
		$(\mu\mu)_0$	1.1×10^{-14}	(this work)	–	–	✘	✘
		$(\tau\tau)_0$	3.2×10^{-12}	(this work)	–	–	✘	✘

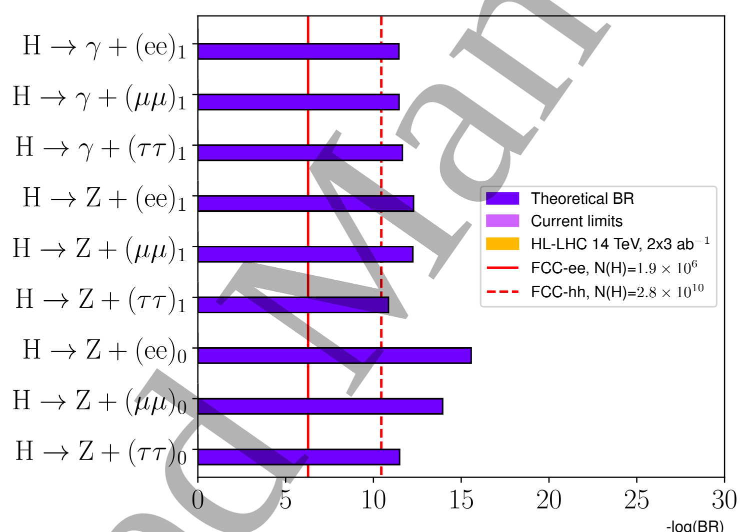

FIG. 9. Branching fractions (in negative log scale) of exclusive $H\to\gamma, Z+$leptonium decays: The theoretical predictions computed here are shown as blue bars. The red vertical lines indicate the FCC-ee (solid) and FCC-hh (dashed) reach based only on the total number of H bosons to be produced at both facilities.

bosons. First estimates of these processes were performed ignoring the internal motion of the produced quark-antiquark pairs [115], and then further improved within different approaches for the meson-pair formation [116–121]. Except for a channel involving the ϕ meson, only exclusive decays involving charmonium and/or bottomonium final states have been computed to date, i.e., no calculations of decays to a pair of light mesons exist to our knowledge (due to the difficulties explained in Section IV D for the similar $Z\to M+M$ case).

Table IX lists the corresponding theoretical predictions and experimental limits for concrete $H\to 2(Q\overline{Q})$ and $H\to(Q\overline{Q})(Q\overline{Q}')$ decay modes. The calculations are carried out in multiple frameworks (LC + LCDA, RQM, NRQCD/NRCSM, NRQCD + LDME) and predict rates in the $O(10^{-9}$–$10^{-11})$ range[4], with some differences in the results for the same final state driven by the partial inclusion of the diagrams shown in Fig. 10. As a matter of fact,

[4] Semiexclusive decays $H\to B_c+Q,+Q'$, B_c^*+Q+Q' have much larger rates [122] and, since they are not rare, nor exclusive, not covered here.

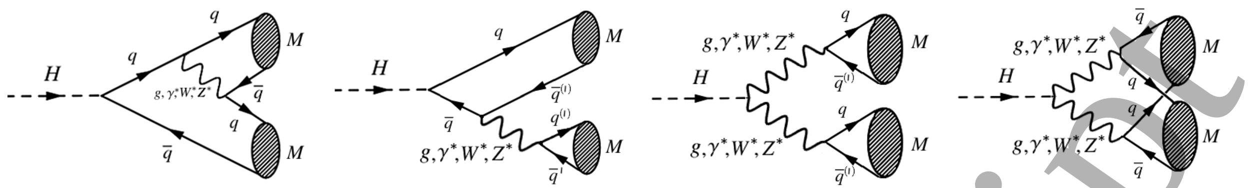

FIG. 10. Schematic diagrams of exclusive decays of the H boson into two mesons. The wavy lines indicate gauge bosons, the solid fermion lines represent quarks and the gray blobs are the meson bound states.

the existing predictions have not fully included all processes shown in the figure with, e.g., the W-induced and quark "crossed" decays often considered subleading and not added to the rates. The $H \to \phi + J/\psi$ decay is the only process computed to date that includes the $H \to W^*W^*$ intermediate diagram. The direct (quark-induced) contributions are only relevant for the heavier double bottomonia with larger Yukawa couplings, and final decays involving charmonium ignore them.

TABLE IX. Compilation of exclusive Higgs decays to two mesons. For each decay, we provide the predicted branching fraction(s) and the theoretical approach used to compute it, as well as the current experimental upper limit and that estimated for HL-LHC. The last two columns indicate whether the decay can be produced at FCC-ee/FCC-hh.

						Exp. limits		Producible at	
$H \to$	M	+	M	Branching fraction	Framework	2023	HL-LHC	FCC-ee	FCC-hh
$H \to$	ϕ	+	J/ψ	1.0×10^{-9}	LC+LCDA [116]	–	–	✗	✓
	J/ψ	+	J/ψ	$(5.8-6.0) \times 10^{-9}$	NRQCD+LDME [121]	$< 3.8\times 10^{-4}$ [106]	$\lesssim 5.8\times 10^{-5}$	✗	✓
				1.7×10^{-10}	RQM [118]				
				2.1×10^{-10}	RQM [120]				
				$(5.9 \pm 2.3) \times 10^{-10}$	NRQCD/NRCSM [119]				
				1.5×10^{-10}	LC+LCDA [116]				
	$\psi(2S)$	+	J/ψ	$\mathcal{O}(5) \times 10^{-11}$	–	$< 2.1\times 10^{-3}$ [106]	$\lesssim 3.2\times 10^{-4}$	✗	✓
			$\psi(2S)$	$(5.1 \pm 2.0) \times 10^{-11}$	NRQCD/NRCSM [119]	$< 3.0\times 10^{-3}$ [106]	$\lesssim 4.5\times 10^{-4}$	✗	✓
	$B_c^{*\mp}$	+	$B_c^{*\pm}$	$(1.4-1.7) \times 10^{-10}$	RQM [117]	–	–	✗	✓
	$B_c^{\mp}$	+	$B_c^{\pm}$	$(2.0-3.0) \times 10^{-10}$	RQM [117]	–	–	✗	✓
	$\Upsilon(1S)$	+	J/ψ	$(2.7-3.6) \times 10^{-10}$	NRQCD+LDME [121]	–	–	✗	✓
				1.6×10^{-11}	LC+LCDA [116]				
			$\Upsilon(1S)$	$(8.5-9.2) \times 10^{-10}$	NRQCD+LDME [121]	$< 1.7\times 10^{-3}$ [106]	$\lesssim 2.6\times 10^{-4}$	✗	✓
				1.8×10^{-10}	RQM [118]				
				2.3×10^{-9}	RQM [120]				
				$(4.3 \pm 0.9) \times 10^{-10}$	NRQCD/NRCSM [119]				
				2.3×10^{-9}	LC+LCDA [116]				
	$\Upsilon(2S)$	+	$\Upsilon(2S)$	$(1.0 \pm 0.2) \times 10^{-10}$	NRQCD/NRCSM [119]	–	–	✗	✓
	$\Upsilon(3S)$	+	$\Upsilon(3S)$	$(5.7 \pm 1.2) \times 10^{-11}$	NRQCD/NRCSM [119]	–	–	✗	✓
	$\Upsilon(mS)$	+	$\Upsilon(nS)$		–	$< 3.5\times 10^{-4}$ [106]	$\lesssim 1.1\times 10^{-5}$ [64]	✗	✗

Experimentally, the double-$(Q\overline{Q})$ and $(Q\overline{Q})(Q\overline{Q}')$ decays have been searched for at the LHC [106], but the current $\mathcal{O}(10^{-3}\text{–}10^{-4})$ limits are 4–5 orders-of-magnitude larger than the predictions. Their production at the HL-LHC, as well as at any future lepton collider, appears unfeasible, and only a machine like FCC-hh will have the Higgs production rates required to reach those decay modes, as indicated in Fig. 11.

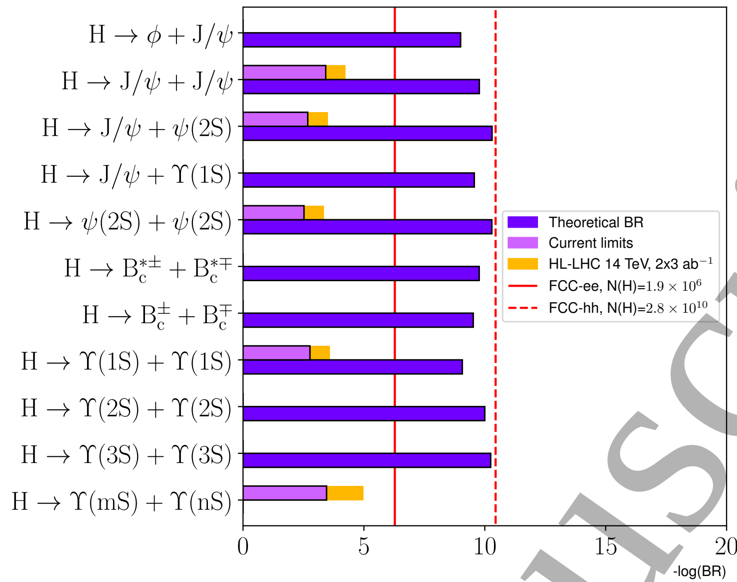

FIG. 11. Branching ratios (in negative log scale) of exclusive H → meson + meson decays. Most recent theoretical predictions (blue bars) are compared to current experimental upper limits (violet) and expected HL-LHC bounds (orange). The red vertical lines indicate the FCC-ee (solid) and FCC-hh (dashed) reach based only on the total number of H bosons to be produced at both machines.

IV. RARE Z BOSON DECAYS

A. Rare three-body Z boson decays

The two-body decay of the Z boson into two massless vector particles ($Z \to \gamma\gamma, gg$) is forbidden by the Landau–Yang theorem, which states that a spin-1 boson cannot decay into two massless bosons [123, 124], and of course the $Z \to \gamma g$ decay is forbidden by conservation of colour. On the other hand, three-body decays into gauge bosons, or into a photon plus two neutrinos, are possible but can only be induced at the loop level in the SM (Fig. 12). Calculations for these virtual processes exist for many years [125–128] but they are not all always consistent among each other and, to our knowledge, have not been revised since then although key underlying parameters, such as the $\alpha_s(m_Z)$ coupling constant, hadronic Z boson partial widths, and top quark mass, have (noticeably) changed. For example, the original $Z \to 3\gamma$ calculations from [126] used $m_t = 124$ GeV, whereas the calculation of the $Z \to 3g$ decay of [127] used the $m_b \to 0$, $m_t \to \infty$ limits, and the prediction for $Z \to g + g + \gamma$ from [125] used $\alpha_s(m_Z) = 0.17$, $m_t = 20$ GeV, and $\Gamma_Z = \Gamma_{Z\to q\bar{q}} \approx 2$ GeV. We note also that many of these older works, including the review of Ref. [18], provide contradictory values for some of these different branching fractions. We have therefore recalculated the rates for all these Z boson rare decays with MG5_aMC in the SM framework with QCD and EW loop corrections computed up to NLO accuracy using the input parameters of Table II. The updated branching fractions (Table X) change with respect to the existing ones (using the old formulas with updated SM parameters, where needed) by 10–25% up or down, except for the $Z \to \gamma + \nu\bar{\nu}$ case, where our result is six times smaller than that estimated in [128]. This older work quoted a partial width for the triangle diagram which is smaller than our results for this contribution, whereas the relative impact of box diagrams was not clearly specified. So we suspect that a larger cancellation of contributions is present in our setup compared to that in this previous study.

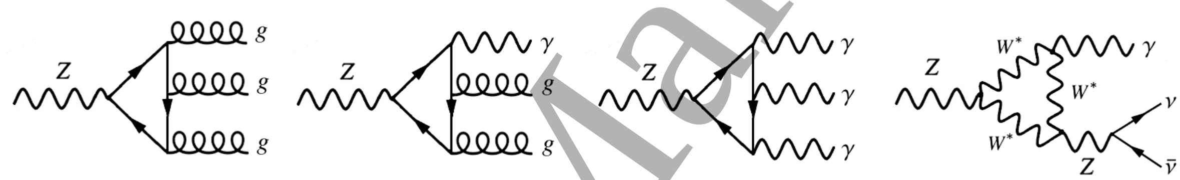

FIG. 12. Representative diagrams of rare 3-body decays of the Z boson into gluons and/or photons and into a photon plus neutrinos. The solid fermion lines represent quarks in the first and second diagrams, and quarks and leptons in the third one.

TABLE X. Compilation of exclusive Z decays to three gauge bosons (photons and/or gluons, with two additional channels requiring one soft photon, $E_\gamma < 1$ GeV, as explained in the text) and a photon plus two neutrinos. For each decay, we provide the predicted branching fraction and the theoretical approach used to compute it, as well as the current experimental limit and that estimated for HL-LHC. The last column indicates whether the decay can be produced at FCC-ee.

	Branching fraction	Framework	Exp. limits 2023	Exp. limits HL-LHC	Producible at FCC-ee
$Z \to g + g + g$	1.9×10^{-6}	NLO SM [127]	$< 1.1\times 10^{-2}$ [129]	–	✓
	1.9×10^{-6}	NLO SM, MG5_aMC (this work)			
$Z \to g + g + \gamma$	7.0×10^{-7}	NLO SM[a] [125]	–	–	✓
	6.8×10^{-7}	NLO SM, MG5_aMC (this work)			
$Z \to g + g + \gamma_{soft}$	1.2×10^{-9}	NLO SM, MG5_aMC (this work)	–	–	✓
$Z \to \gamma + \gamma + \gamma$	5.4×10^{-10}	NLO SM [126]	$< 2.2\times 10^{-6}$ [68]	$\lesssim 1.3 \times 10^{-7}$	✓
	6.4×10^{-10}	NLO SM, MG5_aMC (this work)			
$Z \to \gamma + \gamma + \gamma_{soft}$	2.2×10^{-12}	NLO SM, MG5_aMC (this work)	$< 1.5\times 10^{-5}$ [130]	$\lesssim 2.1 \times 10^{-7}$	✓
$Z \to \gamma + \nu + \hat{\nu}$	7.2×10^{-10}	NLO SM [128]	–	–	✓
	1.3×10^{-10}	NLO SM, MG5_aMC (this work)			

[a] With updated SM parameters. The original result was $\mathcal{B} = 1.8 \times 10^{-6}$ [125]

Among the four rare Z boson decays shown in Fig. 12, those with final-state gluons have the largest rates, $\mathcal{O}(10^{-6})$, whereas the pure electroweak processes have much smaller, $O(10^{-10})$, branching fractions. Experimentally, limits exist for $Z \to 3g$ and $Z \to 3\gamma$ of $O(10^{-2})$ and $O(10^{-6})$, respectively, although no searches have been yet performed to our knowledge for $Z \to \gamma\, g\, g$ and $Z \to \gamma\, \nu\bar{\nu}$ decays. The study of the 3-gluon decay appears hopeless at hadronic machines given the huge QCD trijet backgrounds, although the triphoton decay can be constrained to 100 times the expected SM value at the HL-LHC. Observation of all such decays appears only feasible at a lepton collider such as FCC-ee[5], as indicated by the red vertical line in Fig. 13. We also provide estimates of the branching fraction for the $Z \to gg\,\gamma_{\rm soft}$ and $Z \to \gamma\gamma\,\gamma_{\rm soft}$ decays (where the soft photon has $E_\gamma < 1$ GeV) that can mimic the forbidden $Z \to gg, \gamma\gamma$ channels if the low-energy photon goes experimentally undetected. The branching ratios for both such "fake" Landau–Yang-violating decay modes are $O(10^{-9})$ and $O(10^{-12})$, respectively.

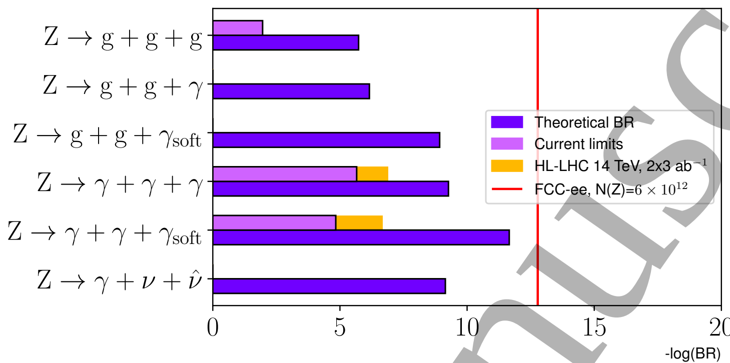

FIG. 13. Branching fractions (in negative log scale) of rare three-body Z boson decays. The most recent theoretical predictions (blue bars) are compared to current experimental upper limits (violet) and expected HL-LHC bounds (orange). The red vertical line indicates the expected FCC-ee reach based only on the total number of Z bosons to be produced.

B. Exclusive Z boson decays into a gauge boson plus a meson

Figure 14 shows the schematic diagrams of the exclusive decay of the Z boson into a photon (or a W boson) plus a meson. Due to the similarity of these diagrams to those of the Higgs boson (Fig. 3), and since the Z boson yields at colliders are about three orders-of-magnitude larger than for the scalar boson (Table I), the study of such processes provides valuable information on, both, theoretical elements (SCET and NRQCD validation, LCDAs/LDMEs constraints, etc.) and experimental aspects (optimization of search techniques) for the corresponding studies of exclusive Higgs boson decays. The observation of any such exclusive decays would provide unique opportunities to reconstruct the Z boson from isolated hadrons, and would improve our knowledge of meson transition form-factors, which describe the $M \to \gamma^*\gamma^{(*)}$ decays. In addition, exclusive Z boson decays into flavoured mesons such as that shown in Fig. 14 (left) probe FCNC processes.

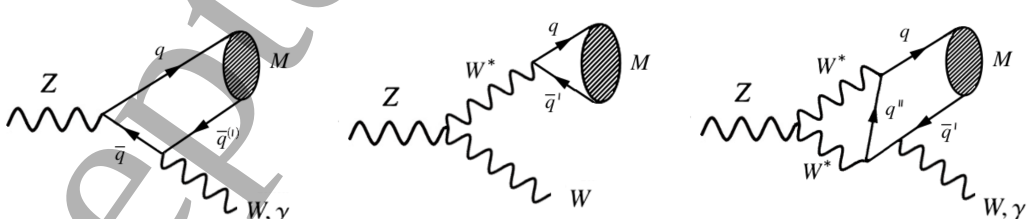

FIG. 14. Schematic diagrams of exclusive decays of the Z boson into a photon or W boson plus a meson. The solid fermion lines represent quarks, and the gray blobs the mesonic bound state.

[5] In this whole section, we will be providing future Z-boson limits expectations for the FCC-ee alone because, although the FCC-hh will produce twice more Z bosons (Table I), the backgrounds are much larger for this collider.

1. *Z boson decays into a photon plus an unflavoured meson*

The theoretical predictions and experimental limits for the branching fractions of the radiative Z boson decay into light, charm, and bottom unflavoured mesons ($Z \to \gamma + q\bar{q}, c\bar{c}, b\bar{b}$, proceeding through the right and center diagrams of Fig. 14) are listed in Table XI, XII, and XIII, respectively, and shown in graphical form in Fig. 15. After forty years from their discovery, no hadronic radiative decay of the electroweak bosons has yet been observed, despite searches performed by the CDF [130, 131], ATLAS [88, 91, 93, 132, 133], CMS [90, 92, 134, 135], and LHCb [136] collaborations. In some cases, such as for the $Z \to \gamma\eta$, $\gamma\eta'$ channels, LEP measurements at the Z pole still provide the best upper limits [137].

The exclusive Z-boson radiative decays into light unflavoured mesons ($Z \to \gamma + M$), listed in Table XI, have theoretical branching fractions in the range of $\mathcal{O}(10^{-8}$–$10^{-12})$, whereas the current experimental limits are in the $\mathcal{O}(10^{-5}$–$10^{-7})$ range with seven channels searched for by ATLAS (3), LHCb (1), CDF at Tevatron (1), and ALEPH at LEP (2). The $Z \to \gamma\omega$ decay is very close to being detected at HL-LHC because its predicted $\mathcal{B}$ is about half of our projected limit. Otherwise, all channels are producible at the FCC-ee.

TABLE XI. Compilation of exclusive Z decays to a photon plus a light unflavoured meson. For each decay, we provide the predicted branching fraction(s) and the theoretical approach used to compute it, as well as the current experimental upper limit and that estimated for HL-LHC. The last column indicates whether the decay can be produced at FCC-ee.

$Z \to \gamma$ +	M	Branching fraction	Framework	Exp. limits 2023	Exp. limits HL-LHC	Producible at FCC-ee
$Z \to \gamma$ +	π^0	$(9.8 \pm 1.0) \times 10^{-12}$	SCET+LCDA [45]	$< 2.0\times 10^{-5}$ [130]	$\lesssim 2.8 \times 10^{-7}$	✓
	η	$(1.0 - 17.0) \times 10^{-10}$	SCET+LCDA [138]	$< 5.1\times 10^{-5}$ [137]	–	✓
	ρ^0	$(4.19 \pm 0.47) \times 10^{-9}$	SCET+LCDA [45]	$< 2.5\times 10^{-5}$ [88]	$\lesssim 1.8 \times 10^{-6}$	✓
	ω	$(2.82 \pm 0.41) \times 10^{-8}$	SCET+LCDA [45]	$< 3.8\times 10^{-7}$ [91]	$\lesssim 5.7 \times 10^{-8}$	✓
	η'	$(3.1 - 4.8) \times 10^{-9}$	SCET+LCDA [138]	$< 4.2\times 10^{-5}$ [137]	–	✓
	ϕ	$(1.17 \pm 0.08) \times 10^{-8}$	LC+LCDA [139]	$< 9.0\times 10^{-7}$ [88]	$\lesssim 6.6 \times 10^{-8}$	✓
		$(1.04 \pm 0.12) \times 10^{-8}$	SCET+LCDA [45]			

The exclusive Z-boson radiative decays to charmonium mesons ($Z \to \gamma + c\bar{c}$), collected in Table XII, have rates in the $\mathcal{O}(10^{-8}$–$10^{-10})$ range as computed within multiple approaches (LC, SCET, NRQCD), which are in general consistent among themselves for the same process. Only one single channel has been searched for, $Z \to \gamma + J/\psi$, with $\mathcal{O}(10^{-6})$ experimental upper bounds [92, 134]. This decay may be visible at HL-LHC, because its predicted rate is about 1/5 of our projected limit. All channels are producible at FCC-ee.

The exclusive Z-boson radiative decays to bottomonium mesons ($Z \to \gamma + b\bar{b}$), listed in Table XIII, have also branching fractions in the $\mathcal{O}(10^{-8}$–$10^{-10})$ range. Three $Z \to \gamma + \Upsilon(nS)$ channels have been searched for at the LHC, setting limits in the $\mathcal{O}(10^{-6})$ range. The $Z \to \gamma + \Upsilon(1S)$ channel might be visible at HL-LHC, as the predicted branching fraction is about 1/4 of our projected limit. As for the photon-plus-charmonium case, all photon-plus-bottomonium channels are producible at FCC-ee.

TABLE XII. Compilation of exclusive Z decays to a photon plus a charmonium state. For each decay, we provide the predicted branching fraction(s) and the theoretical approach used to compute it, as well as the current experimental upper limit and that estimated for HL-LHC. The last column indicates whether the decay can be produced at FCC-ee.

				Exp. limits		Producible at
$Z \to \gamma$ +	M	Branching fraction	Framework	2023	HL-LHC	FCC-ee
	η_c	$(9.5 \pm 0.2) \times 10^{-9}$	NRQCD (NNLO+NLL) [140]	–	–	✓
		$\left(1.32^{+0.56}_{-0.54}\right) \times 10^{-8}$	NRQCD+LDME [141]			
		$(7.42 \pm 0.61) \times 10^{-9}$	NRQCD (NLO+NLL) [142]			
		6.6×10^{-9}	NRQCD+LDME [143]			
		$(9.4 \pm 1.0) \times 10^{-9}$	LC+LCDA [143]			
	J/ψ	$\left(5.75^{+0.08}_{-0.09}\right) \times 10^{-8}$	NRQCD (NNLO+NLL) [140]	$< 6.0\times 10^{-7}$ [92, 134]	$\lesssim 3.1\times 10^{-7}$ [62]	✓
		$\left(1.04^{+0.18}_{-0.16}\right) \times 10^{-7}$	NRQCD+LDME [141]			
		$\left(8.96^{+1.51}_{-1.38}\right) \times 10^{-8}$	LC+LCDA [144]			
		4.5×10^{-8}	NRQCD+LDME [143]			
		$(8.8 \pm 0.9) \times 10^{-8}$	LC+LCDA [143]			
		$(9.96 \pm 1.86) \times 10^{-8}$	NRQCD+LDME [139]			
		$(8.02 \pm 0.45) \times 10^{-8}$	SCET+LCDA [45]			
$Z \to \gamma$ +	$\psi(2S)$		–	$< 1.3\times 10^{-6}$ [92, 134]	$\lesssim 1.0\times 10^{-7}$	✘
	χ_{c0}	$(3.74 \pm 0.05) \times 10^{-10}$	NRQCD+LDME [145]	–	–	✓
		1.4×10^{-10}	NRQCD+LDME [143]			
		$(5.0 \pm 2.0) \times 10^{-10}$	LC+LCDA [143]			
	χ_{c1}	$\left(2.383^{+0.014}_{-0.017}\right) \times 10^{-9}$	NRQCD+LDME [145]	–	–	✓
		8.7×10^{-10}	NRQCD+LDME [143]			
		$(5.6 \pm 2.0) \times 10^{-9}$	LC+LCDA [143]			
	h_c	$\left(3.487^{+0.206}_{-0.230}\right) \times 10^{-9}$	NRQCD+LDME [145]	–	–	✓
		3.0×10^{-9}	NRQCD+LDME [143]			
		$(1.0 \pm 0.4) \times 10^{-8}$	LC+LCDA [143]			
	χ_{c2}	$\left(3.38^{+0.19}_{-0.22}\right) \times 10^{-10}$	NRQCD+LDME [145]	–	–	✓
		2.9×10^{-10}	NRQCD+LDME [143]			
		$(1.0 \pm 0.4) \times 10^{-9}$	LC+LCDA [143]			

TABLE XIII. Compilation of exclusive Z decays to a photon plus a bottomonium state. For each decay, we provide the predicted branching fraction(s) and the theoretical approach used to compute it, as well as the current experimental upper limit and that estimated for HL-LHC. The last column indicates whether the decay can be produced at FCC-ee.

				Exp. limits		Producible at
$Z \to \gamma$ +	M	Branching fraction	Framework	2023	HL-LHC	FCC-ee
$Z \to \gamma$ +	η_b	$(2.43 \pm 0.01) \times 10^{-8}$	NRQCD (NNLO+NLL) [140]	–	–	✓
		$\left(2.79^{+0.20}_{-0.19}\right) \times 10^{-8}$	NRQCD+LDME [141]			
		$(2.8 \pm 0.5) \times 10^{-8}$	NRQCD (NLO+NLL) [142]			
	$\Upsilon(1S)$	$(4.63 \pm 0.02) \times 10^{-8}$	NRQCD (NNLO+NLL) [140]	$< 1.1\times 10^{-6}$ [93]	$\lesssim 1.7\times 10^{-7}$	✓
		$(5.41 \pm 0.39) \times 10^{-8}$	NRQCD+LDME [141]			
		$(5.61 \pm 0.29) \times 10^{-8}$	NRQCD+LDME [146]			
		$\left(4.8^{+0.3}_{-0.2}\right) \times 10^{-8}$	LC+LCDA [144]			
		$(4.93 \pm 0.51) \times 10^{-8}$	NRQCD+LDME [139]			
		$(5.39 \pm 0.16) \times 10^{-8}$	SCET+LCDA [45]			
	$\Upsilon(2S)$	$(2.66 \pm 0.31) \times 10^{-8}$	NRQCD+LDME [146]	$< 1.3\times 10^{-6}$ [93]	$\lesssim 2.0\times 10^{-7}$	✓
		$\left(2.44^{+0.14}_{-0.13}\right) \times 10^{-8}$	LC+LCDA [144]			
	$\Upsilon(3S)$	$(1.93 \pm 0.25) \times 10^{-8}$	NRQCD+LDME [146]	$< 2.4\times 10^{-6}$ [93]	$\lesssim 3.7\times 10^{-7}$	✓
		$\left(1.88^{+0.11}_{-0.10}\right) \times 10^{-8}$	LC+LCDA [144]			
	$\Upsilon(4S)$	$(1.22 \pm 0.13) \times 10^{-8}$	SCET+LCDA [45]	–	–	✓
	$\Upsilon(nS)$	$\left(9.96^{+0.28}_{-0.26}\right) \times 10^{-8}$	SCET+LCDA [45]	–	–	✓
	χ_{b0}	$\left(2.73^{+0.05}_{-0.04}\right) \times 10^{-10}$	NRQCD+LDME [145]	–	–	✓
	χ_{b1}	$\left(1.473^{+0.010}_{-0.011}\right) \times 10^{-9}$	NRQCD+LDME [145]	–	–	✓
	h_b	$\left(9.27^{+0.36}_{-0.41}\right) \times 10^{-10}$	NRQCD+LDME [145]	–	–	✓
	χ_{b2}	$\left(2.92^{+0.12}_{-0.14}\right) \times 10^{-10}$	NRQCD+LDME [145]	–	–	✓

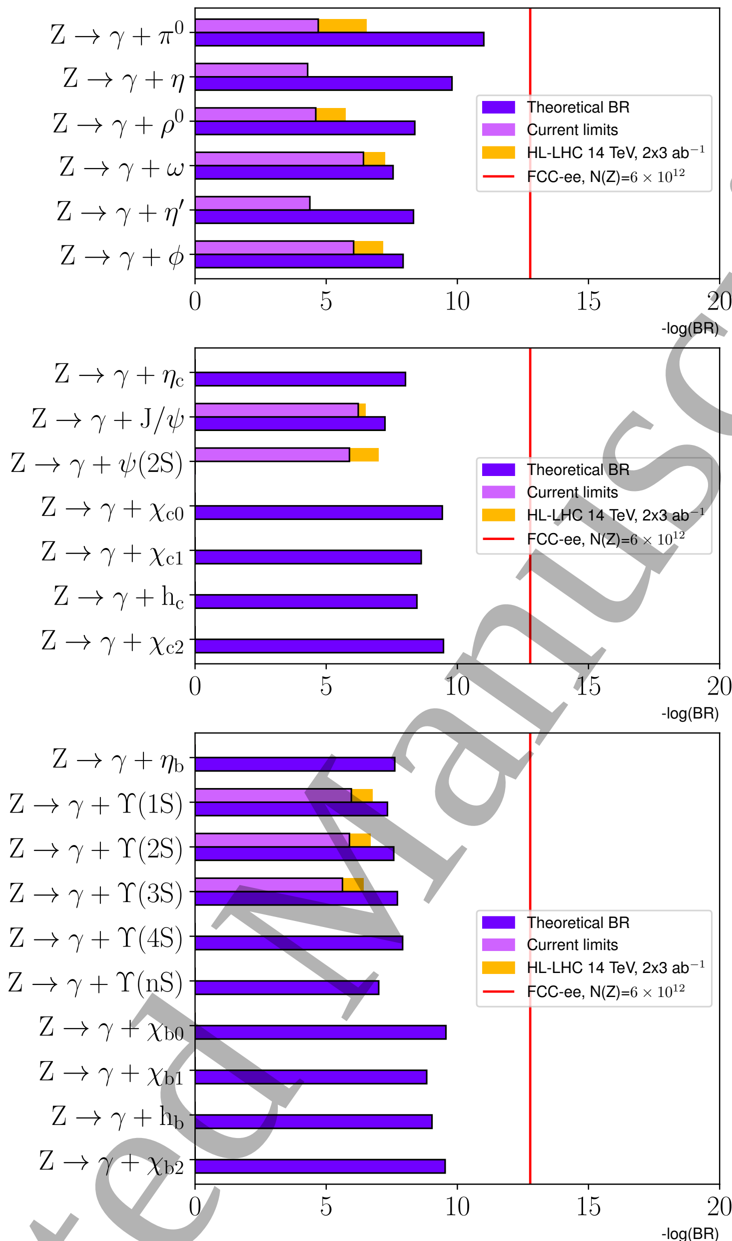

FIG. 15. Branching fractions (in negative log scale) of exclusive $Z \to \gamma + M$ decays, with M being light (upper), charm (middle), and bottom (lower) unflavoured mesons. The most recent theoretical predictions (blue bars) are compared to current experimental upper limits (violet) and expected HL-LHC bounds (orange). The red vertical line indicates the expected FCC-ee reach based only on the total number of Z bosons to be produced.

2. Z boson decays into a photon plus a flavoured meson

In the SM, the absence of direct FCNC decays of the Z boson implies that the only possible exclusive radiative Z boson decays into flavoured mesons can proceed through the (extremely suppressed) left diagram of Fig. 14. We are not aware of existing evaluations of the branching fractions for such exclusive decays in the SM, but only of indirect limits for them determined in Ref. [45] using different SM constraints. Therefore, we estimate the numerical value of these exclusive FCNC channels here next. The standard Lagrangian density describing the Z boson coupling to quarks is given by the interaction term

$$\mathcal{L}_{\mathrm{Z}\to\mathrm{q}\bar{\mathrm{q}}} \subset -\frac{e}{\sin\theta_{\mathrm{w}}\cos\theta_{\mathrm{w}}} Z^{\mu}\bar{q}\gamma_{\mu}(v_q - a_q\gamma_5)q, \tag{28}$$

with vector $v_q \equiv T_3^q/2 - Q_q\sin^2\theta_{\mathrm{w}}$ and axial $a_q \equiv T_3^q/2$ couplings of a quark of electric charge Q_q and third component of weak isospin T_3^q. One can extend this Lagrangian to include interactions between quarks of different generations, as follows

$$\mathcal{L}_{\mathrm{Z}\to\mathrm{q_i}\bar{\mathrm{q_j}}} \subset -\frac{e}{\sin\theta_{\mathrm{w}}\cos\theta_{\mathrm{w}}} Z^{\mu}\bar{q}_i\gamma_{\mu}(v_{ij} - a_{ij}\gamma_5)q_j, \tag{29}$$

where $i, j \in \{\mathrm{u, d, c, s, t, b}\}$. The offdiagonal interaction couplings $v_{i,j\neq i}$ and $a_{i,j\neq i}$ are zero in the SM, but are used here as an effective coupling to encode contributions from higher-order loop processes (such as those shown in Fig. 14, right), which can take on a very small value. The work [45] provides generic expressions for the calculation of partial widths of exclusive Z boson decays into a flavoured meson plus a photon in the SCET + LCDA framework, using offdiagonal quark couplings v_{ij}, a_{ij} as inputs. For arbitrary $\mathrm{q}_i\overline{\mathrm{q}_j}$ combinations, the decay width for the $\mathrm{Z}\to\mathrm{q}\bar{\mathrm{q}}'$ process can be written at tree level as

$$\Gamma_{\mathrm{Z}\to\mathrm{qq'}} = \frac{\alpha(m_{\mathrm{Z}})(|v_{\mathrm{qq'}}|^2 + |a_{\mathrm{qq'}}|^2)}{2m_{\mathrm{Z}}^5\cos^2\theta_{\mathrm{w}}\sin^2\theta_{\mathrm{w}}}\lambda^{1/2}\left(m_{\mathrm{Z}}^2, m_1^2, m_2^2\right)\left[2m_{\mathrm{Z}}^4 - m_1^4 - m_2^4 - m_2^2m_{\mathrm{Z}}^2 - m_1^2(m_{\mathrm{Z}}^2 - 2m_2^2)\right]. \tag{30}$$

where $\lambda(a,b,c) = a^2 + b^2 + c^2 - 2(ab + ac + bc)$ is the Källén function, and $m_{1,2}$ the quark masses. Ignoring quark masses ($m_1 = m_2 = 0$) and setting $v_{\mathrm{qq'}} = a_{\mathrm{qq'}}$, the equation above simplifies to

$$\Gamma_{\mathrm{Z}\to\mathrm{qq'}} = \frac{2\alpha(m_{\mathrm{Z}})m_{\mathrm{Z}}|v_{\mathrm{qq'}}|^2}{\sin^2\theta_{\mathrm{w}}\cos^2\theta_{\mathrm{w}}}. \tag{31}$$

Using this last expression, the numerical values of the effective couplings $v_{\mathrm{qq'}} = a_{\mathrm{qq'}}$ can now be estimated from the offdiagonal Z boson quark decay widths computed at NLO accuracy in [87]: $\Gamma_{\mathrm{Z}\to\bar{\mathrm{b}}\mathrm{s}} = 5.2\times10^{-8}$ GeV, $\Gamma_{\mathrm{Z}\to\bar{\mathrm{b}}\mathrm{d}} = 2.3\times10^{-9}$ GeV, $\Gamma_{\mathrm{Z}\to\bar{\mathrm{c}}\mathrm{u}} = 1.7\times10^{-18}$ GeV; and amount to

$$\begin{cases} |v_{\mathrm{bs}}|^2 = |a_{\mathrm{bs}}|^2 & \approx 6.6\times10^{-9} \\ |v_{\mathrm{bd}}|^2 = |a_{\mathrm{bd}}|^2 & \approx 2.9\times10^{-10} \\ |v_{\mathrm{cu}}|^2 = |a_{\mathrm{cu}}|^2 & \approx 2.2\times10^{-19}. \end{cases} \tag{32}$$

The decay $\mathrm{Z}\to\mathrm{sd}$ was first computed in [147], with vector and axial couplings equal since the photon contribution is zero, and with the offdiagonal coupling obtained via

$$v_{\mathrm{sd}} = a_{\mathrm{sd}} = \frac{\alpha(m_{\mathrm{Z}})}{16\pi\sin^2\theta_{\mathrm{w}}}\sum_{i=\mathrm{u,c,t}} V_{is}V_{id}^*\left[-\frac{3x_i}{1-x_i} + \frac{x_i^2}{2(1-x_i)} - \frac{3x_i^2\log(x_i)}{2(1-x_i)^2} - \frac{x_i\log(x_i)}{(1-x_i)^2}\right], \tag{33}$$

with $x_i = m_{\mathrm{q}_i}^2/m_{\mathrm{W}}^2$. Using the parameters of Table II, this coupling squared can be numerically evaluated as

$$|v_{\mathrm{sd}}|^2 = |a_{\mathrm{sd}}|^2 \approx 4.27\times10^{-13}. \tag{34}$$

Plugging in the values of the effective couplings (32) and (34) into the SCET + LCDA expressions of Ref. [45] enables us to determine the numerical branching fractions for Z-boson radiative decays to flavoured mesons listed in Table XIV. All such exclusive FCNC decays of the Z boson are extremely suppressed, amounting to $\mathcal{O}(10^{-15}\text{–}10^{-25})$. The experimentally negligible branching fractions for such decays make those interesting channels to search for BSM FCNC decays of the Z boson with a negligible SM background. Two decays have been experimentally searched-for to date: $\mathrm{Z}\to\gamma+\mathrm{D}^0$ [100, 136] and $\mathrm{Z}\to\gamma+\mathrm{K}_\mathrm{s}^0$ [100], where experimental limits are at the $\mathcal{O}(10^{-6})$ level, and can be improved by a factor of ~10 at the end of the HL-LHC phase as per our extrapolations here.

TABLE XIV. Compilation of exclusive Z decays to a photon plus a flavoured meson. For each decay, we provide the predicted branching fraction(s) and the theoretical approach used to compute it, as well as the current experimental upper limits (if any) and those estimated for HL-LHC. The last column indicates whether the decay can be produced at FCC-ee.

				Exp. limits		Producible at
$Z \to \gamma$ +	M	Branching fraction	Framework	2023	HL-LHC	FCC-ee
$Z \to \gamma$ +	K^0	3.3×10^{-20}	SCET+LCDA (this work)	$< 3.0\times 10^{-6}$ [100]	$\lesssim 4.5 \times 10^{-7}$	✘
	D^0	$< 1.0 \times 10^{-15}$	SCET+LCDA [45, 136]	$< 4.0\times 10^{-6}$ [100]	$\lesssim 6.0 \times 10^{-7}$	✘
		1.4×10^{-25}	SCET+LCDA (this work)			
	B^0	8.3×10^{-17}	SCET+LCDA (this work)	–	–	✘
	B^0_s	2.3×10^{-15}	SCET+LCDA (this work)	–	–	✘

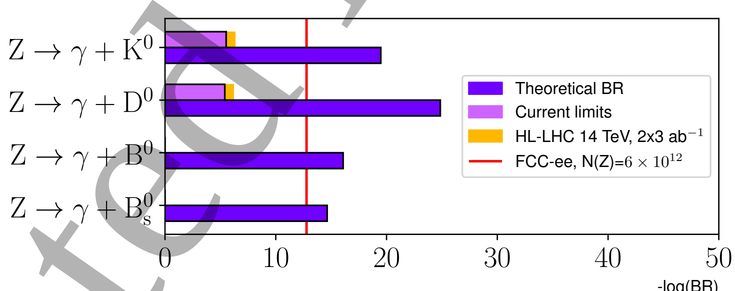

FIG. 16. Branching fractions (in negative log scale) of exclusive $Z \to \gamma + M$ decays, with M being a flavoured meson. The theoretical predictions computed here (blue bars) are compared to current experimental upper limits (violet) and expected HL-LHC bounds (orange). The red vertical line indicates the expected FCC-ee reach based only on the total number of Z bosons to be produced.

3. *Z boson triphoton decays*

As seen in Table X, the Z → 3γ decay is extremely suppressed in the SM ($\mathcal{B} = 6.4\cdot 10^{-10}$, as computed here) making of such a final state a particularly clean means to search for exotic Z decays into BSM particles with EW couplings. Many new physics scenarios contain new light (pseudo)scalar or tensor particles that couple to the electroweak (or Higgs) bosons and decay primarily to photons. Searches for $\mathrm{Z} \to \gamma\, a(\gamma\gamma)$, with a being an ALP [20, 148] or a graviton [21] decaying into photons, have attracted an increasing interest in the last years [19]. Figure 17 shows possible diagrams leading to the triphoton decay of the Z boson. The direct decay (left diagram) and the exclusive radiative decays into C-even mesons followed by their diphoton decays (center) can mimic the BSM processes signals (right), and constitute a background to the latter. The direct and mesonic backgrounds have been neglected so far in all ALP/graviton upper limits set in studies based on current and future triphoton Z decay data. Such an assumption is justified so far given the null sensitivity to such rare SM processes, but it will not be the case at the FCC-ee facility where, as we see below, a few thousands such events are expected during the whole Z-pole run. Here, we quantify the triphoton branching fractions from meson decays by combining the exclusive $\mathrm{Z} \to \gamma + \mathrm{M}$ results for spin-0,2 mesons of Tables XI–XIII with their corresponding two-photon branching fractions [60]. The results are listed in Table XV. The sum of all exclusive mesonic decay channels amounts to $\mathcal{B} = 1.8 \cdot 10^{-10}$, representing an increase of about 30% from the direct 3γ decay. The yields of SM triphoton decays will therefore amount to about 1 000 events for the $N(\mathrm{Z}) = 6 \cdot 10^{12}$ Z bosons expected to be collected during the full Z-pole operation at the FCC-ee. Searches for ALPs and gravitons will have to be carried out on top of such a relatively large number of background events that have been neglected so far in the derivation of ALP limits at future $\mathrm{e^+e^-}$ facilities [148].

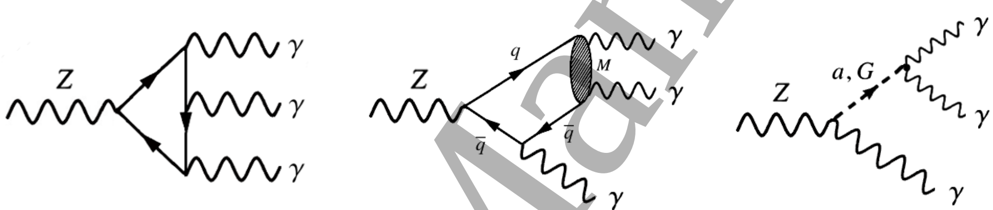

FIG. 17. Triphoton decays of the Z boson: SM direct decay (left), exclusive γ + meson($\gamma\gamma$) decay (center), radiative decay into a BSM (ALP or graviton) diphoton system (right).

TABLE XV. Compilation of exclusive Z decays into triphoton final states. The predictions of relevant $\mathrm{Z} \to \gamma + \mathrm{M}$ radiative decays listed in Tables XI–XIII are combined with the diphoton branching fractions of the produced mesons, $\mathrm{M} \to \gamma\gamma$ [60].

$\mathrm{Z} \to \gamma$	+	$\mathrm{M}(\gamma\gamma)$	Branching fraction
		$\pi^0(\gamma\gamma)$	9.7×10^{-12}
		$\eta(\gamma\gamma)$	6.3×10^{-11}
		$\eta'(\gamma\gamma)$	1.1×10^{-10}
		$\eta_c(\gamma\gamma)$	2.1×10^{-12}
$\mathrm{Z} \to \gamma$	+	$\chi_{c0}(\gamma\gamma)$	7.6×10^{-14}
		$\chi_{c1}(\gamma\gamma)$	1.5×10^{-14}
		$\chi_{c2}(\gamma\gamma)$	9.6×10^{-14}
		$\chi_{b0}(\gamma\gamma)$	1.6×10^{-14}
		$\chi_{b2}(\gamma\gamma)$	1.6×10^{-14}
Sum			1.8×10^{-10}
Z	$\longrightarrow$	$\gamma\gamma\gamma$	6.4×10^{-10}
Total			8.2×10^{-10}

4. *Z boson decays into a W boson plus a meson*

Table XVI lists the theoretical predictions for Z boson decays into a $W^{\pm}$ boson plus a charged vector meson (corresponding to the diagrams of Fig. 14 with W bosons in the final state). All branching fractions are in the 10^{-10}–10^{-11} range, and only two channels have been searched for in the Z-pole run at LEP. Experimental observation will only be possible at FCC-ee for all of them. The same results compiled in Table XVI are shown in graphical form in Fig. 18.

TABLE XVI. Compilation of exclusive Z decays to W plus a meson. For each decay, we provide the predicted branching fraction(s) and the theoretical approach used to compute it, as well as the current experimental upper limit and that estimated for HL-LHC. The last column indicates whether the decay can be produced at FCC-ee.

					Exp. limits		Producible at
$Z \to W$	+	M	Branching fraction	Framework	2023	HL-LHC	FCC-ee
$Z \to W^{\mp}$	+	$\pi^{\pm}$	$(1.51 \pm 0.01) \times 10^{-10}$	SCET+LCDA [45]	$< 7.0 \times 10^{-5}$ [137]	–	✓
		$\rho^{\pm}$	$(4.0 \pm 0.1) \times 10^{-10}$	SCET+LCDA [45]	$< 8.3 \times 10^{-5}$ [137]	–	✓
		$K^{\pm}$	$(1.16 \pm 0.01) \times 10^{-11}$	SCET+LCDA [45]	–	–	✓
		$K^{*\pm}$	$(1.96 \pm 0.12) \times 10^{-11}$	SCET+LCDA [45]	–	–	✓
		$D^{\pm}$	$(1.99 \pm 0.17) \times 10^{-11}$	SCET+LCDA [45]	–	–	✓
		$D_s^{\pm}$	$(6.04 \pm 0.30) \times 10^{-10}$	SCET+LCDA [45]	–	–	✓

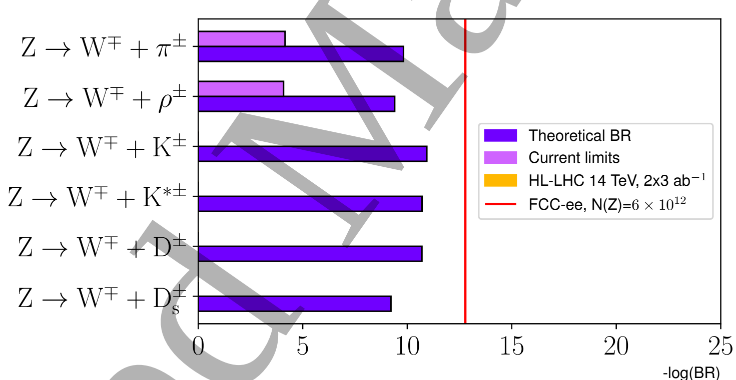

FIG. 18. Branching fractions (in negative log scale) of exclusive $Z \to W^{\pm}$ + meson decays. The most recent theoretical predictions (blue bars) are compared to current experimental upper limits (violet) and expected HL-LHC bounds (orange). The red vertical line indicates the expected FCC-ee reach based only on the total number of Z bosons to be produced.

C. Radiative Z boson leptonium decays

Figure 14 shows the diagrams for the decay of the Z boson into a photon plus a leptonium state. Depending on the relative helicities of the outgoing leptons, their bound state can be in the spin singlet (paraleptonium, $(\ell\ell)_0$) or triplet (ortholeptonium, $(\ell\ell)_1$) states. No calculation for such processes exists to our knowledge, but the key ingredients can be obtained from the determination of the $e^+e^- \to \gamma + (\tau^+\tau^-)_0$ cross section at the Z pole provided in the ditauonium studies of Ref. [149]. The motivations for their study are the same as for the similar Higgs decays, namely, the search for LFV or LFUV phenomena.

The leading-order partial decay width of a Z boson into a leptonium-plus-a-photon can be derived from the ratio of the $\sigma(e^+e^- \to \gamma + (\ell^+\ell^-))$ cross section at the Z pole over the total resonant Z boson cross section in e^+e^- collisions,

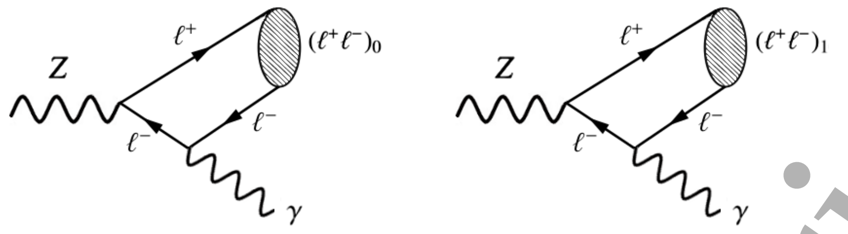

FIG. 19. Schematic diagrams of exclusive decays of the Z boson into para- (left) and ortho- (right) leptonium plus a photon. The solid fermion lines represent leptons, the gray blobs represent the leptonium bound state.

and amounts to

$$\mathcal{B}(\mathrm{Z} \to \gamma + (\ell^+\ell^-)_0) = \frac{\alpha(0)^4 \alpha(m_\mathrm{Z})^2}{9 \cdot 256\, n^3} \frac{m_{\ell\ell}^2}{m_\mathrm{Z}^2} \frac{\left(1 - 4s_w^2\right)^2 \left(8s_w^4 - 4s_w^2 + 1\right)\left(m_\mathrm{Z}^2 - m_{\ell\ell}^2\right)}{\Gamma_\mathrm{ee}\Gamma_\mathrm{Z} s_w^4 c_w^4} \tag{35}$$

for the paraleptonium case, and to

$$\mathcal{B}(\mathrm{Z} \to \gamma + (\ell^+\ell^-)_1) = \frac{\alpha(0)^4 \alpha(m_\mathrm{Z})^2}{9 \cdot 256\, n^3} \frac{m_{\ell\ell}^2}{m_\mathrm{Z}^4} \frac{\left(8s_w^4 - 4s_w^2 + 1\right)\left(m_\mathrm{Z}^4 - m_{\ell\ell}^4\right)}{\Gamma_\mathrm{ee}\Gamma_\mathrm{Z} s_w^4 c_w^4} \tag{36}$$

for the ortho-leptonium one, where n is the principal quantum number of the leptonium resonance, and $s_w \equiv \sin\theta_\mathrm{W}$, and $c_w \equiv \cos\theta_\mathrm{W}$ are the sine and cosine of the Weinberg angle (Table II). In both expressions above, $\alpha(0)$ and $\alpha(m_\mathrm{Z})$ are the electromagnetic coupling evaluated at zero[6] and at the Z pole mass, respectively, that, together with the rest of parameters, are listed in Table II. The obtained branching fractions are tabulated in Table XVII, and plotted in Fig. 20. The dependence of these Z-boson radiative rates on $\alpha^6 m_{\ell\ell}^2$, leads to vanishingly small branching fractions, $\mathcal{O}(10^{-13}$–$10^{-23})$, with ditauonium (positronium) featuring the largest (smallest) values. No experimental search has been conducted to date, although the relatively long lifetime of the leptonium objects (significantly boosted in the decay of the much heavier Z boson) would lead to a clean signature characterized by a displaced vertex from secondary decays of the $(\ell^+\ell^-)$ into photons, $\mathrm{e}^\pm$, and/or $\mu^\pm$ [110], akin to many BSM long-lived particles (but with an invariant mass at the corresponding leptonium mass). Given the negligible rates, only an FCC-ee run at the Z pole would be able to provide limits approaching the SM values for the $\mathrm{Z} \to \gamma\,(\tau^+\tau^-)_0$ case.

TABLE XVII. Compilation of exclusive Z decays into a photon plus a ground state ($n = 1$) of ortho- and para-leptonium. For each decay, we provide the prediction of its branching fraction computed via Eq. (35) or (36). The last column indicates whether the decay can be produced at FCC-ee.

$\mathrm{Z} \to \gamma\ +$	$(\ell\ell)$	Branching fraction	Framework	Exp. limits 2023	Exp. limits HL-LHC	Producible at FCC-ee
$\mathrm{Z} \to \gamma\ +$	$(\mathrm{ee})_1$	7.3×10^{-21}	(this work)	–	–	✘
	$(\mu\mu)_1$	3.1×10^{-16}	(this work)	–	–	✘
	$(\tau\tau)_1$	8.9×10^{-14}	(this work)	–	–	✘
	$(\mathrm{ee})_0$	4.7×10^{-23}	(this work)	–	–	✘
	$(\mu\mu)_0$	2.0×10^{-18}	(this work)	–	–	✘
	$(\tau\tau)_0$	5.7×10^{-16}	(this work)	–	–	✘

[6] The leptonium wavefunction is proportional to $\alpha(0)^3$, Eq. (18), which combined with the emission of a final-state onshell photon, gives the $\alpha(0)^4$ dependence shown in Eqs. (35) and (36).

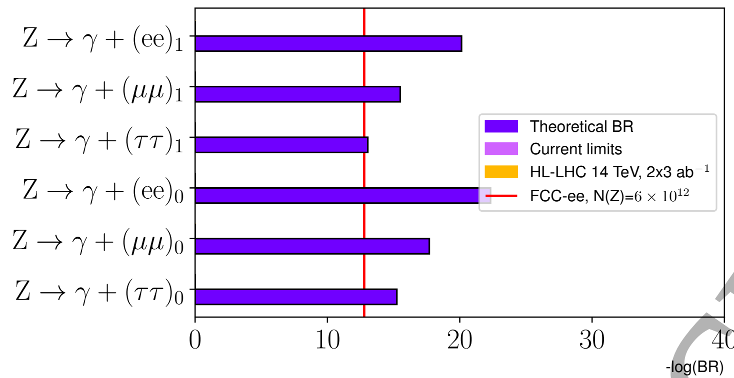

FIG. 20. Branching ratios (in negative log scale) of exclusive $Z \to \gamma$ + leptonium decays. Theoretical predictions computed here are shown as blue bars. The red vertical line indicates the expected FCC-ee reach based on the total number of Z bosons to be produced.

D. Exclusive Z boson decays into two mesons

Figure 21 displays the diagrams of exclusive Z boson decays into two mesons, with contributions from direct quark decays (left and center), as well as from indirect $V^* \to M$ transitions (right). Due to the coincidence of diagrams with those of the Higgs boson (Fig. 10), and since the Z boson yields at colliders are ~1000 times larger (Table I), the study of such processes provides valuable information for the corresponding Higgs rates. The two-body decays into the same pair of pseudo-scalar mesons, $Z \to M + M$, are quantum-mechanically forbidden due to the presence of two identical final-state particles and conservation of angular momentum (thus violating the spin-statistics theorem), but the mesons M can be in a vector state. The decays of Z bosons into double quarkonia, first studied in 1990 [150], have been investigated as a means to provide clean information on the quarkonium bound-state dynamics at large momentum transfers. As explained below, there is still a relatively large uncertainty in the theoretical predictions, but this is still the most promising place to search for exclusive double-charmonia/bottomonia decays.

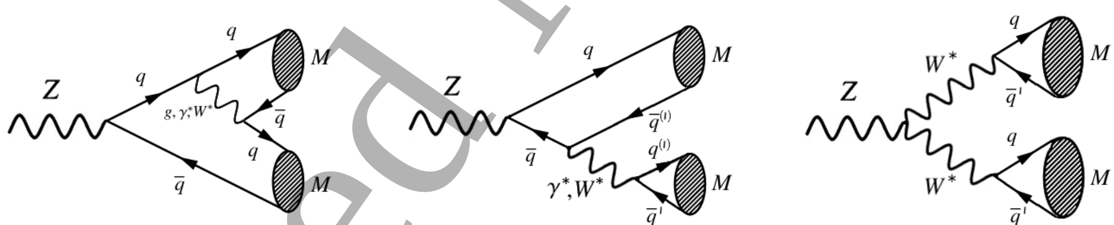

FIG. 21. Schematic diagrams of exclusive decays of the Z boson into two mesons. The solid fermion lines represent quarks, and the gray blobs the mesonic bound state.

To our knowledge, there are no calculations of exclusive decays of the Z boson involving light mesons, but only into charmonium and/or bottomonium states. We have evaluated here for the first time the double light vector meson decay $Z \to VM + VM$ via the two direct (left and center) diagrams of Fig. 21, using the EFT + NRQM formalism of [151] in which the width can be written as

$$\Gamma_{Z\to VM\,VM} = \Gamma^1_{VM\,VM}(1 + 2R + R^2), \tag{37}$$

where $\Gamma^1_{VM\,VM}$ is the partial width corresponding to the left diagram of Fig. 21, amounting to

$$\Gamma^1_{VM\,VM} = \frac{2048\pi^2\alpha(0)\alpha_s(m_Z)^2}{27c_w^2 s_w^2 m_Z^5}|\phi_{VM}(0)|^4\left(1 - \frac{4m^2_{VM}}{m^2_Z}\right)^{5/2}, \tag{38}$$

and where R is the ratio of the direct amplitudes $\mathcal{A}_1$ and $\mathcal{A}_2$ corresponding, respectively, to the left and center diagrams of Fig. 21, given by

$$R = \frac{\mathcal{A}_2}{\mathcal{A}_1} = -\frac{9Q_q^2\alpha(0)}{8\alpha_s(m_Z)}\frac{m_Z}{m_{VM}}. \tag{39}$$

For the light meson wavefunction at the origin $\phi_M(0)$ in Eq. (38), we derive it from its decay constant using the Van Royen–Weisskopf expression, Eq. (22), as follows

$$|\phi_{VM}(0)|^2 = \frac{m_{VM}f_{VM}^2}{4N_c}, \tag{40}$$

for $N_c = 3$ colours, and without higher-order QCD corrections. We can only estimate the rate for the $Z \to \phi+\phi$ channel because it is the only pure $|q\bar{q}\rangle$ state among the light mesons. Using Eqs. (37)–(40) and the parameters of Table II, we obtain a $\mathcal{B} = 2.1 \cdot 10^{-12}$ rate (Table XVIII). There is no $Z \to \phi + \phi$ experimental search performed to date, and only a machine like FCC-ee can provide enough Z bosons to start producing the decay. The table also quotes the forbidden $Z \to \pi^0+\pi^0$ channel, for which the CDF upper bound could be improved by a factor of 100 at the HL-LHC. To provide a reasonable evaluation for exclusive double decays into other light mesons, rotation from flavour eigenstates $|u\bar{u}\rangle$, $|d\bar{d}\rangle$ to physical eigenstates such as ρ, ω, η... would need to be performed. One can, however, anticipate branching fractions of the same order as the double-ϕ channel, $\mathcal{O}(10^{-12})$, since they only differ from a rotation and they are enhanced by the second and third diagram of Fig. 21 involving extra γ^*, W^* contributions. The scenario where Z decays into light pseudoscalar plus vector mesons suffers from the same complications of mixed states, but their rates are expected to be of the same order-of-magnitude as the double vector meson case because they have the same enhancing effect from the photon propagator contribution (Fig. 21, center) [151].

TABLE XVIII. Compilation of exclusive Z decays to a pair of light mesons. For the forbidden two-pion decay, we provide the current experimental upper limit. For the double-ϕ decay, we provide the branching fraction predicted using Eqs. (37)–(40). The last column indicates whether the decay can be produced at FCC-ee.

$Z \to$	M + M	Branching fraction	Framework	Exp. limits 2023	Exp. limits HL-LHC	Producible at at FCC-ee
$Z \to$	$\pi^0 + \pi^0$		–	$< 1.5\times 10^{-5}$ [130]	$\lesssim 2.1\times 10^{-7}$	✘
	$\phi + \phi$	2.1×10^{-12}	EFT+NRQM (this work)	–	–	✓

Tables XIX and XX list the theoretical predictions and experimental limits for concrete two-meson decay modes with pairs of charmonium mesons and bottomonium plus other mesons, respectively. The same results are shown in graphical form in Figs. 22 and 23. The decay rates are very small, $\mathcal{B}(Z \to M + M) \lesssim 10^{-10}$, and quite sensitive to the model details and ingredients. All heavy-quarkonium channels have rates obtained within the NRQCD + LDMEs formalism. Alternative LC calculations show a good agreement with the latter [38] but, unfortunately, they can only provide predictions for final states with different mesons or with mesons in different excited states. The NRQCD predictions from the work [38] show discrepancies with other later works, because they did not consider diagrams involving a photon propagator (Fig. 21, center) that can enhance the rates by more than two orders-of-magnitude. In contrast, this latter study provides results for some excited states that have not been calculated elsewhere (although their results for channels such as $Z \to \chi_{c1}+\chi_{c1}$, $\chi_{c2}+\chi_{c2}$, $\chi_{c0}+\chi_{c2}$,..., which cannot be predicted using LC formalism, may need to be revisited for the same reasons stated above). In addition, recent calculations including higher-order QED [152] and QCD + QED [153] corrections yield significant enhancements in the branching ratios for double-quarkonia production. All that said, and within the relatively large theoretical uncertainties for those processes, the largest branching fractions expected are for double-charmonium with $\mathcal{O}(10^{-10})$ rates. Despite a few searches carried out at LEP (and one at the LHC), experimental observation will only be possible at FCC-ee for about half of them.

TABLE XIX. Compilation of exclusive Z decays to two charmonium mesons. For each decay, we provide the predicted branching fraction(s) and the theoretical approach used to compute it, as well as the current experimental upper limit and that estimated for HL-LHC. The last column indicates whether the decay can be produced at FCC-ee.

						Exp. limits		Producible at
Z →	M	+	M	Branching fraction	Framework	2023	HL-LHC	at FCC-ee
Z →	η_c	+	J/ψ	$(1.5 \pm 0.4) \times 10^{-11}$	NRQCD/NRCSM [151]	–	–	✓
				$(1.8 - 2.7) \times 10^{-11}$	NRQCD+LDME (NLO) [152]			
				2.7×10^{-14}	NRQCD+LDME [38]			
			χ_{c0}	2.3×10^{-12}	NRQCD+LDME [38]	–	–	✓
				$(2.3 \pm 1.0) \times 10^{-12}$	LC+LCDA [38]			
			χ_{c1}	5.4×10^{-14}	NRQCD+LDME [38]	–	–	✘
			h_c	2.1×10^{-13}	NRQCD+LDME [38]	–	–	✓
				$(1.0 \pm 0.5) \times 10^{-12}$	LC+LCDA [38]			
			χ_{c2}	9.7×10^{-13}	NRQCD+LDME [38]	–	–	✓
				$(4.6 \pm 2.0) \times 10^{-12}$	LC+LCDA [38]			
	J/ψ	+	J/ψ	$(1.1 \pm 0.3) \times 10^{-10}$	NRQCD/NRCSM [151]	$< 1.1 \times 10^{-6}$ [106]	$\lesssim 1.7 \times 10^{-7}$	✓
				$\left(1.11^{+0.34}_{-0.24}\right) \times 10^{-10}$	NRQCD+LDME [153]			
				$(1.1 - 1.3) \times 10^{-10}$	NRQCD+LDME (NLO) [152]			
				2.3×10^{-14}	NRQCD+LDME [38]			
				2.7×10^{-11}	NRQCD [150]			
			χ_{c0}	$(1.1 - 4.1) \times 10^{-12}$	NRQCD+LDME (NLO) [152]	–	–	✓
				8.3×10^{-14}	NRQCD+LDME [38]			
				$(4.7 \pm 2.0) \times 10^{-13}$	LC+LCDA [38]			
			χ_{c1}	$(3.5 - 4.4) \times 10^{-12}$	NRQCD+LDME (NLO) [152]	–	–	✓
				3.5×10^{-15}	NRQCD+LDME [38]			
			h_c	1.5×10^{-12}	NRQCD+LDME [38]	–	–	✓
				$(9.5 \pm 5.0) \times 10^{-12}$	LC+LCDA [38]			
			χ_{c2}	$(9.6 - 24.8) \times 10^{-13}$	NRQCD+LDME (NLO) [152]	–	–	✓
				1.4×10^{-13}	NRQCD+LDME [38]			
				$(9.3 \pm 4.0) \times 10^{-13}$	LC+LCDA [38]			
	χ_{c0}	+	χ_{c1}	7.6×10^{-14}	NRQCD+LDME [38]	–	–	✘
				$(1.4 \pm 1.0) \times 10^{-12}$	LC+LCDA [38]			
			h_c	3.5×10^{-16}	NRQCD+LDME [38]	–	–	✘
			χ_{c2}	6.4×10^{-15}	NRQCD+LDME [38]	–	–	✘
	χ_{c1}	+	χ_{c1}	3.9×10^{-16}	NRQCD+LDME [38]	–	–	✘
			h_c	2.9×10^{-14}	NRQCD+LDME [38]	–	–	✘
				$(6.1 \pm 5.0) \times 10^{-13}$	LC+LCDA [38]			
			χ_{c2}	1.3×10^{-13}	NRQCD+LDME [38]	–	–	✘
				$(2.8 \pm 2.0) \times 10^{-12}$	LC+LCDA [38]			
	h_c	+	h_c	9.9×10^{-17}	NRQCD+LDME [38]	–	–	✘
			χ_{c2}	2.3×10^{-16}	NRQCD+LDME [38]	–	–	✘
	χ_{c2}	+	χ_{c2}	1.3×10^{-16}	NRQCD+LDME [38]	–	–	✘

FIG. 22. Branching fractions (in negative log scale) of exclusive Z boson decays into two light mesons (upper) or two charmonium mesons (lower). The most recent theoretical predictions (blue bars) are compared to current experimental upper limits (violet) and expected HL-LHC bounds (orange). The red vertical line indicates the expected FCC-ee reach based only on the total number of Z bosons to be produced.

TABLE XX. Compilation of exclusive Z decays to one bottomonium meson plus another meson (or anything else, in a few cases). For each decay, we provide the predicted branching fraction(s) and the theoretical approach used to compute it, as well as the current experimental upper limit and that estimated for HL-LHC. The last column indicates whether the decay can be produced at FCC-ee.

$Z \to$	M	+	M	Branching fraction	Framework	Exp. limits 2023	HL-LHC	Producible at at FCC-ee
$Z \to$	J/ψ	+	$\Upsilon(1S)$	4.6×10^{-11}	NRQCD [150]	–	–	✓
	$\eta_b(1S)$	+	$\Upsilon(1S)$	$(1.9 \pm 0.2) \times 10^{-11}$	NRQCD/NRCSM [151]	–	–	✓
	$\Upsilon(1S)$	+	$\Upsilon(1S)$	$\left(4.4^{+0.6}_{-0.3}\right) \times 10^{-13}$	NRQCD/NRCSM [151]	$< 1.8\times 10^{-6}$ [106]	$\lesssim 2.7\times 10^{-7}$	✓
	$\Upsilon(mS)$	+	$\Upsilon(nS)$	2.1×10^{-12}	NRQCD [150]	$< 3.9\times 10^{-7}$ [106]	$\lesssim 5.9\times 10^{-8}$	✓
$Z \to$	$\Upsilon(1S)$	+	X	$(2.6 - 2.9) \times 10^{-6}$	NRQCD+LDME (NLO) [154]	$< 4.4\times 10^{-5}$ [155]	–	✓
	$\Upsilon(2S)$	+	X	$(3.7 - 4.3) \times 10^{-6}$	NRQCD+LDME (NLO) [154]	$< 1.4\times 10^{-4}$ [156]	–	✓
	$\Upsilon(3S)$	+	X	$(7.6 - 8.3) \times 10^{-6}$	NRQCD+LDME (NLO) [154]	$< 9.4\times 10^{-5}$ [156]	–	✓
	$\Upsilon(nS)$	+	X	$(1.4 - 1.5) \times 10^{-5}$	NRQCD+LDME (NLO) [154]	$(1.0 \pm 0.5)\times 10^{-4}$ [157]	–	✓

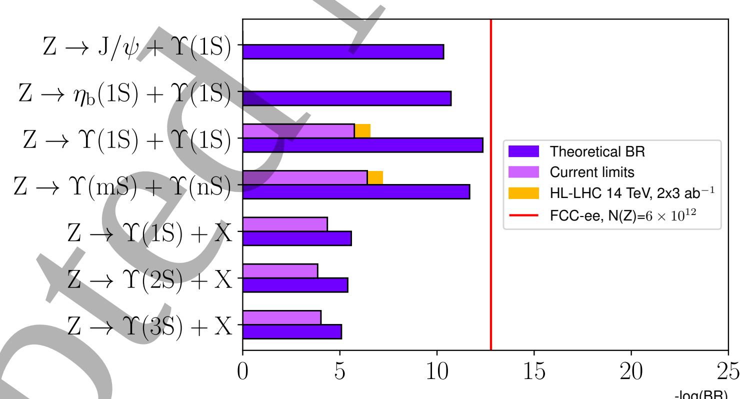

FIG. 23. Branching fractions (in negative log scale) of exclusive $Z \to$ b-meson + X decays. The most recent theoretical predictions (blue bars) are compared to current experimental upper limits (violet) and expected HL-LHC bounds (orange). The red vertical line indicates the expected FCC-ee reach based only on the total number of Z bosons to be produced.

V. RARE W BOSON DECAYS

A. Exclusive W decays into a photon plus a meson

Figure 24 displays the two generic diagrams contributing to exclusive decays of a W boson into a photon (the only gauge boson kinematically accessible for the least massive weak boson) plus a meson. Table XXI compiles the corresponding theoretical predictions and experimental limits for branching ratios of the eight radiative exclusive decay modes considered to date. The theoretical branching fractions are in the $\mathcal{O}(10^{-8}\text{–}10^{-12})$ range, whereas current experimental upper bounds are three to five orders-of-magnitude larger, $\mathcal{O}(10^{-4}\text{–}10^{-6})$. Four channels have been searched for to date at the LHC (3 by CMS, 1 by ATLAS, and 1 by LHCb), and the HL-LHC will improve the existing limits by about one order-of-magnitude, but still far from any possible observation. The FCC-ee will be able to produce events for three decay modes, and the FCC-hh will produce all of them. The results listed in Table XXI are presented in graphical form in Fig. 25.

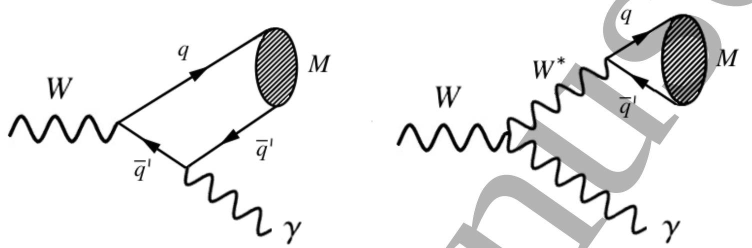

FIG. 24. Schematic diagrams of exclusive decays of the W bosons into a photon plus a meson. The solid fermion lines represent quarks, and the gray blobs represent the mesonic bound state.

TABLE XXI. Compilation of exclusive W decays to a photon plus a meson. For each decay, we provide the predicted branching fraction(s) and the theoretical approach used to compute it, as well as the current experimental upper limit and that estimated for HL-LHC. The last two columns indicate whether the decay can be produced at FCC-ee/FCC-hh.

				Exp. limits		Producible at	
$W^\pm \to \gamma\ +$	M	Branching fraction	Framework	2023	HL-LHC	FCC-ee	FCC-hh
$W^\pm \to \gamma\ +$	$\pi^\pm$	$(4.0 \pm 0.8) \times 10^{-9}$	SCET+LCDA [45]	$< 1.9\times 10^{-6}$ [158, 159]	$\lesssim 2.9\times 10^{-7}$	✓	✓
	$\rho^\pm$	$(8.74 \pm 1.91) \times 10^{-9}$	SCET+LCDA [45]	$< 5.2\times 10^{-6}$ [158]	$\lesssim 7.9\times 10^{-7}$	✓	✓
	$K^\pm$	$(3.25 \pm 0.69) \times 10^{-10}$	SCET+LCDA [45]	$< 1.7\times 10^{-6}$ [158]	$\lesssim 2.6\times 10^{-7}$	✘	✓
	$K^{*\pm}$	$(4.78 \pm 1.15) \times 10^{-10}$	SCET+LCDA [45]	–	–	✘	✓
	$D^\pm$	$\left(1.38^{+0.51}_{-0.33}\right) \times 10^{-9}$	SCET+LCDA [45]	–	–	✘	✓
	$D_s^\pm$	$\left(3.66^{+1.49}_{-0.85}\right) \times 10^{-8}$	SCET+LCDA [45]	$< 6.5\times 10^{-4}$ [136]	$\lesssim 1.2\times 10^{-5}$	✓	✓
		4.7×10^{-9}	NRQCD+LDME [160]				
		3.4×10^{-9}	LC+LCDA [160]				
	$D_s^{*\pm}$	8.9×10^{-10}	NRQCD+LDME [160]	–	–	✘	✓
		3.4×10^{-9}	LC+LCDA [160]				
	$B^\pm$	$\left(1.55^{+0.79}_{-0.60}\right) \times 10^{-12}$	SCET+LCDA [45]	–	–	✘	✓
		$\left(2.616^{+3.146}_{-1.330}\right) \times 10^{-12}$	HQET+LCDA [161]				
		$\left(1.99^{+2.49}_{-0.82}\right) \times 10^{-12}$	SCET+LCDA[a] [161]				

[a] updated inputs from [161] for the result from [45]

B. Exclusive W decays into two mesons

Figure 26 shows the schematic diagrams of the exclusive decay of the W boson into two mesons proceeding through quark decays (left and center), or through intermediate W^*, $\gamma^* \to$ M transitions (right). Table XXII lists the corre-

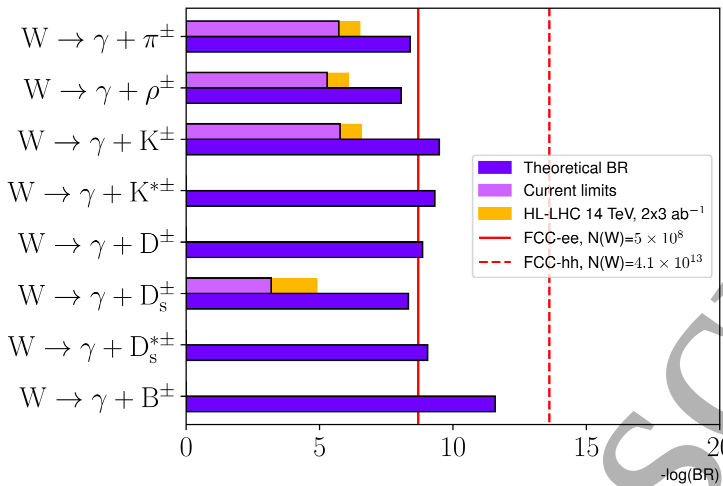

FIG. 25. Branching ratios (in negative log scale) of exclusive $W^{\pm} \to \gamma$ + meson decays. Most recent theoretical predictions (blue bars) are compared to current experimental upper limits (violet) and expected HL-LHC bounds (orange). The red vertical lines indicate the FCC-ee (solid) and FCC-hh (dashed) reach based only on the total number of W bosons to be produced at both machines.

sponding theoretical predictions and experimental limits for concrete decay modes, all of them involving charm and/or bottom quarks mesons. We are not aware of any study of exclusive W-boson decays involving one or two light mesons in the literature[7]. The expected rates are truly tiny, of order $\mathcal{O}(10^{-11}$–$10^{-14})$, with relatively large uncertainties. The work of [163] compared the branching fractions predicted within two approaches (LC and NRCSM), which differ by factors of 5–10, whereas Ref. [160] computed those within the NRQCD framework. For decays with a small ratio m_M/m_W, the results from the LC approach should be preferable. Differences among predictions for the same process appear in some cases as due to not consistently considering all diagrams of Fig. 26. The effect of the center diagram in Fig. 26 was partially discussed in [163], but none of the two theoretical works that have so far studied these processes, has considered the rightmost diagram of Fig. 26. Experimentally, none of the listed decays has been searched for at LEP, Tevatron, or the LHC to date. Only FCC-hh has possibilities to produce about eight decay channels (Fig. 27), but the expected tiny rates seemingly preclude their observation in the complex hadron-collider environment.

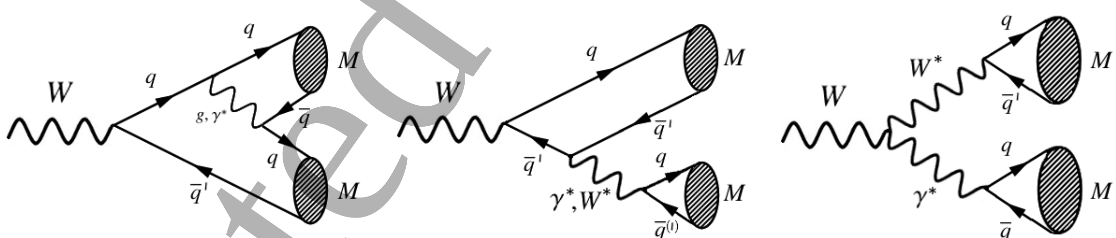

FIG. 26. Schematic diagrams of exclusive decays of the W boson into two mesons. The solid fermion lines represent quarks, and the gray blobs the mesonic bound state.

[7] The exclusive three-pion decay, $W^{\pm} \to \pi^+\pi^-\pi^{\pm}$, estimated to have a $\mathcal{B} \approx 10^{-7}$ [162], has been however searched-for by the CMS experiment at the LHC [135].

TABLE XXII. Compilation of exclusive W decays into two mesons. For each decay, we provide the predicted branching fraction(s) and the theoretical approach used to compute it. The last two columns indicate whether the decay can be produced at FCC-ee/FCC-hh.

						Exp. limits		Producible at	
$W^\pm \to$	M	+	M	Branching fraction	Framework	2023	HL-LHC	FCC-ee	FCC-hh
$W^\pm \to$	η_c	+	$D_s^\pm$	2.1×10^{-12}	NRCSM+LCDA [163]	–	–	✘	✓
				$\left(1.31^{+0.34}_{-0.22}\right)\times10^{-11}$	LC+LCDA [163]				
			$D_s^{*\pm}$	3.0×10^{-12}	NRCSM+LCDA [163]	–	–	✘	✓
				$\left(1.48^{+0.36}_{-0.22}\right)\times10^{-11}$	LC+LCDA [163]				
	J/ψ	+	$D_s^\pm$	2.6×10^{-12}	NRQCD+LDME [160]	–	–	✘	✓
				2.1×10^{-12}	NRCSM+LCDA [163]				
				$\left(1.8^{+0.4}_{-0.2}\right)\times10^{-11}$	LC+LCDA [163]				
			$D_s^{*\pm}$	1.7×10^{-12}	NRQCD+LDME [160]	–	–	✘	✓
				3.0×10^{-12}	NRCSM+LCDA [163]				
				$\left(2.03^{+0.46}_{-0.24}\right)\times10^{-11}$	LC+LCDA [163]				
	$\psi(2S)$	+	$D_s^\pm$	5.1×10^{-11}	NRQCD+LDME [160]	–	–	✘	✓
			$D_s^{*\pm}$	7.4×10^{-12}	NRQCD+LDME [160]	–	–	✘	✓
	χ_{c0}	+	$D_s^\pm$	9.4×10^{-14}	NRQCD+LDME [160]	–	–	✘	✓
				4.7×10^{-14}	NRCSM+LCDA [163]				
				$\left(7.1^{+3.5}_{-3.1}\right)\times10^{-13}$	LC+LCDA [163]				
			$D_s^{*\pm}$	1.2×10^{-13}	NRQCD+LDME [160]	–	–	✘	✓
				8.1×10^{-14}	NRCSM+LCDA [163]				
				$\left(8.0^{+3.7}_{-3.1}\right)\times10^{-13}$	LC+LCDA [163]				
	χ_{c1}	+	$D_s^\pm$	2.0×10^{-13}	NRQCD+LDME [160]	–	–	✘	✓
				2.9×10^{-13}	NRCSM+LCDA [163]				
				$\left(7.83^{+3.40}_{-3.05}\right)\times10^{-12}$	LC+LCDA [163]				
			$D_s^{*\pm}$	2.0×10^{-13}	NRQCD+LDME [160]	–	–	✘	✓
				4.0×10^{-13}	NRCSM+LCDA [163]				
				$\left(8.83^{+3.50}_{-3.06}\right)\times10^{-12}$	LC+LCDA [163]				
	h_c	+	$D_s^\pm$	1.4×10^{-13}	NRCSM+LCDA [163]	–	–	✘	✓
				$\left(2.13^{+0.97}_{-0.83}\right)\times10^{-12}$	LC+LCDA [163]				
			$D_s^{*\pm}$	2.0×10^{-13}	NRCSM+LCDA [163]	–	–	✘	✓
				$\left(2.4^{+1.1}_{-0.9}\right)\times10^{-12}$	LC+LCDA [163]				
	χ_{c2}	+	$D_s^\pm$	3.9×10^{-14}	NRQCD+LDME [160]	–	–	✘	✓
				9.6×10^{-14}	NRCSM+LCDA [163]				
				$\left(1.42^{+0.62}_{-0.53}\right)\times10^{-12}$	LC+LCDA [163]				
			$D_s^{*\pm}$	3.9×10^{-14}	NRQCD+LDME [160]	–	–	✘	✓
				1.4×10^{-13}	NRCSM+LCDA [163]				
				$\left(1.6^{+0.7}_{-0.6}\right)\times10^{-12}$	LC+LCDA [163]				
	B_s^0	+	$B_c^{*\pm}$	2.0×10^{-12}	NRQCD+LDME [160]	–	–	✘	✓
			$B_c^\pm$	2.5×10^{-12}	NRQCD+LDME [160]	–	–	✘	✓
	B_s^*	+	$B_c^{*\pm}$	2.7×10^{-12}	NRQCD+LDME [160]	–	–	✘	✓
			$B_c^\pm$	2.7×10^{-12}	NRQCD+LDME [160]	–	–	✘	✓

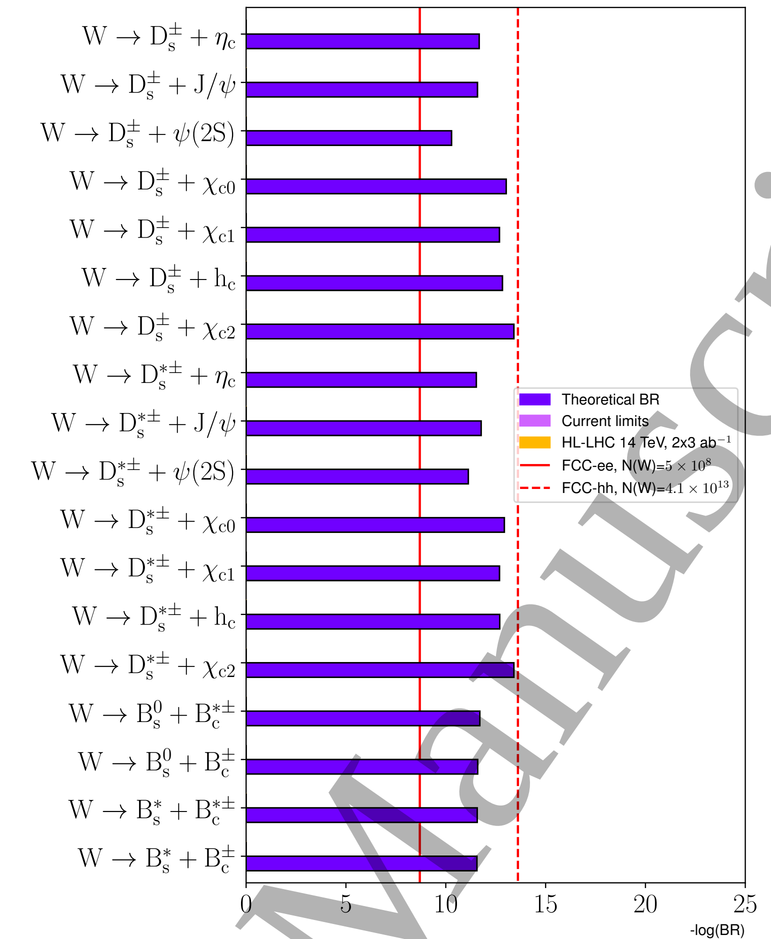

FIG. 27. Branching fractions (in negative log scale) of exclusive $W^\pm \to$ meson + meson decays: Most recent theoretical predictions are shown as blue bars. The red vertical lines indicate the FCC-ee (solid) and FCC-hh (dashed) reach based only on the total number of W bosons expected at both facilities.

VI. RARE TOP QUARK DECAYS

A. Two-body top quark decays

The top quark decays to a W boson and a bottom quark, t → W b, with a branching fraction of nearly 100%, with the other tree-level decays t → W s and t → W d comparatively suppressed by factors of 10^{-3} and 10^{-4}, respectively, as per the CKM element hierarchy $V_{tb} \gg V_{ts} > V_{td}$ (Table II). The FCNC top-quark decays to a gauge boson plus a light up-type quark (q = u or c; for charge conservation), t → q Z, t → γ c, and t → g c, occur only at the level of quantum loop corrections (Fig. 28), and are extremely suppressed in the SM. More precisely, they are 1-loop-, CKM-, and GIM-suppressed (with a GIM suppression factor[8] given by $f(m_b^2/m_W^2) \approx 10^{-9}$), leading to tiny amplitudes. In many BSM models, however, the GIM suppression can be relaxed, and one-loop diagrams mediated by new bosons may also contribute, yielding effective couplings orders of magnitude larger, and correspondingly enhancing such ultrarare branching fractions [27, 28].

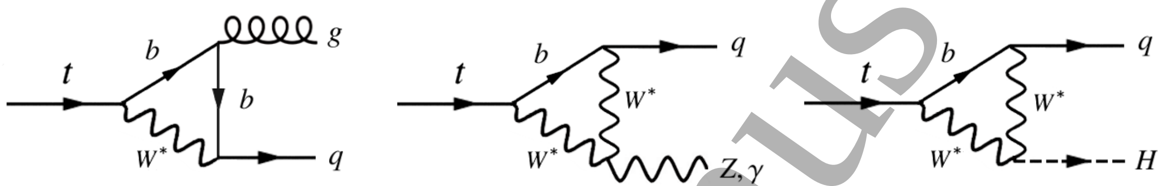

FIG. 28. Schematic diagrams of rare FCNC two-body decays of the top quark into a gauge (g, Z, or γ) boson or a Higgs boson plus an up-type quark (q = c, u).

TABLE XXIII. Compilation of rare two-body top quark decays. For each decay, we provide the predicted branching fraction(s) and the theoretical approach used to compute it, as well as the current experimental upper limit and that estimated for HL-LHC. The last two columns indicate whether the decay can be produced at FCC-ee/FCC-hh.

					Exp. limits		Producible at	
t →	V +	q	Branching fraction	Framework	2023	HL-LHC	FCC-ee	FCC-hh
t →	γ +	c	$(4.55 \pm 0.23) \times 10^{-14}$	NLO SM [164]	$< 4.0\times 10^{-4}$ [165]	$\lesssim 5.2 \times 10^{-5}$ [64]	✘	✘
			$\left(4.6^{+2.0}_{-1.0}\right) \times 10^{-14}$	NLO SM [28]				
		u	$(3.26 \pm 0.34) \times 10^{-16}$	NLO SM [164]	$< 8.9\times 10^{-5}$ [165]	$\lesssim 6.1 \times 10^{-6}$ [64]	✘	✘
			3.7×10^{-16}	NLO SM [28]				
	g +	c	$(5.31 \pm 0.27) \times 10^{-12}$	NLO SM [164]	$< 4.1\times 10^{-4}$ [166]	$\lesssim 2.3 \times 10^{-5}$ [64]	✘	✓
			$\left(4.6^{+3.0}_{-1.0}\right) \times 10^{-12}$	NLO SM [28]				
			5.7×10^{-12}	NLO SM [167]				
		u	$(3.81 \pm 0.34) \times 10^{-14}$	NLO SM [164]	$< 2.0\times 10^{-5}$ [166]	$\lesssim 2.7 \times 10^{-6}$ [64]	✘	✘
			3.7×10^{-14}	NLO SM [28]				
	Z +	c	1.0×10^{-14}	NLO SM [28]	$< 2.4\times 10^{-4}$ [133]	$\lesssim 2.3 \times 10^{-5}$ [65]	✘	✘
		u	8.0×10^{-17}	NLO SM [28]	$< 1.7\times 10^{-4}$ [133]	$\lesssim 7.3 \times 10^{-6}$ [65]	✘	✘
	H +	c	$\left(4.19^{+1.09}_{-0.86}\right) \times 10^{-15}$	NLO SM [168]	$< 7.3\times 10^{-4}$ [169]	$\lesssim 8.5 \times 10^{-5}$ [66]	✘	✘
			3.0×10^{-15}	NLO SM [28]				
		u	$\left(3.66^{+1.15}_{-0.97}\right) \times 10^{-17}$	NLO SM [168]	$< 1.9\times 10^{-4}$ [169]	$\lesssim 8.5 \times 10^{-5}$ [66]	✘	✘
			2.0×10^{-17}	NLO SM [28]				

[8] Theoretically, the b-quark running mass must be evaluated at the top pole mass scale (at which the t quark decays) in the $\overline{\text{MS}}$ scheme, otherwise rates are artificially enhanced.

Table XXIII lists the branching fractions of FCNC top decays, and Fig. 29 displays them graphically. The predicted SM rates are tiny, $\mathcal{O}(10^{-12}$–$10^{-17})$, and very sensitive to the value of the b-quark mass used to calculate them[8]. The decay branching fractions $\mathrm{t} \to \mathrm{Z\,q}$, $\mathrm{t} \to \gamma\,\mathrm{q}$, $\mathrm{t} \to \mathrm{g\,q}$, $\mathrm{t} \to \mathrm{H\,q}$, are further suppressed for q = u compared to the q = c case, by a CKM factor $(|V_{\mathrm{ub}}|/|V_{\mathrm{cb}}|)^2 \approx 0.008$. Experimentally, FCNC decays of the top quark have attracted lots of interest in the quest for BSM phenomena at the LHC, and all eight channels have been searched for. The current experimental upper limits are set in the $\mathcal{O}(10^{-4}$–$10^{-5})$ range, and will be improved by about a factor of ten at the end of the HL-LHC. In the absence of BSM effects enhancing such FCNC top decays, only the FCC-hh will reach top production rates capable of probing the $\mathrm{t} \to \mathrm{g\,c}$ decay.

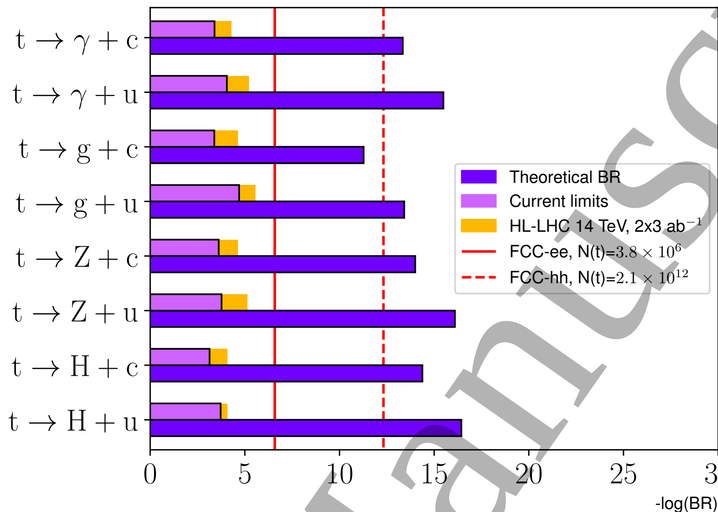

FIG. 29. Branching fractions (in negative log scale) of rare two-body $\mathrm{t} \to \mathrm{V+q}, \mathrm{H+q}$ decays (with V = gauge boson, and q = u, c). The most recent theoretical predictions (blue bars) are compared to current experimental upper limits (violet) and expected HL-LHC bounds (orange). The red vertical lines indicate the FCC-ee (solid) and FCC-hh (dashed) reach based only on the total number of top quarks expected at both facilities.

B. Three-body top quark decays

Thanks to its large mass, the top quark has different rare decays kinematically accessible involving the presence of multiple heavy bosons in the final state [27, 170]. The possibility of 3-body radiative decays of the top quark $\mathrm{t} \to \mathrm{W\,b\,X}$, where X can be a Z or a Higgs boson has been considered, e.g., in Refs. [171–173] (the cases $\mathrm{X} = \gamma, \mathrm{g}$ are simply NLO real QED or QCD corrections to the dominant tW b decay, for which one needs also an energy threshold to avoid infrared/collinear divergences in the decay rates, and not considered here as they are not rare). The corresponding diagrams are shown in Fig. 30. Properly taking into account the finite width effects is key to compute any close-to-threshold 3-body decays with (partially) offshell particles [167, 173].

Table XXIV collects the branching fractions for rare three-body decays of the top quark, and Fig. 31 presents them in graphical form. No experimental search has been performed to date. By an amusing coincidence, the $\mathrm{t} \to \mathrm{Z\,W\,b}$ decay is kinematically allowed because $m_{\mathrm{t}} \approx (m_{\mathrm{W}} + m_{\mathrm{b}}) + m_{\mathrm{Z}}$ to within a few GeV, which can be satisfied within the $\mathcal{O}(2\ \mathrm{GeV})$ widths of the onshell electroweak bosons (Table II). The corresponding branching fraction is $\mathcal{B}(\mathrm{t} \to \mathrm{Z\,W\,b}) \approx 2 \cdot 10^{-6}$ and, although no experimental limits exist yet from the LHC data, it could be potentially discovered at the HL-LHC, and for sure observed at FCC-ee and FCC-hh. The branching fraction of $\mathrm{t} \to \mathrm{H\,W\,b}$, first evaluated in [174], has been recomputed here at NLO using MG5_aMC (via $\mathrm{t} \to \mathrm{H\,W^*}(\mu\nu)\mathrm{b}$, with $m_{\mathrm{b}}(m_{\mathrm{t}}) = 2.6$ GeV) with the parameters listed in Table II, and found to be $\mathcal{B} = 1.6 \cdot 10^{-9}$. Other decays are highly GIM-suppressed (Fig. 30, bottom) and have much smaller rates. The $\mathrm{t} \to \mathrm{ZZq}$ is below $\mathcal{O}(10^{-13})$, and is likely impossible to observe anywhere unless some BSM mechanism enhances it. The top quark can also decay into three up-type quarks, either through the same diagrams shown in Fig. 28 where the emitted boson further decays/splits into $\mathrm{u\bar{u}}$ or $\mathrm{c\bar{c}}$, or through a virtual W boson exchange. This process is dominated by the gluon splitting into two up-type quarks shown in the Fig. 30 (lower right panel), and has a decay rate of $\mathcal{O}(10^{-12})$ [175] commensurate with that of the "parent" $\mathrm{t} \to \mathrm{u\,g}$ two-body decay (Table XXIII).

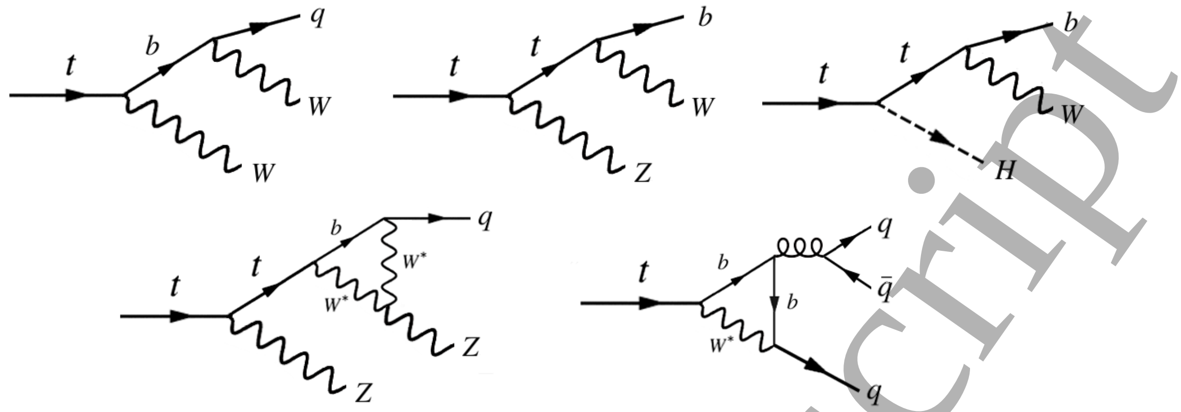

FIG. 30. Representative diagrams of rare three-body decays of the top quark into a pair of bosons plus a quark at tree-level (upper), and via loops into ZZq (lower left) and into three quarks (lower right). The outgoing quarks are either b, or up-type quarks (q = c, u), by charge conservation.

TABLE XXIV. Compilation of rare three-body top quark decays ($u_{1,2}$ = u, c quarks). For each decay, we provide the predicted branching fraction(s) and the theoretical approach used to compute it. The last two columns indicate whether the decay can be produced at FCC-ee/FCC-hh.

								Exp. limits		Producible at	
t →	X	+	Y	+	Z	Branching fraction	Framework	2023	HL-LHC	FCC-ee	FCC-hh
	W^+	+	W^-	+	c	1.0×10^{-13}	LO SM [27]	–	–	✘	✘
						2.0×10^{-13}	LO SM [176]				
	Z	+	W^+	+	b	1.8×10^{-6}	LO SM [177]	–	–	✓	✓
						$\left(5.4^{+4.7}_{-2.0}\right)\times10^{-7}$	LO SM [178]				
t →						2.0×10^{-6}	LO SM [173]				
	H	+	W^+	+	b	1.8×10^{-9}	LO SM [174]	–	–	✘	✓
						1.6×10^{-9}	NLO SM, MG5_aMC (this work)				
	Z	+	Z	+	c	$<1.0\times10^{-13}$	LO SM [176]	–	–	✘	✘
	u_1	+	u_2	+	$\bar{u}_2$	3.4×10^{-12}	NLO SM [175]	–	–	✘	✓

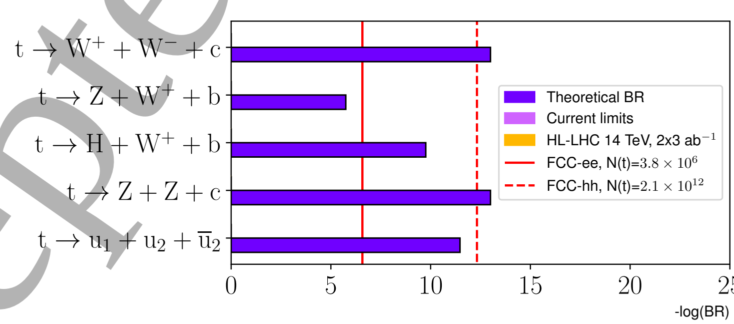

FIG. 31. Branching fractions (in negative log scale) of rare three-body top quark decays: Most recent theoretical predictions are shown as blue bars. The red vertical lines indicate the FCC-ee (solid) and FCC-hh (dashed) reach based only on the total number of top quarks expected at both facilities.

C. Semiexclusive top quark decays into a quark plus a meson

There are also theoretical studies of semiexclusive top quark decays in which interactions among the decay quarks (either from the W decay, or combining the primary bottom quark with the W-decay quarks) lead to the formation of final states with one meson recoiling against a jet [26, 179–181]. Such decays can provide a new method to measure the top-quark mass via a two-body (jet-meson) invariant mass analysis, with different systematic uncertainties of those of the currently existing approaches [26]. Typical diagrams for the process are shown in Fig. 32 with the meson recoiling against a q = u, c quark (right), or against a b quark (left).

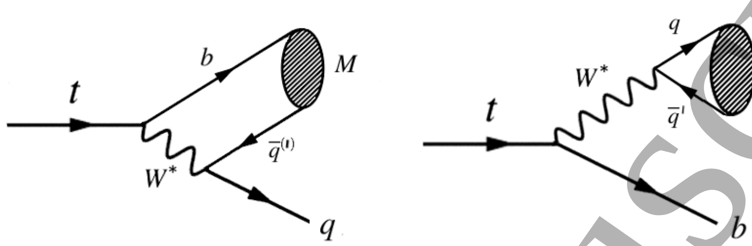

FIG. 32. Schematic diagrams of semiexclusive two-body decays of the top quark into a meson plus a q = c, u quark (left) or a b quark (right).

Branching fractions are listed in Table XXV for a bottom meson plus a c or u quark. The results of this table are shown in graphical form in Fig. 33. Theoretical branching fractions are in the $\mathcal{O}(10^{-5}$–$10^{-12})$ range. No experimental study has been performed to date. The combined $t \to B_{(s)} + u/c$ decays have a relatively large rate of $\mathcal{B} \approx 10^{-4}$, that makes them worth an experimental search at the LHC. Dedicated studies exist that prove the feasibility to observe them via t → b-jet + c-jet at the HL-LHC [26]. Four channels are producible at FCC-ee, and all of them can be produced at FCC-hh.

TABLE XXV. Compilation of exclusive decays of the top quark into a c or u quark plus a meson. For each decay, we provide the predicted branching fraction(s) and the theoretical approach used to compute it, as well as the current experimental upper limit and that estimated for HL-LHC. The last two columns indicate whether the decay can be produced at FCC-ee/FCC-hh.

						Exp. limits		Producible at	
t →	M	+	q	Branching fraction	Framework	2023	HL-LHC	FCC-ee	FCC-hh
t →	$\overline{B}^0$	+	c	$\left(2.1^{+2.1}_{-1.1}\right) \times 10^{-6}$	NRQCD+LDME [26]	–	–	✓	✓
			u	$\left(4.0^{+4.0}_{-2.0}\right) \times 10^{-5}$	NRQCD+LDME [26]	–	–	✓	✓
	$\overline{B}^0_s$	+	c	$\left(4.0^{+4.0}_{-2.0}\right) \times 10^{-5}$	NRQCD+LDME [26]		$\lesssim 4.0 \times 10^{-5}$ [26]	✓	✓
			u	$\left(2.1^{+2.1}_{-1.1}\right) \times 10^{-6}$	NRQCD+LDME [26]	–	–	✓	✓
	$\Upsilon(1S)$	+	c	4.3×10^{-10}	NRQCD+CSM [181]	–	–	✘	✓
				$(1.0 - 1.5) \times 10^{-9}$	NRQCD+LDME [26]				
				$(6.4 \pm 1.3) \times 10^{-10}$	NRQCD+COM [180]				
			u	$(1.0 - 1.5) \times 10^{-11}$	NRQCD+LDME [26]	–	–	✘	✓
	$\Upsilon(2S)$	+	c	2.1×10^{-10}	NRQCD+CSM [181]	–	–	✘	✓
				$(1.7 - 5.3) \times 10^{-10}$	NRQCD+LDME [26]				
			u	$(1.7 - 5.3) \times 10^{-12}$	NRQCD+LDME [26]	–	–	✘	✓
	$\Upsilon(3S)$	+	c	1.6×10^{-10}	NRQCD+CSM [181]	–	–	✘	✓
				$(2.7 - 3.8) \times 10^{-10}$	NRQCD+LDME [26]				
			u	$(2.7 - 3.8) \times 10^{-12}$	NRQCD+LDME [26]	–	–	✘	✓
	$\Upsilon(nS)$	+	c	$\left(1.9^{+0.2}_{-0.1}\right) \times 10^{-9}$	NRQCD+LDME [26]	–	–	✘	✓
			u	$\left(1.9^{+0.2}_{-0.1}\right) \times 10^{-11}$	NRQCD+LDME [26]	–	–	✘	✓

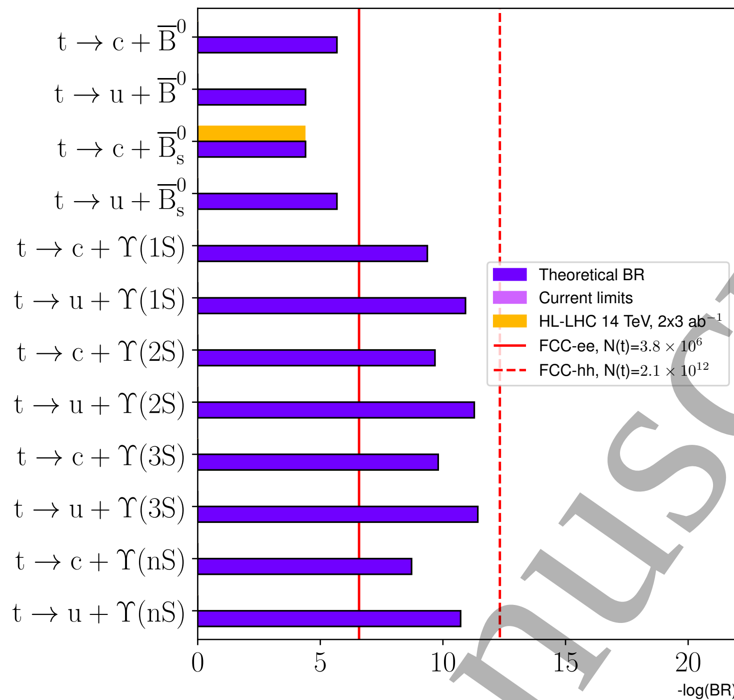

FIG. 33. Branching fractions (in negative log scale) of semiexclusive t → c/u quark + meson decays. Most recent theoretical predictions are shown as blue bars. The red vertical lines indicate the FCC-ee (solid) and FCC-hh (dashed) reach based only on the total number of top quarks expected at both facilities.

The right diagram of Fig. 32 corresponds to the process of a top quark decaying through an offshell W boson with virtual mass $m_{W^*} \approx m_M$ close to a mesonic resonance M that recoils against a b-jet. Estimates for the partial width of W^* decays into $M = \pi^\pm, D_s^\pm$ have been given in Refs. [27, 179] in the EFT + LCDA approach, based on the expression

$$\Gamma(t \to b + M) \approx \frac{G_F{}^2 m_t^3}{144\pi} f_M^2 \, |V_{qq'}|^2 = 1.55 \cdot 10^{-6} \, [\mathrm{GeV}^{-1}] \, f_M^2 \, |V_{qq'}|^2 \ , \tag{41}$$

where f_M is the decay constant of the meson, and $|V_{qq'}|^2$ the relevant CKM matrix element, and where the last numerical equality is obtained with the parameters of Table II. We extend here the study of semiexclusive t → meson + b-jet decays to include also the $M = \rho^\pm$, $K^\pm$, $D^\pm$, $D_s^\pm$, $B^\pm$, $B_c^\pm$ cases (and their corresponding excited states) by employing the decay constants from the recent compilation [45] for the light mesons, and from lattice calculations [71, 74] for the heavy ones (Table II). The resulting t → b + M branching fractions are tabulated in Table XXVI, and also shown in graphical form in Fig. 34. Estimated theoretical branching fractions are in the $\mathcal{O}(10^{-7}$–$10^{-13})$ range. No experimental search has been performed to date at the LHC. Although no channel is producible in the clean FCC-ee environment, most channels will be accessible at FCC-hh.

TABLE XXVI. Compilation of exclusive decays of the top quark into a b quark plus a meson. For each decay, we provide the predicted branching fraction(s) and the theoretical approach used to compute it, or derived here using Eq. (41). The last two columns indicate whether the decay can be produced at FCC-ee/FCC-hh.

						Exp. limits		Producible at	
t →	M	+	b	Branching fraction	Framework	2023	HL-LHC	FCC-ee	FCC-hh
t →	π^+	+	b	2.0×10^{-8}	EFT+LCDA [27]	–	–	✘	✓
				1.9×10^{-8}	EFT+LCDA (this work)				
	ρ^+	+	b	5.0×10^{-8}	EFT+LCDA (this work)	–	–	✘	✓
	K^+	+	b	1.4×10^{-9}	EFT+LCDA (this work)	–	–	✘	✓
	K^{*+}	+	b	2.4×10^{-9}	EFT+LCDA (this work)	–	–	✘	✓
	D^+	+	b	2.6×10^{-9}	EFT+LCDA (this work)	–	–	✘	✓
	D^{*+}	+	b	4.3×10^{-9}	EFT+LCDA (this work)	–	–	✘	✓
	D_s^+	+	b	1.0×10^{-7}	EFT+LCDA [27]	–	–	✘	✓
				6.9×10^{-8}	EFT+LCDA (this work)				
	D_s^{*+}	+	b	1.1×10^{-7}	EFT+LCDA (this work)	–	–	✘	✓
	B^+	+	b	6.1×10^{-13}	EFT+LCDA (this work)	–	–	✘	✓
	B^{*+}	+	b	5.4×10^{-13}	EFT+LCDA (this work)	–	–	✘	✓
	B_c^{*+}	+	b	3.6×10^{-10}	EFT+LCDA (this work)	–	–	✘	✓
	B_c^+	+	b	3.6×10^{-10}	EFT+LCDA (this work)	–	–	✘	✓

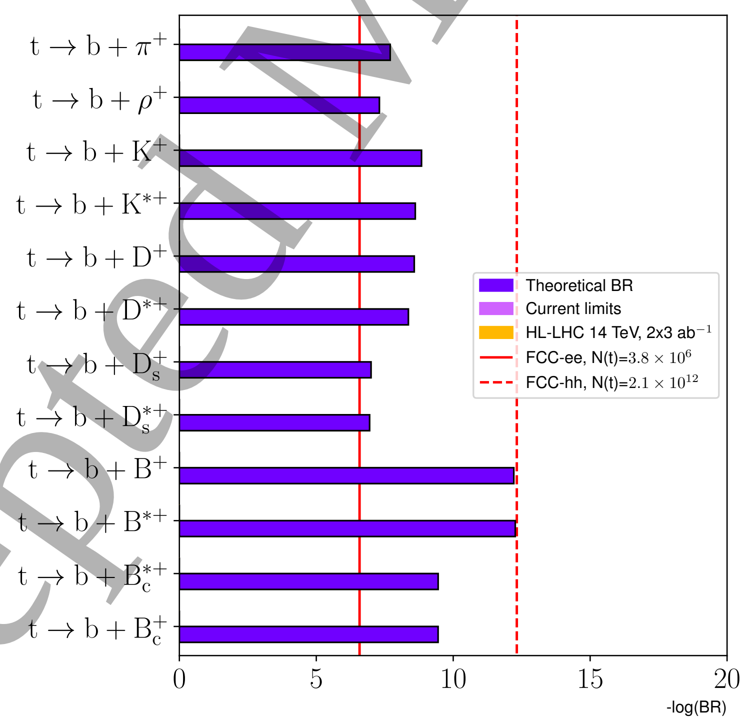

FIG. 34. Branching fractions (in negative log scale) of semiexclusive t → b quark + meson decays. The theoretical rates obtained with Eq. (41) are shown as blue bars. The red vertical lines indicate the FCC-ee (solid) and FCC-hh (dashed) reach based only on the total number of top quarks expected at both facilities.

VII. SUMMARY

We have presented a comprehensive survey of the theoretical and experimental status of about 200 rare and exclusive few-body decays of the four heaviest Standard Model (SM) particles: the Higgs, the electroweak (W, Z) bosons, and the top quark. Rare decays are defined here as those having branching fractions below $\mathcal{B} \approx 10^{-5}$, and we focus on those with two- or three-particles in the final state. Such decay processes remain experimentally unobserved and only upper limits have been set for about 50 of them. The study of these decay processes provides a powerful window into physics beyond the Standard Model (BSM) either directly, by probing SM suppressed or forbidden processes (such as flavour-changing neutral currents FCNC, lepton-flavour or lepton-flavour-universality violating processes, or spin-selection-rules violating decays), or indirectly as SM backgrounds to multiple exotic BSM decays (e.g., into axion-like particles ALPs, gravitons, or dark photons). Additionally, such decays offer a unique opportunity to constrain the light-quark Yukawa couplings, can provide alternative means to measure the W and/or top-quark masses, and help improve our understanding of quantum chromodynamics (QCD) factorization with small nonperturbative corrections.

First, we have systematically collected and organized in tabular form the theoretical branching fractions of almost 200 rare decay channels, indicating the model(s) used for the calculations, while providing any existing experimental upper limits on them. Among those, we have estimated for the first time the rates of about 50 new processes including ultrarare Higgs boson decays into photons and/or neutrinos (with rates 10^{-12}–10^{-40}), radiative H and Z boson decays into leptonium states (with rates 10^{-10}–10^{-23}), exclusive radiative H and Z boson quark-flavour-changing decays (with rates 10^{-14}–10^{-27}), exclusive Z decays into a pair of ϕ mesons (with an $\mathcal{O}(10^{-12})$ rate), three-body H W b top-quark decay (with an $\mathcal{O}(10^{-10})$ rate), and semiexclusive top-quark decays into a quark plus a meson (with rates 10^{-7}–10^{-13}). In addition, we have revised and updated predictions for a few other rare Z-boson and top-quark partial widths. We have also studied in detail all Z decay channels leading to a triphoton final state, and found that the sum of all relevant exclusive photon-plus-meson decays amounts to $\mathcal{B}(Z \to \gamma + M \to 3\gamma) = 1.8 \cdot 10^{-10}$, which is about one-third of the direct rate estimated here to be $\mathcal{B}(Z \to 3\gamma) = 6.4 \cdot 10^{-10}$. All such decays will need to be taken into account as backgrounds for future searches of $Z \to \gamma a(\gamma\gamma)$ processes, where a can be a BSM particle such as spin-0 (axion-like) or spin-2 (graviton-like) object.

Secondly, the feasibility of measuring each of these unobserved decays has been estimated for p-p collisions at the high-luminosity Large Hadron Collider (HL-LHC), as well as for e^+e^- and p-p collisions at the future circular

TABLE XXVII. Selection of rare and exclusive decays of the H, Z, W bosons and top quark potentially observable in pp(14 TeV) collisions at the HL-LHC. The last column indicates the approximate ratio of theoretical to our expected projected rates, $\mathcal{B}$(th)/$\mathcal{B}$(exp).

			Exp. limits		
		Branching fraction	2023	HL-LHC	$\mathcal{B}$(th)/$\mathcal{B}$(exp)
H →	$\gamma\gamma\gamma\gamma$	$(4.56 \pm 0.01) \times 10^{-12}$	–	–	–
	$\gamma + \rho^0$	$(1.68 \pm 0.08) \times 10^{-5}$	$< 8.8\times 10^{-4}$ [88]	$\lesssim 6.8 \times 10^{-5}$	~ 1/4
	$\gamma + J/\psi$	$(2.95 \pm 0.17) \times 10^{-6}$	$< 2.6\times 10^{-4}$ [90, 92]	$\lesssim 3.9 \times 10^{-5}$ [62]	~ 1/10
	$W^{\mp} + \rho^{\pm}$	$(1.5 \pm 0.1) \times 10^{-5}$	–	–	–
	$W^{\mp} + D_s^{*\pm}$	$(3.5 \pm 0.2) \times 10^{-5}$	–	–	–
	$Z + \rho^0$	$(1.4 \pm 0.1) \times 10^{-5}$	$< 1.2\times 10^{-2}$ [103]	$\lesssim 1.8 \times 10^{-3}$	~ 1/100
	$Z + \Upsilon(1S)$	1.7×10^{-5}	–	–	–
Z →	$\gamma + \rho^0$	$(4.19 \pm 0.47) \times 10^{-9}$	$< 2.5\times 10^{-5}$ [88]	$\lesssim 1.8 \times 10^{-6}$	~ 1/400
	$\gamma + \omega$	$(2.82 \pm 0.41) \times 10^{-8}$	$< 3.8\times 10^{-7}$ [91]	$\lesssim 5.7 \times 10^{-8}$	~ 1/2
	$\gamma + \phi$	$(1.17 \pm 0.08) \times 10^{-8}$	$< 9.0\times 10^{-7}$ [88]	$\lesssim 6.6 \times 10^{-8}$	~ 1/6
	$\gamma + J/\psi$	$(9.96 \pm 1.86) \times 10^{-8}$	$< 6.0\times 10^{-7}$ [92, 134]	$\lesssim 3.1 \times 10^{-7}$ [62]	~ 1/3
	$\gamma + \Upsilon(1S)$	$(4.93 \pm 0.51) \times 10^{-8}$	$< 2.8\times 10^{-6}$ [89]	$\lesssim 2.2 \times 10^{-7}$	~ 1/4
W →	$\gamma + \pi^{\pm}$	$(4.0 \pm 0.8) \times 10^{-9}$	$< 1.9\times 10^{-6}$ [158, 159]	$\lesssim 2.9 \times 10^{-7}$	~ 1/70
	$\gamma + D_s^{\pm}$	$\left(3.66^{+1.49}_{-0.85}\right) \times 10^{-8}$	$< 6.5\times 10^{-4}$ [136]	$\lesssim 1.2 \times 10^{-5}$	~ 1/300
t →	$c + \overline{B}_s^0$	$\left(4.0^{+4.0}_{-2.0}\right) \times 10^{-5}$	–	$\lesssim 4.0 \times 10^{-5}$ [26]	~ 1/1
	$W + Z + b$	$\left(5.4^{+4.7}_{-2.0}\right) \times 10^{-7}$	–	–	–

collider (FCC-ee and FCC-hh). From the number of H, Z, W bosons, and top quarks expected to be produced at the HL-LHC, FCC-ee, and FCC-hh colliders, and by statistically extrapolating the current 95% confidence-level limits set, we provide estimates of the ultimately achievable experimental upper bounds (or observations) in those machines. Among those, in Table XXVII we have selected a few interesting channels that can be observed and/or deserve further study in p-p collisions at the HL-LHC. The last column indicates the approximate ratio of theoretical to expected experimental rates, $\mathcal{B}(\mathrm{th})/\mathcal{B}(\mathrm{exp})$. Two reasons motivate this selection of channels: either (i) they have relatively large rates, $O(10^{-5})$ (with a measurement having been attempted or not, to date), or (ii) they have lower rates, $\mathcal{B} \lesssim 10^{-8}$, but measurements of upper bounds have been performed, and our projections indicate $\mathcal{B}(\mathrm{th})/\mathcal{B}(\mathrm{exp})$ not far from unity. For the Higgs boson, we list first the rare $\mathrm{H} \to 4\gamma$ decay that has not been directly searched for at the LHC to date, but limits exist on the process $\mathrm{H} \to \mathrm{a}(\gamma\gamma)\mathrm{a}(\gamma\gamma)$ with two intermediate ALPs decaying into photons [68, 83–86]. Although its rate makes its observation impossible at the LHC in the absence of enhancing BSM effects, it would not be difficult for ATLAS/CMS to recast any current and future similar ALP searches into upper bounds on the $\mathrm{H} \to 4\gamma$ "continuum" decay. Next, we find that the HL-LHC can set upper bounds on the exclusive $\mathrm{H} \to \gamma\rho$ and $\mathrm{H} \to \gamma\,\mathrm{J}/\psi$ decays at about four and ten times their expected SM values, respectively. Similarly, we find that HL-LHC can potentially observe $\mathrm{Z} \to \gamma\,\omega$, $\mathrm{Z} \to \gamma\,\mathrm{J}/\psi$, and $Z \to \gamma\,\Upsilon(1S)$ with ratios between the theoretical rates and projected experimental limits as large as 1/2, 1/3, and 1/4, respectively. In the W boson case, the least suppressed rare decays are $\mathrm{W} \to \gamma\,\pi$, $\gamma\,\mathrm{D_s}$ but with experimental bounds expected at about two orders-of-magnitude their SM values. Finally, the semiexclusive decay of the top quark into a charm jet and B meson (identified experimentally as a b-jet) has $O(10^{-4})$ rates that make it observable at the HL-LHC [26], and the three-body $\mathrm{t} \to \mathrm{W\,Z\,b}$ decay can occur in about one out of one million top-quark decays, and a search should also be attempted. Of course, the HL-LHC channel selection of Table XXVII is driven by the SM rates and their potential visibility, but as explained in this work there are many other suppressed decays of the four heaviest particles that can be enhanced in many BSM scenarios, and should be an active part of target searches in the next years.

Finally, we have shown that a future high-luminosity $\mathrm{e}^+\mathrm{e}^-$ electroweak factory, such as the FCC-ee with $6 \cdot 10^{12}$ Z bosons, $5 \cdot 10^{8}$ W bosons, $1.9 \cdot 10^{6}$ Higgs bosons, and $3.8 \cdot 10^{6}$ top quarks produced in very clean experimental conditions, can discover about half of the 200 rare decays discussed here. Eventually, the FCC-hh with huge data samples expected, can produce most of the decay channels listed in this work, although their experimental observation will be difficult in a challenging hadronic collider environment. We hope that this document can help guide and prioritize upcoming experimental and theoretical studies of rare and exclusive few-body decays of the most massive SM particles, as well as further motivate BSM searches, at the LHC and future colliders.

Acknowledgments.— Informative discussions and valuable feedback from Hua-Sheng Shao and J.-Ph. Lansberg are gratefully acknowledged. We thank Dao-Neng Gao, Richard Ruiz, and Bin Yan for feedback on a previous version of the paper. Support from the EU STRONG-2020 project under the program H2020-INFRAIA-2018-1, grant agreement No. 824093 is acknowledged.

Data availability statement.— All data that support the findings of this study are included within the article.

REFERENCES

[1] **ATLAS** Collaboration, G. Aad *et al.*, "Observation of a new particle in the search for the Standard Model Higgs boson with the ATLAS detector at the LHC," *Phys. Lett. B* **716** (2012) 1–29, arXiv:1207.7214 [hep-ex].

[2] **CMS** Collaboration, S. Chatrchyan *et al.*, "Observation of a New Boson at a Mass of 125 GeV with the CMS Experiment at the LHC," *Phys. Lett. B* **716** (2012) 30–61, arXiv:1207.7235 [hep-ex].

[3] P. Azzi *et al.*, "Report from Working Group 1: Standard Model Physics at the HL-LHC and HE-LHC," *CERN Yellow Rep. Monogr.* **7** (2019) 1–220, arXiv:1902.04070 [hep-ph].

[4] **FCC** Collaboration, A. Abada *et al.*, "FCC-ee: The Lepton Collider: Future Circular Collider Conceptual Design Report Volume 2," *Eur. Phys. J. ST* **228** (2019) 261–623.

[5] **CEPC Study Group** Collaboration, M. Dong *et al.*, "CEPC Conceptual Design Report: Volume 2 - Physics & Detector," arXiv:1811.10545 [hep-ex].

[6] **FCC** Collaboration, A. Abada *et al.*, "FCC-hh: The Hadron Collider: Future Circular Collider Conceptual Design Report Volume 3," *Eur. Phys. J. ST* **228** (2019) 755–1107.

[7] **LHCb** Collaboration, R. Aaij *et al.*, "Physics case for an LHCb Upgrade II - Opportunities in flavour physics, and beyond, in the HL-LHC era," arXiv:1808.08865 [hep-ex].

[8] **Belle-II** Collaboration, W. Altmannshofer *et al.*, "The Belle II Physics Book," *PTEP* **2019** (2019) 123C01, arXiv:1808.10567 [hep-ex]. [Erratum: PTEP 2020 (2020) 029201].

[9] D. Curtin *et al.*, "Exotic decays of the 125 GeV Higgs boson," *Phys. Rev. D* **90** (2014) 075004, arXiv:1312.4992 [hep-ph].
[10] **LHC Higgs Cross Section Working Group** Collaboration, D. de Florian *et al.*, "Handbook of LHC Higgs Cross Sections: 4. Deciphering the Nature of the Higgs Sector," arXiv:1610.07922 [hep-ph].
[11] G. T. Bodwin, F. Petriello, S. Stoynev, and M. Velasco, "Higgs boson decays to quarkonia and the $H\bar{c}c$ coupling," *Phys. Rev. D* **88** (2013) 053003, arXiv:1306.5770 [hep-ph].
[12] G. Isidori, A. V. Manohar, and M. Trott, "Probing the nature of the Higgs-like Boson via $h \to V\mathcal{F}$ decays," *Phys. Lett. B* **728** (2014) 131–135, arXiv:1305.0663 [hep-ph].
[13] A. L. Kagan, G. Perez, F. Petriello, Y. Soreq, S. Stoynev, and J. Zupan, "Exclusive window onto Higgs Yukawa couplings," *Phys. Rev. Lett.* **114** (2015) 101802, arXiv:1406.1722 [hep-ph].
[14] M. König and M. Neubert, "Exclusive radiative Higgs decays as probes of light-quark Yukawa couplings," *JHEP* **08** (2015) 012, arXiv:1505.03870 [hep-ph].
[15] G. Perez, Y. Soreq, E. Stamou, and K. Tobioka, "Prospects for measuring the Higgs boson coupling to light quarks," *Phys. Rev. D* **93** (2016) 013001, arXiv:1505.06689 [hep-ph].
[16] S. L. Glashow, J. Iliopoulos, and L. Maiani, "Weak Interactions with Lepton-Hadron Symmetry," *Phys. Rev. D* **2** (1970) 1285–1292.
[17] B. Guberina, J. H. Kuhn, R. D. Peccei, and R. Ruckl, "Rare Decays of the Z^0," *Nucl. Phys. B* **174** (1980) 317–334.
[18] M. A. Perez, G. Tavares-Velasco, and J. J. Toscano, "New physics effects in rare Z decays," *Int. J. Mod. Phys. A* **19** (2004) 159–178, arXiv:hep-ph/0305227.
[19] P. Agrawal *et al.*, "Feebly-interacting particles: FIPs 2020 workshop report," *Eur. Phys. J. C* **81** (2021) 1015, arXiv:2102.12143 [hep-ph].
[20] D. d'Enterria, "Collider constraints on axion-like particles," arXiv:2102.08971 [hep-ex].
[21] D. d'Enterria, M. A. Tamlihat, L. Schoeffel, H.-S. Shao, and Y. Tayalati, "Collider constraints on massive gravitons coupling to photons," *Phys. Lett. B* **846** (2023) 138237, arXiv:2306.15558 [hep-ph].
[22] D. Curtin, R. Essig, S. Gori, and J. Shelton, "Illuminating dark photons with high-energy colliders," *JHEP* **02** (2015) 157, arXiv:1412.0018 [hep-ph].
[23] L. Arnellos, W. J. Marciano, and Z. Parsa, "Radiative Decays $W^\pm \to \rho^\pm\gamma$ and $Z^0 \to \rho^0\gamma$," *Nucl. Phys. B* **196** (1982) 378–393.
[24] M. Mangano and T. Melia, "Rare exclusive hadronic W decays in a $t\bar{t}$ environment," *Eur. Phys. J. C* **75** (2015) 258, arXiv:1410.7475 [hep-ph].
[25] E. Jones and W. J. Murray, "Mass biases in exclusive radiative hadronic decays of W bosons at the LHC," *New J. Phys.* **23** (2021) 113035, arXiv:2009.01073 [hep-ex].
[26] D. d'Enterria and H.-S. Shao, "Rare two-body decays of the top quark into a bottom meson plus an up or charm quark," *JHEP* **07** (2020) 127, arXiv:2005.08102 [hep-ph].
[27] M. Beneke *et al.*, "Top quark physics," in *Workshop on Standard Model Physics (and more) at the LHC (First Plenary Meeting)*, pp. 419–529. 3, 2000. arXiv:hep-ph/0003033.
[28] J. A. Aguilar-Saavedra, "Top flavor-changing neutral interactions: Theoretical expectations and experimental detection," *Acta Phys. Polon. B* **35** (2004) 2695–2710, arXiv:hep-ph/0409342.
[29] G. P. Lepage and S. J. Brodsky, "Exclusive Processes in Quantum Chromodynamics: Evolution Equations for Hadronic Wave Functions and the Form-Factors of Mesons," *Phys. Lett. B* **87** (1979) 359–365.
[30] G. P. Lepage and S. J. Brodsky, "Exclusive Processes in Perturbative Quantum Chromodynamics," *Phys. Rev. D* **22** (1980) 2157.
[31] A. V. Efremov and A. V. Radyushkin, "Asymptotical Behavior of Pion Electromagnetic Form-Factor in QCD," *Theor. Math. Phys.* **42** (1980) 97–110.
[32] A. V. Efremov and A. V. Radyushkin, "Factorization and Asymptotical Behavior of Pion Form-Factor in QCD," *Phys. Lett. B* **94** (1980) 245–250.
[33] V. L. Chernyak and A. R. Zhitnitsky, "Asymptotic Behavior of Exclusive Processes in QCD," *Phys. Rept.* **112** (1984) 173.
[34] J.-P. Lansberg, "New Observables in Inclusive Production of Quarkonia," *Phys. Rept.* **889** (2020) 1–106, arXiv:1903.09185 [hep-ph].
[35] E. Chapon *et al.*, "Prospects for quarkonium studies at the high-luminosity LHC," *Prog. Part. Nucl. Phys.* **122** (2022) 103906, arXiv:2012.14161 [hep-ph].
[36] M. A. Shifman, A. I. Vainshtein, and V. I. Zakharov, "QCD and Resonance Physics. Theoretical Foundations," *Nucl. Phys. B* **147** (1979) 385–447.
[37] P. Colangelo and A. Khodjamirian, "QCD sum rules, a modern perspective," arXiv:hep-ph/0010175.
[38] A. K. Likhoded and A. V. Luchinsky, "Double Charmonia Production in Exclusive Z Boson Decays," *Mod. Phys. Lett. A* **33** (2018) 1850078, arXiv:1712.03108 [hep-ph].
[39] C. W. Bauer, D. Pirjol, and I. W. Stewart, "Soft collinear factorization in effective field theory," *Phys. Rev. D* **65** (2002) 054022, arXiv:hep-ph/0109045.
[40] H. Georgi, "Effective field theory," *Ann. Rev. Nucl. Part. Sci.* **43** (1993) 209–252.
[41] A. Manohar and H. Georgi, "Chiral quarks and the Nonrelativistic Quark Model," *Nucl. Phys. B* **234** (1984) 189–212.
[42] M. Beneke, G. Buchalla, M. Neubert, and C. T. Sachrajda, "QCD factorization for exclusive, nonleptonic B meson decays: General arguments and the case of heavy light final states," *Nucl. Phys. B* **591** (2000) 313–418, arXiv:hep-ph/0006124.

[43] M. Neubert, "Heavy quark symmetry," *Phys. Rept.* **245** (1994) 259–396, arXiv:hep-ph/9306320.
[44] M. König, *Effective field theories in the standard model and beyond*. PhD thesis, Mainz U., 2018.
[45] Y. Grossman, M. König, and M. Neubert, "Exclusive Radiative Decays of W and Z Bosons in QCD Factorization," *JHEP* **04** (2015) 101, arXiv:1501.06569 [hep-ph].
[46] G. T. Bodwin, E. Braaten, and G. P. Lepage, "Rigorous QCD analysis of inclusive annihilation and production of heavy quarkonium," *Phys. Rev. D* **51** (1995) 1125–1171, arXiv:hep-ph/9407339. [Erratum: Phys. Rev. D 55 (1997) 5853].
[47] E. J. Eichten and C. Quigg, "Quarkonium wave functions at the origin," *Phys. Rev. D* **52** (1995) 1726–1728, arXiv:hep-ph/9503356.
[48] G. T. Bodwin, H. S. Chung, D. Kang, J. Lee, and C. Yu, "Improved determination of color-singlet nonrelativistic QCD matrix elements for S-wave charmonium," *Phys. Rev. D* **77** (2008) 094017, arXiv:0710.0994 [hep-ph].
[49] D. Ebert, R. N. Faustov, and V. O. Galkin, "Properties of heavy quarkonia and B_c mesons in the relativistic quark model," *Phys. Rev. D* **67** (2003) 014027, arXiv:hep-ph/0210381.
[50] E. Braaten, Y. Jia, and T. Mehen, "*B* production asymmetries in perturbative QCD," *Phys. Rev. D* **66** (2002) 034003, arXiv:hep-ph/0108201.
[51] H.-S. Shao and D. d'Enterria, "gamma-UPC: automated generation of exclusive photon-photon processes in ultraperipheral proton and nuclear collisions with varying form factors," *JHEP* **09** (2022) 248, arXiv:2207.03012 [hep-ph].
[52] **LEP/SLD Electroweak Working Groups** Collaboration, S. Schael *et al.*, "Precision electroweak measurements on the Z resonance," *Phys. Rept.* **427** (2006) 257–454, arXiv:hep-ex/0509008.
[53] **LEP Electroweak Working Group** Collaboration, S. Schael *et al.*, "Electroweak measurements in electron-positron collisions at W-boson-pair energies at LEP," *Phys. Rept.* **532** (2013) 119–244, arXiv:1302.3415 [hep-ex].
[54] **LEP Working Group for Higgs boson searches, ALEPH, DELPHI, L3, OPAL** Collaboration, R. Barate *et al.*, "Search for the standard model Higgs boson at LEP," *Phys. Lett. B* **565** (2003) 61–75, arXiv:hep-ex/0306033.
[55] D. d'Enterria, P. Rebello Teles, and D. E. Martins, "Measurements of $\gamma\gamma \to$ Higgs and $\gamma\gamma \to W^+W^-$ in e^+e^- collisions at the Future Circular Collider," in *17th conference on Elastic and Diffractive Scattering*. 12, 2017. arXiv:1712.07023 [hep-ph].
[56] **FCC-ee** Collaboration, C. Grojean, P. Janot, M. Mangano, *et al.*, "FCC-ee Midterm report: Physics and Experiments." CERN-FCC-2023-000i, 2023.
[57] M. L. Mangano *et al.*, "Physics at a 100 TeV pp Collider: Standard Model Processes," arXiv:1607.01831 [hep-ph].
[58] R. Boughezal, J. M. Campbell, R. K. Ellis, C. Focke, W. Giele, X. Liu, F. Petriello, and C. Williams, "Color singlet production at NNLO in MCFM," *Eur. Phys. J. C* **77** (2017) 7, arXiv:1605.08011 [hep-ph].
[59] **NNPDF** Collaboration, R. D. Ball *et al.*, "Parton distributions from high-precision collider data," *Eur. Phys. J. C* **77** (2017) 663, arXiv:1706.00428 [hep-ph].
[60] **Particle Data Group** Collaboration, R. L. Workman *et al.*, "Review of Particle Physics," *PTEP* **2022** (2022) 083C01.
[61] **ATLAS** Collaboration, G. Aad *et al.*, "Sensitivity of ATLAS at HL-LHC to flavour changing neutral currents in top quark decays t $\to$ cH, with H $\to \gamma\gamma$." ATL-PHYS-PUB-2013-012, 2013.
[62] **ATLAS** Collaboration, G. Aad *et al.*, "Search for the Standard Model Higgs and Z Boson decays to J/$\psi\,\gamma$: HL-LHC projections." ATL-PHYS-PUB-2015-043, 2015.
[63] **CMS** Collaboration, A. Tumasyan *et al.*, "Search for rare Higgs boson decays with mesons at the HL-LHC." CMS-PAS-FTR-21-009, 2022.
[64] A. Cerri *et al.*, "Report from Working Group 4: Opportunities in Flavour Physics at the HL-LHC and HE-LHC," *CERN Yellow Rep. Monogr.* **7** (2019) 867–1158, arXiv:1812.07638 [hep-ph].
[65] Y.-B. Liu and S. Moretti, "Probing tqZ anomalous couplings in the trilepton signal at the HL-LHC, HE-LHC and FCC-hh," *Chin. Phys. C* **45** (2021) 043110, arXiv:2010.05148 [hep-ph].
[66] **ATLAS** Collaboration, "Expected sensitivity of ATLAS to FCNC top quark decays $t \to Zu$ and $t \to Hq$ at the High Luminosity LHC," tech. rep., 2016.
[67] **CMS** Collaboration, S. Chatrchyan *et al.*, "Search for a Higgs Boson Decaying into a Z and a Photon in *pp* Collisions at $\sqrt{s} = 7$ and 8 TeV," *Phys. Lett. B* **726** (2013) 587–609, arXiv:1307.5515 [hep-ex].
[68] **ATLAS** Collaboration, G. Aad *et al.*, "Search for new phenomena in events with at least three photons collected in pp collisions at $\sqrt{s} = 8$ TeV with the ATLAS detector," *Eur. Phys. J. C* **76** (2016) 210, arXiv:1509.05051 [hep-ex].
[69] **Flavour Lattice Averaging Group (FLAG)** Collaboration, Y. Aoki *et al.*, "FLAG Review 2021," *Eur. Phys. J. C* **82** (2022) 869, arXiv:2111.09849 [hep-lat].
[70] L.-S. Lu, "Factorization of radiative leptonic D-meson decay with sub-leading power corrections," *Chin. Phys. C* **45** (2021) 073101, arXiv:2104.01562 [hep-ph].
[71] D. Becirevic, V. Lubicz, F. Sanfilippo, S. Simula, and C. Tarantino, "D-meson decay constants and a check of factorization in non-leptonic B-decays," *JHEP* **02** (2012) 042, arXiv:1201.4039 [hep-lat].
[72] R. Mandal, S. Nandi, and I. Ray, "Constraining inverse moment of B-meson distribution amplitude using Lattice QCD data," *Phys. Lett. B* **848** (2024) 138345, arXiv:2308.07033 [hep-ph].
[73] **HDECAY** Collaboration, A. Djouadi, J. Kalinowski, M. Muehlleitner, and M. Spira, "HDECAY: Twenty$_{++}$ years after," *Comput. Phys. Commun.* **238** (2019) 214–231, arXiv:1801.09506 [hep-ph].
[74] **HPQCD** Collaboration, B. Colquhoun, C. T. H. Davies, R. J. Dowdall, J. Kettle, J. Koponen, G. P. Lepage, and A. T. Lytle, "B-meson decay constants: a more complete picture from full lattice QCD," *Phys. Rev. D* **91** (2015) 114509, arXiv:1503.05762 [hep-lat].

[75] L.-B. Chen, H. T. Li, J. Wang, and Y. Wang, "Analytic result for the top-quark width at next-to-next-to-leading order in QCD," *Phys. Rev. D* **108** (2023) 054003, arXiv:2212.06341 [hep-ph].

[76] A. Khodjamirian, R. Mandal, and T. Mannel, "Inverse moment of the B_s-meson distribution amplitude from QCD sum rule," *JHEP* **10** (2020) 043, arXiv:2008.03935 [hep-ph].

[77] J. Alwall, R. Frederix, S. Frixione, V. Hirschi, F. Maltoni, O. Mattelaer, H. S. Shao, T. Stelzer, P. Torrielli, and M. Zaro, "The automated computation of tree-level and next-to-leading order differential cross sections, and their matching to parton shower simulations," *JHEP* **07** (2014) 079, arXiv:1405.0301 [hep-ph].

[78] V. Hirschi and O. Mattelaer, "Automated event generation for loop-induced processes," *JHEP* **10** (2015) 146, arXiv:1507.00020 [hep-ph].

[79] R. Frederix, S. Frixione, V. Hirschi, D. Pagani, H. S. Shao, and M. Zaro, "The automation of next-to-leading order electroweak calculations," *JHEP* **07** (2018) 185, arXiv:1804.10017 [hep-ph]. [Erratum: JHEP 11 (2021) 085].

[80] W. Bernreuther and O. Nachtmann, "Weak Interaction Effects in Positronium," *Z. Phys. C* **11** (1981) 235.

[81] A. Pokraka and A. Czarnecki, "Parapositronium can decay into three photons," *Phys. Rev. D* **96** (2017) 093002, arXiv:1707.09466 [hep-ph].

[82] Y. Sun and D.-N. Gao, "Higgs decays to γ and invisible particles in the standard model," *Phys. Rev. D* **89** (2014) 017301, arXiv:1310.8404 [hep-ph].

[83] **CMS** Collaboration, A. Tumasyan *et al.*, "Search for exotic Higgs boson decays $H \to \mathcal{A}\mathcal{A} \to 4\gamma$ with events containing two merged diphotons in proton-proton collisions at $\sqrt{s} = 13$ TeV," *Phys. Rev. Lett.* **131** (2023) 101801, arXiv:2209.06197 [hep-ex].

[84] **CMS** Collaboration, A. Tumasyan *et al.*, "Search for the exotic decay of the Higgs boson into two light pseudoscalars with four photons in the final state in proton-proton collisions at $\sqrt{s} = 13$ TeV," *JHEP* **07** (2023) 148, arXiv:2208.01469 [hep-ex].

[85] **ATLAS** Collaboration, "Search for short- and long-lived axion-like particles in $H \to aa \to 4\gamma$ decays with the ATLAS experiment at the LHC," tech. rep., 2023. http://cds.cern.ch/record/2867933.

[86] **ATLAS** Collaboration, G. Aad *et al.*, "Search for short- and long-lived axion-like particles in $H \to aa \to 4\gamma$ decays with the ATLAS experiment at the LHC," arXiv:2312.03306 [hep-ex].

[87] J. F. Kamenik, A. Korajac, M. Szewc, M. Tammaro, and J. Zupan, "Flavor violating Higgs and Z decays at FCC-ee," arXiv:2306.17520 [hep-ph].

[88] **ATLAS** Collaboration, M. Aaboud *et al.*, "Search for exclusive Higgs and Z boson decays to $\phi\gamma$ and $\rho\gamma$ with the ATLAS detector," *JHEP* **07** (2018) 127, arXiv:1712.02758 [hep-ex].

[89] **ATLAS** Collaboration, M. Aaboud *et al.*, "Searches for exclusive Higgs and Z boson decays into $J/\psi\gamma$, $\psi(2S)\gamma$, and $\Upsilon(nS)\gamma$ at $\sqrt{s} = 13$ TeV with the ATLAS detector," *Phys. Lett. B* **786** (2018) 134–155, arXiv:1807.00802 [hep-ex].

[90] **CMS** Collaboration, A. M. Sirunyan *et al.*, "Search for Higgs and Z boson decays to J/ψ or Υ pairs in the four-muon final state in proton-proton collisions at $\sqrt{s} = 13$ TeV," *Phys. Lett. B* **797** (2019) 134811, arXiv:1905.10408 [hep-ex].

[91] **ATLAS** Collaboration, G. Aad *et al.*, "Search for exclusive Higgs and Z boson decays to $\omega\gamma$ and Higgs boson decays to $K^*\gamma$ with the ATLAS detector," *Phys. Lett. B* **847** (2023) 138292, arXiv:2301.09938 [hep-ex].

[92] **CMS** Collaboration, "Search for the rare decays of the Z and Higgs bosons to a J/ψ or J/ψ' meson and a photon in proton-proton collisions at $\sqrt{s} = 13$ TeV," tech. rep., CERN, Geneva, 2023. http://cds.cern.ch/record/2882656.

[93] **ATLAS** Collaboration, G. Aad *et al.*, "Searches for exclusive Higgs and Z boson decays into a vector quarkonium state and a photon using 139 fb^{-1} of ATLAS $\sqrt{s} = 13$ TeV proton–proton collision data," *Eur. Phys. J. C* **83** (2023) 781, arXiv:2208.03122 [hep-ex].

[94] N. Brambilla, H. S. Chung, W. K. Lai, V. Shtabovenko, and A. Vairo, "Order v^4 corrections to Higgs boson decay into $J/\psi + \gamma$," *Phys. Rev. D* **100** (2019) 054038, arXiv:1907.06473 [hep-ph].

[95] G. T. Bodwin, H. S. Chung, J.-H. Ee, and J. Lee, "Addendum: New approach to the resummation of logarithms in Higgs-boson decays to a vector quarkonium plus a photon [Phys. Rev. D 95, 054018 (2017)]," *Phys. Rev. D* **96** (2017) 116014, arXiv:1710.09872 [hep-ph].

[96] H. Dong, P. Sun, and B. Yan, "Probing the $H\gamma\gamma$ coupling via Higgs boson exclusive decay into quarkonia plus a photon at the HL-LHC," *Phys. Rev. D* **106** (2022) 095013, arXiv:2208.05153 [hep-ph].

[97] L. G. Benitez-Guzmán, I. García-Jiménez, M. A. López-Osorio, E. Martínez-Pascual, and J. J. Toscano, "Revisiting the flavor changing neutral current Higgs decays $H \to q_i q_j$ in the Standard Model," *J. Phys. G* **42** (2015) 085002, arXiv:1506.02718 [hep-ph].

[98] J. I. Aranda, G. González-Estrada, J. Montaño, F. Ramírez-Zavaleta, and E. S. Tututi, "Revisiting the rare $H \to q_i q_j$ decays in the standard model," *J. Phys. G* **47** (2020) 125001, arXiv:2009.07166 [hep-ph].

[99] S. J. Lee and M. Neubert, "Model-independent properties of the B-meson distribution amplitude," *Phys. Rev. D* **72** (2005) 094028, arXiv:hep-ph/0509350.

[100] **ATLAS** Collaboration, G. Aad *et al.*, "Searches for exclusive Higgs boson decays into $D^*\gamma$ and Z boson decays into $D^0\gamma$ and $K_s^0\gamma$ in pp collisions at $\sqrt{s} = 13$ TeV with the ATLAS detector," arXiv:2402.18731 [hep-ex].

[101] **CMS** Collaboration, A. Hayrapetyan *et al.*, "Search for an exotic decay of the Higgs boson into a Z boson and a pseudoscalar particle in proton-proton collisions at $\sqrt{s} = 13$ TeV," arXiv:2311.00130 [hep-ex].

[102] S. Alte, M. König, and M. Neubert, "Exclusive Weak Radiative Higgs Decays in the Standard Model and Beyond," *JHEP* **12** (2016) 037, arXiv:1609.06310 [hep-ph].

[103] **CMS** Collaboration, A. M. Sirunyan *et al.*, "Search for decays of the 125 GeV Higgs boson into a Z boson and a ρ or ϕ meson," *JHEP* **11** (2020) 039, arXiv:2007.05122 [hep-ex].

[104] D. Bečirević, B. Melić, M. Patra, and O. Sumensari, "Seeking a CP -odd Higgs boson via $h \to \eta_{c,b}\ell^+\ell^-$," *Phys. Rev. D* **97** (2018) 015008, arXiv:1705.01112 [hep-ph].

[105] Q.-F. Sun and A.-M. Wang, "Next-to-leading order QCD corrections to the decay of Higgs to vector meson and Z boson," *Chin. Phys. C* **42** (2018) 033105, arXiv:1801.10528 [hep-ph].

[106] **CMS** Collaboration, A. Tumasyan *et al.*, "Search for Higgs boson decays into Z and J/ψ and for Higgs and Z boson decays into J/ψ or Υ pairs in pp collisions at $\sqrt{s}$ = 13 TeV," *Phys. Lett. B* **842** (2023) 137534, arXiv:2206.03525 [hep-ex].

[107] D.-N. Gao, "A note on Higgs decays into Z boson and J/$\psi(\Upsilon)$," *Phys. Lett. B* **737** (2014) 366–368, arXiv:1406.7102 [hep-ph].

[108] R.-F. Zhu, T.-F. Feng, and H.-B. Zhang, "The QCD corrections of the process h $\to \eta$bZ," *Mod. Phys. Lett. A* **33** (2018) 1830008.

[109] M. Fael and T. Mannel, "On the decays B $\to$ K$^{(*)}$+ leptonium," *Nucl. Phys. B* **932** (2018) 370–384, arXiv:1803.08880 [hep-ph].

[110] D. d'Enterria, R. Perez-Ramos, and H.-S. Shao, "Ditauonium spectroscopy," *Eur. Phys. J. C* **82** (2022) 923, arXiv:2204.07269 [hep-ph].

[111] B. Azhothkaran and V. K. Nilakanthan, "Decay Constants of S Wave Heavy Quarkonia," *Int. J. Theor. Phys.* **59** (2020) 2016–2028.

[112] R. Van Royen and V. F. Weisskopf, "Hadron Decay Processes and the Quark Model," *Nuovo Cim. A* **50** (1967) 617–645. [Erratum: Nuovo Cim. A 51 (1967) 583].

[113] A. Y. Korchin and V. A. Kovalchuk, "Polarization effects in the Higgs boson decay to γZ and test of *CP* and *CPT* symmetries," *Phys. Rev. D* **88** (2013) 036009, arXiv:1303.0365 [hep-ph].

[114] L. Nemenov, "Elementary Relativistic Atoms," *Lect. Notes Phys.* **570** (2001) 223–245.

[115] M. N. Doroshenko, V. G. Kartvelishvili, E. G. Chikovani, and S. M. Esakiya, "Vector quarkonium in decays of heavy Higgs particles," *Yad. Fiz.* **46** (1987) 864–868.

[116] V. Kartvelishvili, A. V. Luchinsky, and A. A. Novoselov, "Double vector quarkonia production in exclusive Higgs boson decays," *Phys. Rev. D* **79** (2009) 114015, arXiv:0810.0953 [hep-ph].

[117] I. N. Belov, A. V. Berezhnoy, A. E. Dorokhov, A. K. Likhoded, A. P. Martynenko, and F. A. Martynenko, "Higgs boson decay to paired B$_c$: Relativistic and one-loop corrections," *Nucl. Phys. A* **1015** (2021) 122285, arXiv:2105.02207 [hep-ph].

[118] R. N. Faustov, A. P. Martynenko, and F. A. Martynenko, "Relativistic corrections to paired production of charmonium and bottomonium in decays of the Higgs boson," *Phys. Rev. D* **107** (2023) 056002, arXiv:2209.12321 [hep-ph].

[119] D.-N. Gao and X. Gong, "Higgs boson decays into a pair of heavy vector quarkonia," *Phys. Lett. B* **832** (2022) 137243, arXiv:2203.00514 [hep-ph].

[120] R. N. Faustov, A. P. Martynenko, and F. A. Martynenko, "Pair Quarkonium Production in Higgs Boson Decay," *Phys. Part. Nucl. Lett.* **20** (2023) 368–371.

[121] I. N. Belov, A. V. Berezhnoy, E. A. Leshchenko, and A. K. Likhoded, "QCD one-loop correction to Higgs boson decay into quarkonium pairs," *Phys. Rev. D* **108** (2023) 036013, arXiv:2304.11620 [hep-ph].

[122] J. Jiang and C.-F. Qiao, "B$_c$ Production in Higgs Boson Decays," *Phys. Rev. D* **93** (2016) 054031, arXiv:1512.01327 [hep-ph].

[123] L. D. Landau, "On the angular momentum of a system of two photons," *Dokl. Akad. Nauk SSSR* **60** (1948) 207–209.

[124] C.-N. Yang, "Selection Rules for the Dematerialization of a Particle Into Two Photons," *Phys. Rev.* **77** (1950) 242–245.

[125] M. L. Laursen, M. A. Samuel, G. B. Tupper, and A. Sen, "Z^0 Decay Into Two Gluons and a Photon for Massive Quarks," *Phys. Rev. D* **27** (1983) 196.

[126] E. W. N. Glover and A. G. Morgan, "Z boson decay into photons," *Z. Phys. C* **60** (1993) 175–180.

[127] R. Hopker and J. J. van der Bij, "Z^0 decay into three gluons," *Phys. Rev. D* **49** (1994) 3779–3782.

[128] J. M. Hernandez, M. A. Perez, G. Tavares-Velasco, and J. J. Toscano, "Decay Z $\to \nu\bar{\nu}\gamma$ in the standard model," *Phys. Rev. D* **60** (1999) 013004, arXiv:hep-ph/9903391.

[129] **DELPHI** Collaboration, P. Abreu *et al.*, "An Upper limit for Br(Z^0 $\to$ g g g) from symmetric three jet Z^0 hadronic decays," *Phys. Lett. B* **389** (1996) 405–415.

[130] **CDF** Collaboration, T. A. Aaltonen *et al.*, "First Search for Exotic Z Boson Decays into Photons and Neutral Pions in Hadron Collisions," *Phys. Rev. Lett.* **112** (2014) 111803, arXiv:1311.3282 [hep-ex].

[131] **CDF** Collaboration, F. Abe *et al.*, "Search for the rare decay W$^\pm \to$ D$_s^\pm\gamma$ in p$\bar{\text{p}}$ collisions at $\sqrt{s}$ = 1.8 TeV," *Phys. Rev. D* **58** (1998) 091101.

[132] **ATLAS** Collaboration, M. Aaboud *et al.*, "Search for top-quark decays t $\to$ Hq with 36 fb^{-1} of pp collision data at $\sqrt{s}$ = 13 TeV with the ATLAS detector," *JHEP* **05** (2019) 123, arXiv:1812.11568 [hep-ex].

[133] **ATLAS** Collaboration, M. Aaboud *et al.*, "Search for flavour-changing neutral current top-quark decays t $\to$ qZ in proton-proton collisions at $\sqrt{s}$ = 13 TeV with the ATLAS detector," *JHEP* **07** (2018) 176, arXiv:1803.09923 [hep-ex].

[134] **CMS** Collaboration, A. M. Sirunyan *et al.*, "Search for rare decays of Z and Higgs bosons to J/ψ and a photon in proton-proton collisions at $\sqrt{s}$ = 13 TeV," *Eur. Phys. J. C* **79** (2019) 94, arXiv:1810.10056 [hep-ex].

[135] **CMS** Collaboration, A. M. Sirunyan *et al.*, "Search for W boson decays to three charged pions," *Phys. Rev. Lett.* **122** (2019) 151802, arXiv:1901.11201 [hep-ex].

[136] **LHCb,** Collaboration, R. Aaij *et al.*, "Search for the rare decays $W^+ \to D_s^+\gamma$ and $Z \to D^0\gamma$ at LHCb," *Chin. Phys. C* **47** (2023) 093002, arXiv:2212.07120 [hep-ex].
[137] **ALEPH** Collaboration, D. Decamp *et al.*, "Searches for new particles in Z decays using the ALEPH detector," *Phys. Rept.* **216** (1992) 253–340.
[138] S. Alte, M. König, and M. Neubert, "Exclusive Radiative Z-Boson Decays to Mesons with Flavor-Singlet Components," *JHEP* **02** (2016) 162, arXiv:1512.09135 [hep-ph].
[139] T.-C. Huang and F. Petriello, "Rare exclusive decays of the Z-boson revisited," *Phys. Rev. D* **92** (2015) 014007, arXiv:1411.5924 [hep-ph].
[140] W.-L. Sang, D.-S. Yang, and Y.-D. Zhang, "Z-boson radiative decays to an S-wave quarkonium at NNLO and NLL accuracy," *Phys. Rev. D* **108** (2023) 014021, arXiv:2302.06439 [hep-ph].
[141] G.-Y. Wang, X.-C. Zheng, X.-G. Wu, and G.-Z. Xu, "Z-boson decays into S-wave quarkonium plus a photon up to $O(\alpha_s v^2)$ corrections," arXiv:2312.08796 [hep-ph].
[142] H. S. Chung, J.-H. Ee, D. Kang, U.-R. Kim, J. Lee, and X.-P. Wang, "Pseudoscalar quarkonium+γ production at NLL+NLO accuracy," *JHEP* **10** (2019) 162, arXiv:1906.03275 [hep-ph].
[143] A. V. Luchinsky, "Leading order NRQCD and Light-Cone Analysis of Exclusive Charmonia Production in Radiative Z-boson Decays," arXiv:1706.04091 [hep-ph].
[144] G. T. Bodwin, H. S. Chung, J.-H. Ee, and J. Lee, "Z-boson decays to a vector quarkonium plus a photon," *Phys. Rev. D* **97** (2018) 016009, arXiv:1709.09320 [hep-ph].
[145] W.-L. Sang, D.-S. Yang, and Y.-D. Zhang, "Z boson radiative decays to a P-wave quarkonium at NNLO and LL accuracy," *Phys. Rev. D* **106** (2022) 094023, arXiv:2208.10118 [hep-ph].
[146] H. Dong, P. Sun, B. Yan, and C. P. Yuan, "Probing the Zbb anomalous couplings via exclusive Z boson decay," *Phys. Lett. B* **829** (2022) 137076, arXiv:2201.11635 [hep-ph].
[147] E. Ma and A. Pramudita, "Flavor Changing Effective Neutral Current Couplings in the Weinberg-Salam Model," *Phys. Rev. D* **22** (1980) 214.
[148] M. Bauer, M. Heiles, M. Neubert, and A. Thamm, "Axion-Like Particles at Future Colliders," *Eur. Phys. J. C* **79** (2019) 74, arXiv:1808.10323 [hep-ph].
[149] D. d'Enterria and H.-S. Shao, "Prospects for ditauonium discovery at colliders," *Phys. Lett. B* **842** (2023) 137960, arXiv:2302.07365 [hep-ph].
[150] L. Bergstrom and R. W. Robinett, "On the rare decays $Z \to VV$ and $Z \to VP$," *Phys. Rev. D* **41** (1990) 3513.
[151] D.-N. Gao and X. Gong, "Note on rare Z-boson decays to double heavy quarkonia*," *Chin. Phys. C* **47** (2023) 043106, arXiv:2208.12652 [hep-ph].
[152] X. Luo, H.-B. Fu, H.-J. Tian, and C. Li, "Next-to-leading-order QCD correction to the exclusive double charmonium production via Z decays," arXiv:2209.08802 [hep-ph].
[153] C. Li, Z. Sun, and G.-Y. Zhang, "Analysis of double-J/ψ production in Z decay at next-to-leading-order QCD accuracy," arXiv:2307.08376 [hep-ph].
[154] Z. Sun and H. F. Zhang, "Comprehensive studies of Υ inclusive production in Z boson decay," *JHEP* **06** (2021) 152, arXiv:2104.08711 [hep-ph].
[155] **L3** Collaboration, M. Acciarri *et al.*, "Heavy quarkonium production in Z decays," *Phys. Lett. B* **453** (1999) 94–106.
[156] **L3** Collaboration, M. Acciarri *et al.*, "Υ production in Z decays," *Phys. Lett. B* **413** (1997) 167–175.
[157] **OPAL** Collaboration, G. Alexander *et al.*, "Observation of Υ production in hadronic Z^0 decays," *Phys. Lett. B* **370** (1996) 185–194.
[158] **ATLAS** Collaboration, G. Aad *et al.*, "Search for the exclusive W boson hadronic decays $W^\pm \to \pi^\pm\gamma$, $W^\pm \to K^\pm\gamma$ and $W^\pm \to \rho^\pm\gamma$ with the ATLAS detector," arXiv:2309.15887 [hep-ex].
[159] **CMS** Collaboration, A. M. Sirunyan *et al.*, "Search for the rare decay of the W boson into a pion and a photon in proton-proton collisions at $\sqrt{s} = 13$ TeV," *Phys. Lett. B* **819** (2021) 136409, arXiv:2011.06028 [hep-ex].
[160] A. G. Bagdatova, S. P. Baranov, and A. S. Sakharov, "Study of exclusive two-body W decays with fully reconstructible kinematics," *Mod. Phys. Lett. A* **38** (2023) 2350073, arXiv:2303.02136 [hep-ph].
[161] M. Beneke, G. Finauri, K. K. Vos, and Y. Wei, "QCD light-cone distribution amplitudes of heavy mesons from boosted HQET," *JHEP* **09** (2023) 066, arXiv:2305.06401 [hep-ph].
[162] T. Melia, "Exclusive hadronic W decay: $W \to \pi\gamma$ and $W \to \pi^+\pi^+\pi^-$," *Nucl. Part. Phys. Proc.* **273-275** (2016) 2102–2106.
[163] A. V. Luchinsky and A. K. Likhoded, "Charmonia production in $W \to (c\bar{c})D_s^{(*)}$ decays," *Mod. Phys. Lett. A* **36** (2021) 2150058, 1801.08998.
[164] S. Balaji, "*CP* asymmetries in the rare top decays $t \to c\gamma$ and $t \to cg$," *Phys. Rev. D* **102** (2020) 113010, arXiv:2009.03315 [hep-ph].
[165] **ATLAS** Collaboration, G. Aad *et al.*, "Search for flavour-changing neutral currents in processes with one top quark and a photon using 81 fb^{-1} of pp collisions at $\sqrt{s} = 13$ TeV with the ATLAS experiment," *Phys. Lett. B* **800** (2020) 135082, arXiv:1908.08461 [hep-ex].
[166] **CMS** Collaboration, V. Khachatryan *et al.*, "Search for anomalous Wtb couplings and flavour-changing neutral currents in t-channel single top quark production in pp collisions at $\sqrt{s} = 7$ and 8 TeV," *JHEP* **02** (2017) 028, arXiv:1610.03545 [hep-ex].
[167] G. Eilam, M. Frank, and I. Turan, "Rare decay of the top $t \to cgg$ in the standard model," *Phys. Rev. D* **73** (2006) 053011, arXiv:hep-ph/0601151.

[168] W. Altmannshofer, B. Maddock, and D. Tuckler, "Rare Top Decays as Probes of Flavorful Higgs Bosons," *Phys. Rev. D* **100** (2019) 015003, arXiv:1904.10956 [hep-ph].

[169] **CMS** Collaboration, A. Tumasyan *et al.*, "Search for Flavor-Changing Neutral Current Interactions of the Top Quark and Higgs Boson in Final States with Two Photons in Proton-Proton Collisions at $\sqrt{s} = 13$ TeV," *Phys. Rev. Lett.* **129** (2022) 032001, arXiv:2111.02219 [hep-ex].

[170] E. E. Jenkins, "The Rare top decays $t \to bW^+Z$ and $t \to cW^+W^-$," *Phys. Rev. D* **56** (1997) 458–466, arXiv:hep-ph/9612211.

[171] R. Decker, M. Nowakowski, and A. Pilaftsis, "Dominant three-body decays of a heavy Higgs and top quark," *Z. Phys. C* **57** (1993) 339–348, arXiv:hep-ph/9301283.

[172] G. Mahlon and S. J. Parke, "Finite width effects in top quark decays," *Phys. Lett. B* **347** (1995) 394–398, arXiv:hep-ph/9412250.

[173] G. Altarelli, L. Conti, and V. Lubicz, "The $\mathrm{t} \to \mathrm{WZb}$ decay in the standard model: A Critical reanalysis," *Phys. Lett. B* **502** (2001) 125–132, arXiv:hep-ph/0010090.

[174] T. Han and R. Ruiz, "Higgs Bosons from Top Quark Decays," *Phys. Rev. D* **89** (2014) 074045, arXiv:1312.3324 [hep-ph].

[175] A. Cordero-Cid, J. M. Hernandez, G. Tavares-Velasco, and J. J. Toscano, "Rare top quark decay $\mathrm{t} \to \mathrm{u}_1\bar{\mathrm{u}}_2\mathrm{u}_2$ in the standard model," *Phys. Rev. D* **73** (2006) 094005, arXiv:hep-ph/0411188.

[176] S. Bar-Shalom, G. Eilam, M. Frank, and I. Turan, "Width effects on near threshold decays of the top quark $\mathrm{t} \to \mathrm{cWW}, \mathrm{cZZ}$ and of neutral Higgs bosons," *Phys. Rev. D* **72** (2005) 055018, arXiv:hep-ph/0506167.

[177] A. Papaefstathiou and G. Tetlalmatzi-Xolocotzi, "Rare top quark decays at a 100 TeV proton-proton collider: $\mathrm{t} \to \mathrm{bWZ}$ and $\mathrm{t} \to \mathrm{hc}$," *Eur. Phys. J. C* **78** (2018) 214, arXiv:1712.06332 [hep-ph].

[178] G. Mahlon, "Theoretical expectations in radiative top decays," in *Thinkshop on Top Quark Physics for Run II*. 10, 1998. arXiv:hep-ph/9810485.

[179] L. T. Handoko, "Branching ratio and CP violation in semiinclusive flavor changing top decays," *Nuovo Cim. A* **111** (1998) 1275, arXiv:hep-ph/9803262.

[180] L. T. Handoko and C.-F. Qiao, "$\mathrm{t} \to \mathrm{c}\Upsilon$ within and beyond the Standard Model," *J. Phys. G* **27** (2001) 1391–1404, arXiv:hep-ph/9907375.

[181] S. Slabospitskii, "Top-quark decay into Υ-meson," *Phys. Lett. B* **822** (2021) 136704, arXiv:2107.04398 [hep-ph].